

Technical Report

TR-21-13

February 2022



Compressive strength of bentonites

Factors influencing results from unconfined compression tests

Ann Dueck

Ulf Nilsson

Viktor Jensen

Lennart Börgesson

SVENSK KÄRNBRÄNSLEHANTERING AB

SWEDISH NUCLEAR FUEL
AND WASTE MANAGEMENT CO

Box 3091, SE-169 03 Solna
Phone +46 8 459 84 00
skb.se

SVENSK KÄRNBRÄNSLEHANTERING

ISSN 1404-0344

SKB TR-21-13

ID 1954876

February 2022

Compressive strength of bentonites

Factors influencing results from unconfined compression tests

Ann Dueck, Ulf Nilsson, Viktor Jensen, Lennart Börgesson
Clay Technology AB

Keywords: Unconfined compression tests, Unconfined compressive strength, Bentonite.

This report concerns a study which was conducted for Svensk Kärnbränslehantering AB (SKB). The conclusions and viewpoints presented in the report are those of the authors. SKB may draw modified conclusions, based on additional literature sources and/or expert opinions.

This report is published on www.skb.se

© 2022 Svensk Kärnbränslehantering AB

Abstract

The knowledge of the resistance against fast deformation and shear of the buffer material surrounding the canister in a deposition hole (the shear strength) is important for the dimensioning of the KBS-3V concept, since it has a strong influence on the stresses in the canister caused by a possible rock shear along a fracture intersecting the deposition hole. The higher shear strength the larger stresses in the canister. The shear strength is preferably determined by triaxial tests, but strength can also be determined by the experimentally more simple unconfined compression test. The requirements on strength for the technical design of the buffer is expressed in terms of unconfined compressive strength which is determined by the unconfined compression test which makes this test type suitable for studies on strength. The unconfined compression test has been used in several studies on bentonites, e.g. studies on physical properties and effects of strain rate, for comparative studies and for evaluation of effects of different preparation techniques and influences of different material components. In this study the specimens had a height to diameter ratio of 1:1.

The influence of ion-exchange, different stress paths, drying and heating on the unconfined compressive strength have been studied in this project. Different bentonites have been used in the different test series. The main part of the specimens was saturated before testing but also a series with unsaturated specimens exposed to drying has been included in the study. The strength is often related to mean stress or swelling pressure for modelling purposes so the influence of swelling pressure on the strength has also been studied.

Strength is to a large extent governed by the dry density and the type of bentonite. The results show that there are no indications that ion-equilibrium with an external salt solution (CaCl_2) will influence the strength and for the main part of the bentonites tested no large influence of an ion-exchange (to Ca-dominated bentonite) on strength was seen. In addition, there was no influence of stress path (swelling/consolidation) on the resulting strength when studied as function of final dry density.

When strength is plotted as a function of swelling pressure, the scatter between the results from different types of bentonites is lower than when plotted as a function of dry density. However, to have an unambiguous relationship between swelling pressure and strength for a bentonite, the swelling pressure should refer to a specific condition including e.g. saturation at constant volume condition and equilibrium with de-ionized water. At deviating conditions factors can be introduced into the relationship between average stress and strength although these do not influence the strength as a function of dry density.

The effect of drying by exposure to a combination of CaCl_2 and heating to 90 °C was studied and compared to reference tests. The drying caused no or small deviations in strength for the re-saturated specimens. However, the strain to failure was somewhat lower compared to references. The series with specimens exposed to drying without re-saturation resulted in an increase in strength. In a limited test series, the influence of short time heating to 240 °C, at water saturated and unsaturated conditions, was also studied.

Sammanfattning

Kunskap om mothållet mot snabb deformation och skjuvning av bentonitbufferten som omger kapseln i deponeringshålet (skjuvhållfastheten) är viktig för dimensioneringen av KBS-3V konceptet, eftersom detta har stor inverkan på spänningarna som uppkommer i kapseln vid en eventuell bergskjuvning längs en spricka genom ett deponeringshål. Ju högre skjuvhållfasthet desto större spänningar i kapseln. Skjuvhållfastheten bestäms med fördel med ett triaxialförsök men kan även bestämmas med det försöksmässigt enklare enaxliga tryckförsöket. Eftersom kravet på hållfasthet i den tekniska utformningen av bufferten uttrycks i termer av enaxlig tryckhållfasthet är det enaxliga tryckförsöket en lämplig försökstyp för närmare studier av hållfastheten. Dessutom har det enaxliga tryckförsöket använts i flera tidigare studier av bentonit t.ex. i en studie om fysikaliska egenskaper och inverkan av töjningshastighet, för jämförande studier och för utvärdering av effekten av olika typ av preparering och materialkomponenter.

Inverkan av jon-byte, olika spänningvägar och uttorkning på den enaxliga tryckhållfastheten har studerats i detta projekt. Olika typer av bentonit har använts för de olika försöksserierna. Huvuddelen av proverna har varit vattenmättade vid det enaxliga tryckförsöket men även en serie med omättade uttorkade prover har ingått i studien. Hållfastheten är ofta relaterad till medelspänning eller svälltryck i materialmodeller och inverkan av svälltryck på hållfastheten har därför också undersökts i detta projekt.

Hållfastheten påverkas till stor del av torrdensitet och typen av bentonit. Resultaten från detta projekt visar inga indikationer på att jonjämvikt med en extern saltlösning (CaCl_2) inverkar på hållfastheten och för de flesta materialen kunde ingen stor inverkan på grund av jon-byte (till Ca-dominerat material) observeras. Spänningvägen (svällning/konsolidering) påverkade inte heller hållfastheten då den relaterades till slutlig torrdensitet.

Då hållfastheten uttrycks som en funktion av svälltryck blir spridningen mellan resultat från olika typer av bentonit mindre jämfört med om resultatet tecknas som funktion av torrdensitet. För att hitta en entydig relation mellan svälltrycket och hållfastheten för en viss bentonit måste svälltrycket dock referera till ett specifikt tillstånd med t.ex. vattenmättnad utan volymförändring och jämvikt med avjoniserat vatten. Vid avvikande tillstånd kan faktorer som påverkar medelspänningen introduceras till relationen mellan medelspänning och hållfasthet trots att dessa faktorer inte påverkar hållfastheten som funktion av torrdensitet.

Effekten av uttorkning vid en kombination av tillsatt saltlösning, CaCl_2 , och ökad temperatur, $90\text{ }^\circ\text{C}$, har studerats. Jämfört med referensprover orsakade uttorkningen inga eller endast små förändringar av hållfastheten hos den återmättade bentoniten. Töjningen vid brott var dock mindre jämfört med referensproverna. I en serie prover som utsatts för uttorkning utan att återmättas uppmättes förhöjd hållfasthet. I en begränsad försöksserie undersöktes även inverkan av kortvarig exponering för $240\text{ }^\circ\text{C}$, i vattenmättat och omättat tillstånd.

Contents

1	Introduction	7
1.1	Background	7
1.2	Objective	7
1.3	Structure of the report	8
2	Materials	9
3	Test techniques	11
3.1	General	11
3.2	Determination of base variables and parameters	11
3.2.1	Water content, density, liquid limit and particle density	11
3.2.2	Water retention curve	12
3.3	Ion-exchange	13
3.4	Saturation and measurement of swelling pressure	13
3.5	Exposure to controlled relative humidity	14
3.6	Preparation of specimens	14
3.6.1	General	14
3.6.2	Preparation of ion-exchanged specimens (series TMS1–3)	14
3.6.3	Preparation of specimens with different stress paths (series SC-OE)	16
3.6.4	Preparation of specimens exposed to drying (series DS1 and DS2)	17
3.6.5	Preparation of specimens exposed to high temperature (series UCT)	20
3.7	Unconfined compression tests	21
3.7.1	Equipment	21
3.7.2	Specimens	21
3.7.3	Test procedure	22
3.7.4	Test results	22
3.7.5	Test series	22
4	Results	25
4.1	General	25
4.2	Test series TMS1	25
4.2.1	General	25
4.2.2	Unconfined compression tests	25
4.2.3	Swelling pressure tests	25
4.2.4	Comments	27
4.2.5	Concluding remarks	28
4.3	Test series TMS2	29
4.3.1	General	29
4.3.2	Unconfined compression tests	29
4.3.3	Swelling pressure tests	30
4.3.4	Comments	31
4.3.5	Concluding remarks	31
4.4	Test series TMS3	32
4.4.1	General	32
4.4.2	Unconfined compression tests	32
4.4.3	Swelling pressure tests	33
4.4.4	Comments	34
4.4.5	Concluding remarks	36
4.5	Test series SC-OE	37
4.5.1	General	37
4.5.2	Series with constant axial stress and no radial deformation	37
4.5.3	Series with constant volume conditions	38
4.5.4	Series with controlled final volume	40
4.5.5	Comments	41
4.5.6	Concluding remarks	43

4.6	Test series DS1	43
4.6.1	General	43
4.6.2	Combined effect of content of chloride salts and drying at 90 °C	44
4.6.3	Effect of content of calcium oxide	45
4.6.4	Comments	46
4.6.5	Concluding remarks	47
4.7	Test series DS2	47
4.7.1	General	47
4.7.2	Drying and testing unsaturated specimens	47
4.7.3	Saturated specimens	49
4.7.4	Determinations of characterizing properties	49
4.7.5	Comments	50
4.7.6	Concluding remarks	52
4.8	Test series UCT	53
4.8.1	General	53
4.8.2	Exposure to high temperature	53
4.8.3	Comments	55
4.8.4	Concluding remarks	56
5	Additional analyses	57
5.1	Strength as a function of dry density	57
5.1.1	Different materials	57
5.1.2	Ion-exchanged material	57
5.1.3	Strength as a function of clay dry density	59
5.2	Strength as a function of stress	61
5.2.1	Different materials	61
5.2.2	Ion-exchanged materials	62
5.2.3	Influence of salt solution and other factors on the strength of MX-80	62
5.3	Influence of drying	63
5.4	Influence of exposure to a temperature of 240 °C	64
5.5	Additional observations and comments	67
6	Conclusions	69
6.1	General	69
6.2	Conclusions from each different test series	69
6.3	Concluding remarks	71
	References	73
	Appendix 1 Tables	75
	Appendix 2 Detailed results from TMS1	79
	Appendix 3 Detailed results from TMS2	83
	Appendix 4 Detailed results from TMS3	87
	Appendix 5 Detailed results from SC-OE	91
	Appendix 6 Detailed results from DS1	95
	Appendix 7 Detailed results from DS2	99
	Appendix 8 Detailed results from UCT	107
	Appendix 9 Expected accuracy in unconfined compression tests	113

1 Introduction

1.1 Background

The knowledge of the resistance against fast deformation and shear of the buffer material surrounding the canister in a deposition hole (the shear strength) is important for the dimensioning of the KBS-3V concept, since it has a strong influence on the stresses in the canister caused by a possible rock shear along a fracture intersecting the deposition hole. The higher shear strength the larger stresses in the canister. The shear strength is preferably determined by triaxial tests but an experimentally more simple method is the unconfined compression test from which the shear strength, valid for simplified condition, can be evaluated. In Posiva SKB (2017) the requirement of the strength is mentioned as a technical design requirement of the buffer which should “yield an unconfined compressive strength at failure < 4 MPa at a deformation rate of 0.8 % /min when determined with a specific laboratory test procedure, and for material specimens in contact with waters with less favourable characteristics than site-specific groundwater”.

The unconfined compression test has been used in several studies on bentonites, e.g. a study on physical properties and effects of strain rate (e.g. Börgesson et al. 2004, Dueck et al. 2010) and for comparative studies (e.g. Karnland et al. 2009, Dueck et al. 2011b, Svensson et al. 2011, Åkesson et al. 2012). The method has also been used for evaluation of effects of different preparation techniques or effects of different material components (Dueck and Börgesson 2015, Dueck 2010). In addition to tests on saturated bentonite specimens the method has also been used on unsaturated samples (e.g. Johannesson 2008).

The strength is to a large extent governed by the density but is often related to mean stress or swelling pressure for modelling purposes and such relation has also been verified by triaxial tests (e.g. Börgesson et al. 2010, Dueck et al. 2010). A material model based on mainly triaxial tests was presented by Börgesson et al. (1995) and updated 2010. However, it has been shown that the swelling pressure is generally not uniquely determined by the density and since the swelling pressure can be influenced by e.g. stress paths, low temperatures, ion equilibrium and water pressure (Börgesson et al. 1995, Dueck 2010, Birgersson et al. 2008, Karnland et al. 2006, Birgersson and Karnland 2015) it is important to understand the direct influence of swelling pressure and other parameters on the strength.

Since the swelling pressure instead of the density has been proposed as the parameter to which other properties of the bentonite buffer are related, the relationship between strength and swelling pressure has been further studied and reported. In these studies, swelling pressure is determined separately, just before the unconfined compression test or in separate test series.

The unconfined compressive strength of bentonites with dry densities between 1 300 and 1 800 kg/m³ has been investigated in seven laboratory studies where the influence of factors as ion-exchange, stress paths, drying and heating have been studied. This report comprises compilation and analyses of the laboratory test results of more than 320 specimens of eight different bentonites previously presented in seven Technical Memos 2014 to 2021.

1.2 Objective

The objective of this project has been to study the influences of ion-exchange, stress paths, drying and heat on the unconfined compressive strength of bentonites. In addition, the relationship between swelling pressure and unconfined compressive strength has also been studied. The objective of the report has been to compile and analyse results from studies included in the project where the mentioned issues have been studied. The denominations of the different test series have been kept in this report where the three first studies (TMS1, TMS2 and TMS3) aimed at studying the influence of ion-exchange (to Ca-dominated material), the fourth study (SC-OE) involved studies on stress paths, the fifth and sixth studies (DS1, DS2) aimed at studying the influence of drying and the seventh at the influence of heating to 240 °C (UCT).

1.3 Structure of the report

In Chapter 2 the eight different materials used are briefly described. In Chapter 3 the different types of preparation and the unconfined compression test are described. In Section 3.6 the specimens and how they have been prepared are described and in Section 3.7 all test series are tabulated. In Chapter 4 the test results are shown and the results from each study are presented in separate sections. Some analyses are presented directly together with the test results, but some additional analyses are presented in Chapter 5. In Chapter 6 the conclusions are presented. In Section 6.2 the most important concluding remarks of each study (from Chapter 4) are compiled and some additional remarks given in Section 6.3. The appendices mainly contain tabulated test results and diagrams of the stress-strain curves from all unconfined compression tests. General data is given in Appendix 1 and the accuracy of the test results is commented in Appendix 9. Test results from each study are presented separately in Appendix 2–8.

2 Materials

The material used in this project was the bentonites:

- **Asha505** – Indian Na-bentonite from the Kutch area produced by Ashapura Minechem Co.
- **Calcigel** – German Na-bentonite from Bavaria and produced by Clariant (Süd-Chemie AG)
- **Deponit CaN** (IBECO Deponit CaN) – Greek Ca-bentonite from Milos mined by S&B Industrial Minerals SA
- **FEBEX** – Mg-Ca bentonite extracted from the Cortijo de Archidona deposit in Almería, Spain and exploited by Minas de Gádor SA (Süd-Chemie Espana)
- **GMZ** – Chinese Na-bentonite Gaomiaozhi
- **Ikosorb** – with the commercial name IBECO RWC White is a Ca, Mg, Na bentonite mined in Marocco
- **Kunigel** – Na-bentonite produced by Kunimine Industries Co., Ltd, Japan
- **MX-80** – Wyoming Na dominated bentonite manufactured by American Colloid Company.

Descriptions and properties have been presented by e.g. Karnland et al. (2006) and Svensson et al. (2011). Particle densities and liquid limits for the materials are given in Table 2-1.

Table 2-1. Particle density and liquid limit for the tested materials.

Material	Particle density ρ_s kg/m ³	Liquid limit w_L %	References
Asha505	2907 2869	337	Karnland et al. (2006) Svensson et al. (2011)
Calcigel	2695	119	Svensson et al. (2011)
Deponit CaN	2750 2678	160	Karnland et al. (2006) Svensson et al. (2011)
Febex	2735	109	Svensson et al. (2011)
GMZ			Sandén et al. (2018)
Ikosorb	2740	326	Svensson et al. (2011)
Kunigel	2681	462	Svensson et al. (2011)
MX-80	2777 2735	545	Karnland et al. (2006) Svensson et al. (2011)

3 Test techniques

3.1 General

In this chapter the test technique for unconfined compression tests (UC-tests) is described together with the different types of preparation methods that have been used for the specimens. All specimens were compacted from powder to cylindrical specimens and all specimens were sheared with the height and diameter approximately 20 mm, but different preparation methods were used. During the preparation salt or chemical compounds were added to some specimens and some specimens were saturated while others were kept unsaturated until testing. The test techniques used for the preparation and testing are described in the following sections with focus on

- ion-exchange,
- saturation and measurement of swelling pressure,
- exposure to controlled relative humidity,
- preparation of specimens,
- unconfined compression test.

In addition, determination of base variables and retention properties are also described. The denominations of the original test series have been kept in this section and also in the presented results.

3.2 Determination of base variables and parameters

3.2.1 Water content, density, liquid limit and particle density

The base variables water content w (%), void ratio e (-) and degree of saturation S_r (%) were determined according to Equation 3-1 – Equation 3-3.

$$w = 100 \cdot \frac{m_{tot} - m_s}{m_s} \quad (3-1)$$

$$e = \frac{\rho_s}{\rho} (1 + w/100) - 1 \quad (3-2)$$

$$S_r = \frac{\rho_s \cdot w}{\rho_w \cdot e} \quad (3-3)$$

where

m_{tot} = total mass of the specimen (g)

m_s = dry mass of the specimen (g)

ρ_s = particle density (kg/m³)

ρ_w = density of water (kg/m³)

ρ = bulk density of the specimen (kg/m³)

The dry mass of the specimen was obtained from drying the wet specimen at 105 °C for 24h. The bulk density was calculated from the total mass of the specimen and the volume determined by weighing the specimen above and submerged into paraffin oil. The dry density was then calculated from the determined bulk density and water content.

The liquid limit w_L was determined with the fall-cone one-point method according to the “Consistency limits” part of the Laboratory manual series of the Swedish Geotechnical Society (SGF) and SIS (2007). The method was adjusted to bentonite by letting the clay-water mixtures rest for 24 h before the fall-cone tests were performed.

The particle density ρ_s of the materials was determined according to the method used by Svensson et al. (2011) and Karnland et al. (2006). With this method the density is determined in a volumetric flask. The determination of volume was made with a solution of 1M NaCl in order to prevent swelling of the bentonite.

3.2.2 Water retention curve

The jar method is a method that can be used for the determination of water retention curves. With this method the equilibrium water contents of a material are determined by placing samples in jars each having a controlled climate with a specific RH generated by a salt solution. The method has been described by Wadsö et al. (2004). Results of bentonite have been presented by e.g. Dueck and Nilsson (2010).

Equipment, preparation of specimens and test procedure

Powder specimens of the actual bentonite are prepared to the predetermined initial water content and approximately 10 g is used for each relative humidity RH . Each specimen is placed in a metal cage and suspended inside glass jars with a tight lid, Figure 3-1. A rod through the lid makes it possible to weigh the specimens below a balance without having to remove it from the jars. At equilibrium the measurements are finished, and the specimens are dried at 105 °C for 24 hours and the mass of the dry specimens are determined.

Eight different relative humidity RH were used for the tests (0 %, 11 %, 33 %, 58 %, 75 %, 84 %, 93 %, 97 %) where molecular sieve was used for 0 %, an unsaturated NaCl solution for 93 % and saturated salt solutions (LiCl, MgCl₂, NaBr, NaCl, KCl, K₂SO₄) for the others. The actual values of the saturated salt solutions were taken from Greenspan (1977) and the relative humidity of the unsaturated solution was calculated from values of vapour pressure tabulated by Clarke and Glew (1985). The jars with the samples were placed in an oven with a controlled temperature of 25 °C ± 0.1 °C.

Test results

The time evolution of the water content was determined from the weighing during the time to equilibrium. At equilibrium the tests were terminated, and the final dry mass of the specimens was determined after oven drying. The final water content was then calculated from the total mass before the drying and the dry mass determined after drying. Whether the equilibrium state was reached, was evaluated by a limit of the parameter Ω , Equation 3-4, where m is the mass (g) and t is the time (s). The parameter and the limit value $\Omega \leq 5 \times 10^{-9}$ 1/s were suggested by Wadsö et al. (2004).

$$\Omega = \frac{dm}{dt} \times \frac{(RH_f - RH_i)/100}{m(t) - m_i} \quad (3-4)$$

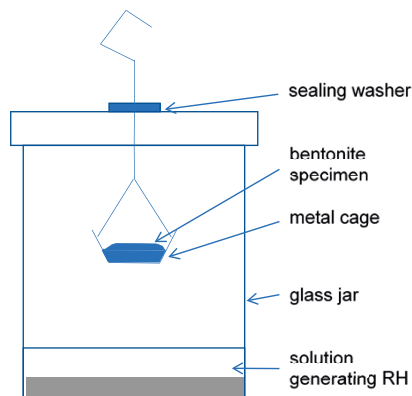


Figure 3-1. Schematic view showing the test equipment (Dueck and Nilsson 2010).

3.3 Ion-exchange

Solutions with one molar CaCl_2 or NaCl solution were used for the ion-exchange (exchangeable ions were exchanged for Ca^{2+} -ions or in some single test Na^+ -ions). The ion-exchange was made either on powder specimens or on confined specimens. After the ion-exchange excess salt was left in some of the specimens but removed from other specimens.

The ion-exchange of powder was made by a method similar to the one introduced and described by Karnland et al. (2006). Samples of the original materials (Asha505, Deponit Ca-N, FEBEX, GMZ, Ikosorb, MX-80, Kunigel) were dispersed in de-ionized water and CaCl_2 or NaCl was added to a concentration of 1M. The material was left to settle, and the supernatant was removed. The procedure was repeated and in case of washing the remaining material was transferred to dialysis membranes and placed in plastic tanks with de-ionized water. The de-ionized water was changed until low electrical conductivity was measured. In test series DS2 the method used was simplified in that no dialysis membrane was used for the washing where the supernatant was removed repeatedly and exchanged for DI water until relatively low electrical conductivity was measured. After the ion-exchange the material was dried in $40\text{ }^\circ\text{C}$ – $50\text{ }^\circ\text{C}$ and crushed before it was used in the preparation for the unconfined compression tests or for the measurement of swelling pressure.

The ion-exchange of confined specimens was made by circulation of 1M CaCl_2 solution on both sides of the compacted specimens (with 20 mm height). A minimum ion-exchange of 80 % in the central part of the samples was used as criterion for the ion-exchange and the estimated time required to reach this was calculated to 40 days based on one dimensional Fickian diffusion, a clay diffusion coefficient of $2 \times 10^{-11}\text{ m}^2/\text{s}$ (Muurinen 1994, Kozaki et al. 1998), and constant boundary conditions. In case of washing out excess salt after the ion-exchange the solution of 1M CaCl_2 solution was exchanged for de-ionized water during additional weeks.

3.4 Saturation and measurement of swelling pressure

The majority of the specimens were saturated before the unconfined compression tests. The specimens were prepared from powder to cylindrical specimens in a compaction device, but the saturation was done in different ways. After the saturation, the specimens were dismantled and used for the unconfined compression tests. The saturation was done in one of the following ways:

- In a saturation device with 3–10 specimens at a time and with the height and diameter 20 mm.
- In a swelling pressure device with one specimen at a time and the height and diameter 20 mm.
- In an oedometer device with axial compression and swelling after the saturation. The final diameter was 35 mm and the height differed between 18 mm and 24 mm.

The majority of the specimens were saturated in a saturation device which consists of two steel endplates bolted together with a middle plate with a height of 20 mm having 3 or 10 cylindrical holes for the compacted specimens. In this device filters are placed on both sides of the specimens for the circulation of fluids which is made in a circulation system including a peristaltic pump.

The swelling pressure device was used for the saturation of some of the specimens and this device consists of a steel ring surrounding the compacted specimen having filters on both sides. Bottom and upper plates are bolted together with the confining ring to keep the volume of the specimen constant. A movable piston is placed above the actual specimen and between the piston and the upper plate a load cell is placed to register the swelling pressure continuously, measured as the stress exerted on the piston. The supply of fluid is made by circulation system including a peristaltic pump.

The oedometer device was used for saturation of some of the specimens where a specific stress path during the preparation was aimed at. In this device the stresses were measured continuously both axially and radially. The device consists of a steel ring surrounding the specimen having filters on both sides. A movable piston and a force transducer were placed vertically above the specimen and also in the radial direction with the piston going through the steel ring. The device with the specimen was placed in a load frame where a constant load was applied. De-ionized water was supplied after evacuating the steel filters and tubes and a water pressure of approximately 2 kPa was applied. The

deformation was measured by a displacement transducer during the saturation and homogenization. After equilibrium the water was evacuated from the filters and tubes and the specimen with diameter 35 mm was dismantled. From the dismantled specimen a sample with diameter 20 mm was trimmed for the unconfined compression tests.

After dismantling, the specimens were sealed and stored approximately 12h before testing. The measured stresses after saturation were used as a measure of swelling pressure, even if different type of water or stress paths were used. Thus, swelling pressure has in this project been used beyond the definition given by Birgersson and Karnland (2015) which is further commented in Section 5.5.

In the results some of the measured stresses are presented as the average stress p which is defined as the average of the principal stresses but is here calculated from the measured axial stress p_a and radial stress p_r , according to Equation 3-5.

$$p = (p_a + 2 \cdot p_r) / 3 \quad (3-5)$$

3.5 Exposure to controlled relative humidity

Cylindrical specimens with different dry density and water content were prepared. Three unsaturated cylindrical specimens were prepared of each combination of water content and dry density. One specimen was used as a reference and the other two were exposed to a relative humidity of either 75 % or 85 % in a climate chamber with a constant temperature of 25 °C. During the exposure the specimens were placed on a tray where any volume change was measured. At equilibrium or at very small changes of mass with time, after approximately three weeks, the exposure was finished. After the exposure the specimens were sealed and stored approximately 12h before testing in an unsaturated state.

3.6 Preparation of specimens

3.6.1 General

The preparation of specimens used for unconfined compression tests is an important part of this project. Some specimens were ion-exchange (test series TMS1-3) and others were prepared with a special stress path (test series SC-OE) before the unconfined compression tests. In the series with ion-exchanged material some tests were also made on the reference materials. Some tests were run to study drying (DS1-2) either as unsaturated specimens or as saturated specimens exposed to a combined effect of salt and increased temperature. In the latter series some specimens were purposely prepared to be cemented. One series (UCT) were run to study any increased strength as a consequence of increased temperature.

The denomination of the test series and specimens are kept in the description below and these are also used in the presentation of results in Chapter 4.

3.6.2 Preparation of ion-exchanged specimens (series TMS1–3)

In the test series with ion-exchanged materials all eight materials mentioned in Table 2-1 were used.

Equipment

All specimens in these series were prepared from powder to cylindrical specimens with the height and diameter 20 mm in a compaction device. All the cylindrical specimens were saturated before the unconfined compression tests which was done in a saturation device for 3 or 10 specimens at a time or in a swelling pressure device for one specimen where the swelling pressure was measured simultaneously. See Section 3.4.

Preparation procedure

The ion-exchange of the material was made either before or after the preparation of cylindrical specimen according to the methodologies A–D:

- ion-exchange of powder specimens with excess salt left (ie A),
- ion-exchange of powder specimens but with excess salt washed out (ie B),
- ion-exchange of compacted specimens at confined conditions with excess salt left (ie C),
- ion-exchange of compacted specimens at confined conditions but with excess salt washed out (ie D).

When the ion-exchange was made on powder a cylindrical specimen was prepared from the ion-exchanged powder by use of the compaction device and then the relatively dry specimen was placed in the saturation device to be saturated. The fluid used for the saturation was either 1M CaCl₂ or de-ionized water, depending on the methodology used for the ion-exchange A or B, respectively, and the saturation was made during more than two weeks.

The ion-exchange of confined specimens, methodology C or D, was made on compacted cylindrical specimens of the original material placed in the saturation device. De-ionized water was introduced into the circulation system and the filters above and under the specimens but was changed to 1M CaCl₂ already after a couple of days. The ion-exchange with 1M CaCl₂ continued for 40 days. Another 40 days was used for washing out excess salt in case of methodology D.

Some specimens prepared by methodology D were put into a swelling pressure device where the swelling pressure was measured during the preparation. The time for the ion-exchange and for the subsequent washing of excess salt was the same as for the specimens placed in the saturation device, see above. The only difference between the specimens prepared in the swelling pressure device and those prepared in the saturation device was that longer time, approximately 14 days, was used for the initial saturation in the swelling pressure device. The longer time was used to get a clear and stable measured value of the initial swelling pressure, before the start of the ion-exchange.

Results from preparation

The prepared specimens were used for the unconfined compression tests. Mass and dimensions were determined on the specimens dismantled from the saturation device or from the swelling pressure device before the unconfined compression tests. The swelling pressure was measured on some of the specimens during the preparation.

Test series

The methodologies A to D (ie A to ie D) used for the ion-exchanged of specimens are further clarified in Table 3-1. In addition to the ion-exchanged specimens, tests were also run on samples of the reference materials, i.e. prepared from the original batches (cf. Appendix 1) of the materials without any ion-exchange. In Table 3-2 the number of specimens prepared by each of the ion-exchange methods and the number of specimens of the reference materials are given.

Table 3-1. Details of the different methodologies used for the ion-exchange (ie A to ie D).

Methodology used for the ion-exchange	Ion-exchange made on powder or confined specimens	Excess salt left or washed out after the ion-exchange	Solution in equilibrium with the specimen just before dismantling	Test series TMS1 to TMS3
ie A	powder	excess salt left	1M CaCl ₂	TMS3
ie B	powder	washed	DI-water	TMS1, TMS3
ie C	confined	excess salt left	1M CaCl ₂	TMS2, TMS3
ie D	confined	washed	DI-water	TMS3

Table 3-2. Number of specimens of ion-exchanged material and reference material prepared for the UC-tests. The number of specimens prepared by each of the methodologies for ion-exchange (ie A to ie D) are given together with number of specimens with reference material. During preparation the swelling pressure was measured on some specimens given as additional specimens, e.g. 3+3. Some specimens were used for swelling pressure only and this is marked as additional numbers within brackets, e.g. 3(+3).

Series	Material	Method of ion-exchange (ie) used and number of prepared specimens				
		Reference	ie A	ie B	ie C	ie D
TMS1	Calcigel	16				
	Dep Ca-N	6		6(+3)		
	Febex	6		6(+3)		
	GMZ	16		6(+3)		
TMS2	Asha 505	2+3			5	
	Ikosorb	3+3			5	
	Kunigel	4+3			6	
TMS3	MX-80	4	3	3	4	8+2
	Ikosorb	3	3	3	3	6+2
	GMZ	3	3	3	3	6+2

3.6.3 Preparation of specimens with different stress paths (series SC-OE)

The material used for the preparation described in this section was MX-80.

Equipment

The specimens in these test series were prepared from powder to cylindrical specimens with the height 20 mm and the diameter 20 mm or 35 mm. All specimens were saturated which was either done in a saturation device for 3 or 10 specimens at a time, in a swelling pressure device or in an oedometer device where one specimen at a time was saturated. See Section 3.4.

Preparation procedure

Different techniques were used in the preparation of specimens in this test series to introduce different stress paths during saturation:

- Saturation at constant axial stress and no radial deformation.
- Saturation at constant volume conditions.
- Saturation with or without volume increase but at controlled final volume.

The specimens exposed to constant axial stress (first bullet point) were prepared in an oedometer device placed in the load frame and the constant axial load was applied before the water was supplied, see Section 3.4. The axial and radial stresses were measured continuously during the saturation together with the deformation. The specimens saturated at constant volume conditions (second bullet point) were mounted in a swelling pressure device according to Section 3.4 with the swelling pressure measured axially and radially continuously during the saturation. The majority of the specimens in this test series were prepared with a controlled final volume (third bullet point) which were saturated, with or without volume increase without any measurement of swelling pressure, in a saturation device mentioned in Section 3.4.

For all specimens de-ionized water was supplied after evacuating the steel filters and tubes and a water pressure of approximately 2 kPa (or a total head of 0.2 m) was applied. After the saturation the water was evacuated from the filters and tubes and those specimens prepared with a diameter of 35 mm were trimmed to a diameter of 20 mm. Efforts were made to ensure that the specimens got parallel end surfaces. The unconfined compression tests were done approximately 12 hours after the dismantling.

Results from preparation

The prepared specimens were used for unconfined compression tests. Mass and dimensions were determined on the specimens dismantled from the saturation device. The specimens dismantled from the swelling pressure device or the oedometer device were trimmed to get a final diameter and height of approximately 20 mm. In addition, the results from these tests was also the swelling pressure, see Equation 3-5, and in some tests with volume change the deformation was also measured.

Test series

The test series run in the SC-OE series are described in Table 3-3.

Table 3-3. Number of specimens prepared by a specific stress path before the unconfined compression tests. Type of preparation, requirements and details are shown.

Series	Material	Type of preparation	Stress measurement	During saturation	After saturation	Number of specimens
SCOEUC	MX-80	Constant axial stress	measured	swelling/consolidation	trimmed	6
SCPUC	MX-80	No volume change	measured	no volume change	trimmed	2
SCUC	MX-80	Controlled final volume	-	large swelling	-	16
	MX-80	Controlled final volume	-	water pressure applied	-	6
	MX-80	Controlled final volume	-	compacted to saturation	-	10

3.6.4 Preparation of specimens exposed to drying (series DS1 and DS2)

The material used for the preparation described in this section was MX-80. The main part of the specimens in series DS1 were exposed to drying at 90 °C and then saturated with salt solutions. The main part of the specimens in series DS2 were exposed to drying and sheared unsaturated. In addition, a few specimens in the former test series were purposely prepared to be cemented.

Equipment

All specimens were prepared from powder to cylindrical specimens with the height and diameter 20 mm in a compaction device. Some specimens were exposed to 90 °C and then saturated at confined conditions. Some specimens were sheared as unsaturated specimens after exposure to drying (dehydration) or water uptake (hydration) under free volume conditions in a climate chamber, see Section 3.5. Other specimens were sheared after water saturation. The saturation was done either in a saturation device, made for several specimens, or in a swelling pressure device, where one specimen at a time was saturated with continuous measurement of swelling pressure, see Section 3.4. The water retention curve of some specimens was determined with the jar method, see Section 3.2.2.

Preparation procedures

The series DS1 were concentrated on

- the combined effect of content of chloride salts and drying at 90 °C on saturated specimens,
- the effect of content of calcium oxide on saturated specimens.

The series DS2 were concentrated on

- drying and testing unsaturated specimens,
- complementary saturated reference specimens,
- subsequent determinations of swelling pressure, water retention properties and compressive strength.

Combined effect of content of chloride salts and drying at 90 °C

The cylindrical specimens in these test series were all exposed to drying at 90 °C and subsequent saturation with 1M solution of CaCl₂ or NaCl before the unconfined compression tests. Before the drying and final saturation, the cylindrical specimens were prepared in one of the following ways:

- by exposing compacted cylindrical specimens to an ion-exchange,
- by using ion-exchanged powder when manufacturing cylindrical specimens,
- by adding excess salt to the powder used for the manufacturing of cylindrical specimens.

The ion-exchange was done according to Section 3.3. The ion-exchange was done either on powder samples (methodology ie A) or on compacted specimens in-situ (methodology ie C) and the methodologies are described in Section 3.6.2.

The cylindrical specimens were exposed to drying, without water supply, placed on a tray in an oven at 90 °C. After 48 hours the specimens were placed in a saturation device to be saturated with 1M CaCl₂ or NaCl for 14 days. The specimens, ion-exchanged as compacted specimens were put back into the swelling pressure devices after drying where they were saturated with the same salt solution used for the ion-exchange.

Effect of content of calcium oxide

The cylindrical specimens in these test series were manufactured by compaction of powder with added contents of calcium oxide or calcium hydroxide. After manufacturing the specimens were put into a saturation device and saturated with de-ionized water for 14 days.

Drying and testing unsaturated specimens

The cylindrical specimens in this series were all exposed to a relative humidity of 75 % or 85 % at a temperature of 25 °C and after the exposure the specimens were sheared unsaturated. The cylindrical specimens were prepared from

- powder mixed to different water contents,
- ion-exchanged powder mixed to a specific water content,
- powder mixed to different water contents and with added salt (5 % of the dry powder).

The ion-exchange of powder was done with the methodology B (ie B) where the simpler method without dialysis-membrane was used, see Section 3.3 and Section 3.6.2. The unsaturated cylindrical specimens were exposed to a relative humidity of 75 % and 85 % placed on a tray in a climate chamber at 25 °C, see Section 3.5. At equilibrium or at very small changes of mass with time, reached after approximately three weeks, the exposure was terminated. After the exposure the specimens were sealed and stored approximately 12h before testing in an unsaturated state.

Complementary saturated reference specimens

Cylindrical specimens were prepared from

- powder mixed to different water contents,
- ion-exchanged powder mixed to a specific water content,
- powder mixed to different water contents and with added salt (14–20 % of the dry powder).

The ion-exchange was made on powder according to methodology B (ie B) where the simpler method without dialysis-membrane was used, see Section 3.3 and Section 3.6.2. After the preparation the specimens were saturated with de-ionized water during approximately 14 days. After dismantling the specimens were sealed and stored approximately 12h before the unconfined compression tests.

Subsequent determinations of characterizing properties

In this series the compressive strength, swelling pressure and retention curves were determined on ion-exchanged Ca-dominated MX-80. The ion-exchange of the cylindrical specimens used for the unconfined compression tests was done either on the powder samples before the compaction (methodology ieB with the simpler method without dialysis-membrane) or on the compacted specimens in-situ (methodology ieD), see Section 3.3 and Section 3.6.2. During the saturation (and ion-exchange) the swelling pressure was measured according to Section 3.4. The ion-exchanged powder was also used for the determination of the retention curves (hydration and dehydration) according to 3.2.2. Before the determination the ion-exchanged powder was either dried to a low water content, which was used for the hydration curve, or was mixed to a water content about 60 %, which was used for the dehydration curve.

Results from preparation

The prepared saturated and unsaturated specimens were used for unconfined compression tests. The swelling and shrinkage of the unsaturated specimens were noted before the unconfined compression tests and the water content and dry density were determined on all specimens after the unconfined compression tests. In addition, the swelling pressure and the water retention curve were determined on some specimens.

Test series

The test series with unconfined compression tests in series DS1 and DS2 are shown in Table 3-4 and Table 3-5, respectively where the type of preparation and the total number of specimens are shown.

In series DS1 the specimens in the series, where the combined effect of content of chloride salts and temperature were studied (PUC1–2, UC1–2 and UC4), were all saturated with salt solutions and thus contained excess salt at dismantling and testing. The specimens in the series, where content of calcium oxide was studied (UC3 and UC5), were saturated with de-ionized water.

In series DS2 unsaturated specimens were sheared after preparation in a climate chamber (UCA, UCB) and two series with complementary saturated specimens (UCC, UCD) were sheared. In a series with characterisation tests the compressive strength was determined after measurement of swelling pressure of ion-exchange material (PUCA, PUCB). In the series with characterisation tests water retention curves were also determined, see Table 3-6.

Table 3-4. Test series of unconfined compression tests in series DS1 with number of specimens and specifications of the preparations used.

Test series	Number of specimens	Excess salt added at compaction	Method of ion-exchange	Temperature	Fluid used for saturation	Measurement of swelling pressure
PUC1	3		in-situ ie C ¹	90 °C	1M CaCl ₂	Yes
PUC2	3		in-situ, ie C ¹	90 °C	1M CaCl ₂	Yes
UC1	6		in-situ, ie C ¹	90 °C	1M CaCl ₂ or 1M NaCl	No
UC2	10	CaCl ₂	powder, ie A ²	90 °C	1M CaCl ₂	No
UC4	10	CaCl ₂	powder, ie A ²	90 °C	1M CaCl ₂	No
UC3	10	CaO or Ca(OH) ₂		20 °C	DI water	No
UC5	10	CaO		20 °C	DI water	No

¹ Ion-exchange as compacted specimen with excess salt left at dismantling (ie C, cf. Section 3.6.2).

² Ion-exchange as powder with excess salt left at dismantling (ie A, cf. Section 3.6.2).

Table 3-5. Test series of unconfined compression tests in series DS2 with number of specimens and specifications of the preparations used. Series UCA and UCB were sheared unsaturated.

Test series	Number of specimens	Excess salt added at compaction	Method of ion-exchange	Temperature	Fluid used for saturation or RH(%) in chamber	Measurement of swelling pressure
UCA	16	CaCl ₂	ieB ²	25 °C	75 %, 85 %	No
UCB	20			25 °C	75 %, 85 %	No
UCC	6	CaCl ₂	ieB ²	22 °C	DI water	No
UCD	10			22 °C	DI water	No
PUCA	3		in-situ ieD ¹	22 °C	DI water	Yes
PUCB	3		ieB ²	22 °C	DI water	Yes

¹ Ion-exchange as compacted specimen with excess salt washed out before dismantling (ieD, cf. Section 3.6.2).

² Ion-exchange as powder with excess salt washed out (ieB, cf. Section 3.6.2).

Table 3-6. Series of water retention curve of ion-exchanged MX-80Ca.

Test series	Type of ion-exchange	Preparation	Aim initial w %	Temperature °C
Jar MX-80Ca	ieB ¹	powder	0	25
	ieB ¹	powder	64	25

¹ Ion-exchange as powder with excess salt washed out (ieB, cf. Section 3.6.2).

3.6.5 Preparation of specimens exposed to high temperature (series UCT)

Equipment

All specimens were prepared in a compaction device where powder was compressed uniaxially to cylindrical specimens with the height and diameter 20 mm. The specimens were saturated in swelling pressure devices or in a specially designed saturation device made for several specimens.

In the swelling pressure devices, one specimen was saturated in each device. Such device consists of an upper piston and a lower plate bolted together with the confining ring containing the specimen. No measurement of swelling pressure was made. In one of the series, a saturation device for 10 specimens was used. This device consists of two steel endplates bolted together with a middle plate with the height 20 mm, having 10 cylindrical holes for the specimens. In the swelling pressure devices and the saturation device filters were placed on both sides of the specimens for the circulation of fluids which was made in a circulation system including a peristaltic pump.

A special set-up was needed for the heating with counter acting constant water pressure applied. A pressure/volume controller was connected with steel pipes to the equipment placed in the oven. A reducing valve was used in the system to avoid any larger pressure build-up during heating.

Preparation procedures

The tests were mainly made on specimens exposed to 240 °C and the specimens were prepared in three different ways:

- saturated confined specimens were heated with constant counteracting water pressure,
- unsaturated specimens were heated, dried and subsequently saturated,
- reference specimens were saturated only.

The saturated specimens, first bullet point, were exposed to heating in two cycles, for 7 hours each. Before the heating, the confined specimens were saturated with water pressure (50 kPa and 500 kPa) during approximately one week. The water pressure was increased to 3900 kPa approximately 24 hours before the heating. The water pressure of 3900 kPa was kept during the heating periods to counteract formation of steam. Between the heating cycles the water pressure was lowered rather rapidly to zero to

change o-rings and improve the sealing of the equipment. After the second heating cycle and additional 24 hours with water supply, the specimens were dismantled. More details are given in Appendix 8.

The unsaturated specimens were placed on a tray and dried in 240 °C in the oven for 7 hours. After drying, the specimens were saturated in the saturation device for two weeks before dismantling. The reference specimens were saturated together with the dried specimens for two weeks and then dismantled. After dismantling, all specimens were sheared after storage in tight plastic bags for approximately 12 hours.

3.7 Unconfined compression tests

The unconfined compression test has previously been used for bentonites to study physical properties and effects of strain rate (e.g. Börgesson et al. 2004, Dueck et al. 2010) and for comparative studies (e.g. Karnland et al. 2009, Dueck et al. 2011a, Svensson et al. 2011, Åkesson et al. 2012). The method has also been used for evaluation of effects of different preparation techniques or effects of different material components (Dueck and Börgesson 2015, Dueck 2010). In addition to tests on saturated bentonite specimens the method has also been used on unsaturated samples (e.g. Johannesson, 2008).

The unconfined compression test is an experimentally simple method where a cylindrical specimen is compressed axially under a constant rate of strain with no radial confinement or external radial stress. From the unconfined compression test the unconfined compressive strength is determined which is equal to the maximum deviator stress in this test. If the shear strength is estimated from the unconfined compression test the shear strength is calculated as $\frac{1}{2}$ of the deviator stress or of the compressive stress at failure. The shear strength can be considered since it is the resistance of the soil to failure in shear which is determined with the method (e.g. Craig 1974).

The unconfined compressive strength is commonly determined on specimens with the height equal to double the size of the diameter to admit the failure surface to fully develop without boundary effects from the end surfaces. In this study specimens with the height equal to the diameter were used, this was chosen to minimize the time for saturation of the specimens. In this case the end effect was minimized by lubrication of the end surfaces. The influence of using the height equal to the diameter on the evaluated maximum deviator stress was commented on in a report by Dueck et al. (2011a) where the influence was considered to be small, see also Appendix 1 and Figure A1-2. In addition, it should be noted that the strength in this actual project has been determined for comparative studies only. The methodology used for the unconfined compression tests is described in previous reports, but a short description is given below.

3.7.1 Equipment

The specimens were placed in a mechanical press where a constant rate of deformation was applied. During the test the deformation and the applied force were measured by means of a load cell and a displacement transducer.

3.7.2 Specimens

At testing the specimens were cylindrical having a height and diameter equal to 20 mm. The majority of the specimens had the diameter 20 ± 0.1 mm and the height 20.1 ± 0.2 mm after saturation in the saturation device. Larger variation was seen from specimens trimmed or tested after equilibrium in the climate chamber, however the specimens still had the height equal or slightly larger than the diameter. The preparation of the specimens was done according to Section 3.6. The unconfined compression tests were made approximately 12 hours after the dismantling of the saturated specimens from the saturation device or from the swelling pressure device. Two test series were made on unsaturated specimens which were removed from the climate chamber and sealed approximately 12h before testing in an unsaturated state.

3.7.3 Test procedure

The specimens were placed in a mechanical press and the axial compression was run at a constant deformation rate of 0.8 %/min which corresponds to 0.16 mm/min for the dimensions used. This rate was used for all tests in this study. The end plates were lubricated when placing the specimens in the press. During the tests the specimens were surrounded by a thin plastic film to minimize evaporation. After failure the water content and density were measured.

3.7.4 Test results

The saturated specimens were considered as undrained during the axial loading and development of shear failure, and no volume change was taken into account. The deviator stress q (kPa) and the strain ε (%) were derived from Equation 3-6 and Equation 3-7, respectively. However, in the series with unsaturated specimens, volume change was expected, and the deviator stress of these specimens was calculated only from the measured force (F) and original cross section area (A_0). The failure was evaluated in terms of maximum deviator stress and corresponding strain.

$$q = \frac{F}{A_0} \cdot \left(\frac{l_0 - \Delta l}{l_0} \right) \quad (3-6)$$

$$\varepsilon = \frac{\Delta l}{l_0} \quad (3-7)$$

where

F = applied vertical load (kN)

A_0 = original cross section area (m²)

l_0 = original length (m)

Δl = change in length (m)

The results were corrected for initial problems with the contact surface by decreasing the strain with the intercept on the x-axis of the tangent to the stress-strain curve taken at a stress of 500 kPa.

For comparison the test results are shown with a reference lines of saturated MX80 from Dueck et al. (2011a) or with a model introduced by B rgesson et al. (1995).

3.7.5 Test series

A total of over 320 specimens have been tested in the project. The number of unconfined compression tests run on specimens with the different types of preparation are given in Table 3-7. The table is focused on the number of each type of preparation and the denomination of each test series is given in Appendix 1.

Table 3-7. Number of unconfined compression tests on specimens with different preparations. The different materials and the different types of preparation are given. The different methods of ion-exchange are given according to Table 3-1 as ie A, ie B, ie C, ie D or ref (no ion-exchange). The special stress paths refers to Table 3-3 and if no paths is given there was a requirement of no or small volume change during saturation.

Study	Material	Preparation of specimens						
		Method of ion-exchange or ref material ¹	Excess salt added	Special stress paths	Exposure to heat, T_{max}	Fluid used ⁴	Stresses measured	Number of specimens tested
TMS1	Calcigel	ref				DI-water		16
	Dep Ca-N	ref				DI-water		6
	Dep Ca-N	ie B				DI-water	Yes ²	6
	FEBEX	ref				DI-water		6
	FEBEX	ie B				DI-water	Yes ²	6
	GMZ	ref				DI-water		6
	GMZ	ie B				DI-water	Yes ²	16
TMS2	Asha	ref				DI-water	Yes ³	5
	Asha	ie C				1M CaCl ₂		5
	Ikosorb	ref				DI-water	Yes ³	6
	Ikosorb	ie C				1M CaCl ₂		6
	Kunigel	ref				DI-water	Yes ³	7
	Kunigel	ie C				1M CaCl ₂		5
TMS3	MX-80	ref				DI-water		4
	MX-80	ie A				1M CaCl ₂		3
	MX-80	ie B				DI-water		3
	MX-80	ie C				1M CaCl ₂		4
	MX-80	ie D				DI-water	Yes ³	10
	Ikosorb	ref				DI-water		3
	Ikosorb	ie A				1M CaCl ₂		3
	Ikosorb	ie B				DI-water		3
	Ikosorb	ie C				1M CaCl ₂		3
	Ikosorb	ie D				DI-water	Yes ³	8
	GMZ	ref				DI-water		3
	GMZ	ie A				1M CaCl ₂		3
	GMZ	ie B				DI-water		3
	GMZ	ie C				1M CaCl ₂		3
	GMZ	ie D				DI-water	Yes ³	8
SC-OE	MX-80	ref		Constant axial stress		DI-water	Yes	6
	MX-80	ref		No volume change		DI-water		2
	MX-80	ref		Large swelling		DI-water		16
	MX-80	ref		Water pressure		DI-water		6
	MX-80	ref		Comp. to saturation		DI-water		10

Study	Material	Preparation of specimens						
		Method of ion-exchange or ref material ¹	Excess salt added	Special stress paths	Exposure to heat, T_{max}	Fluid used ⁴	Stresses measured	Number of specimens tested
DS1	MX-80	ie C, ie A			90 °C	1M CaCl ₂	Yes	6
	MX-80	ie C			90 °C	1M CaCl ₂ or 1M NaCl		6
	MX-80	ie A	CaCl ₂		90 °C	1M CaCl ₂		20
	MX-80		CaO or Ca(OH) ₂			DI water		10
	MX-80		CaO			DI water		10
DS2	MX-80	ie D				DI water	Yes	3
	MX-80	ie B				DI water	Yes	3
	MX-80					75 % or 85 % ⁵		16
	MX-80		CaCl ₂			75 % or 85 % ⁵		20
	MX-80	ie B	CaCl ₂			DI water		6
	MX-80	ref				DI water		10
UCT	MX-80			Water pressure	240 °C	DI water		2
	Asha505			Water pressure	240 °C	DI water		2
	Calcigel			Water pressure	240 °C	DI water		2
	MX-80, Asha505, Calcigel				240 °C	DI water		6
	MX-80, Asha505, Calcigel	ref				DI water		4

¹ The different methods of ion-exchange ie A to ie D which were made according to Table 3-1. Reference, ref, material was also used for some tests.

² These additional specimens were used for measurements of swelling pressure only.

³ Measured on some of the specimens.

⁴ The final fluid before dismantling.

⁵ For unsaturated specimens the relative humidity *RH* is given.

4 Results

4.1 General

This project was carried out in a number of limited studies (TMS1, TMS2 and TMS3, SC-OE, DS1, DS2 and UCT) mentioned in Section 3.7.5 (and in Table A1-4, Appendix 1). Below the results from each of these are presented separately. In addition to the results presented, additional details are given in Appendix 2-8. In Table 4-1 the materials used in this project are mentioned with particle densities and liquid limits. The particle densities (with references) are those used for the calculation of degree of saturation and the liquid limits were determined within this project.

The main part of the specimens was sheared after saturation and deviations from this is clearly mentioned, i.e. when considering the two unsaturated test series (in the study DS2).

In sections 4.2–4.8, which describe results from tests on different materials, different colours are used for the different materials. The colours lilac, pink, brown, grey, green, red, yellow and blue denote the materials Calcigel, Deponit Ca-N, Febex, GMX, Asha505, Ikosorb, Kunigel and MX-80.

Table 4-1. The materials used in this project with particle density (from different references) and liquid limits determined in the project. The seven parts (TMS1, TMS2, TMS3, SC-OE, DS1-2 and UCT) are also mentioned.

Material	Particle density ρ_s , kg/m ³	Liquid limit w_L , %	Part of the project (study)	Particle density presented by
Asha505	2869	181	TMS2	Svensson et al. (2011)
Calcigel	2695	117	TMS1	Svensson et al. (2011)
Deponit Ca-N	2750	157	TMS1	Karlund et al. (2006)
Febex	2735	143	TMS1	Svensson et al. (2011)
GMZ	2713	287	TMS, TMS3	This project
Ikosorb	2740	263	TMS2, TMS3	Svensson et al. (2011)
Kunigel	2681	461	TMS2	Svensson et al. (2011)
MX-80	2780	488 ¹	TMS3, SC-OE, DS1-2, UCT	Karlund et al. (2006)

¹ The value was already presented by Dueck et al. (2018).

4.2 Test series TMS1

4.2.1 General

In the first study TMS1 the materials Calcigel, Deponit Ca-N, Febex and GMZ were tested in nine test series. In addition to the tests of the original materials (reference samples) tests were also made on ion-exchanged specimens and two additional series were run to study the repeatability. Samples of Deponit Ca-N, Febex and GMZ were ion-exchanged and the methodology used in these test series was the methodology B (ie B) where the powder was ion-exchanged and the excess salt washed out, see Section 3.6.2.

4.2.2 Unconfined compression tests

In Figure 4-1 to Figure 4-4 the results are presented in diagrams with maximum deviator stress and corresponding strain as a function of dry density. In the diagrams the colours lilac, pink, brown and grey denote the materials Calcigel, Deponit Ca-N, Febex and GMX. Black marker lines are used for the ion-exchanged specimens (with labels ie B). More details are given in Appendix 2.

4.2.3 Swelling pressure tests

Swelling pressure was measured on ion-exchanged material of Deponit Ca-N, Febex and GMZ and the results are shown in Figure 4-5. The swelling pressure measurements were made on separate specimens not further used for unconfined compression tests.

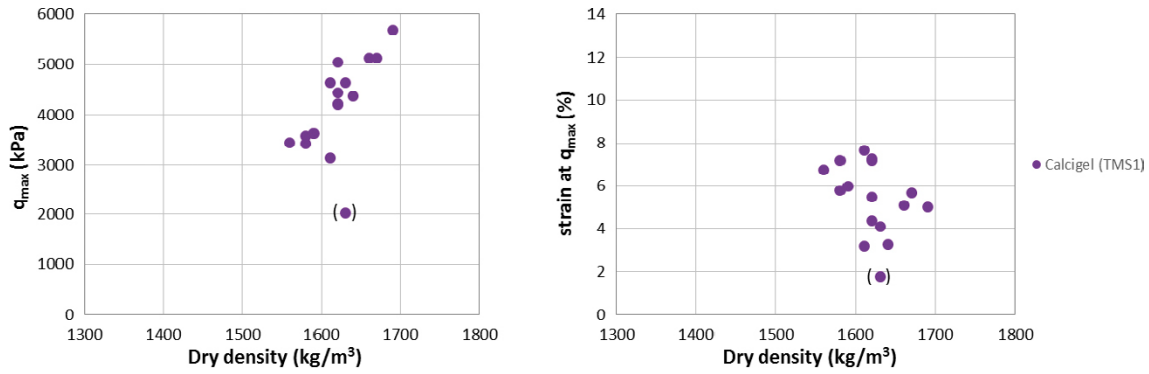


Figure 4-1. Maximum deviator stress and corresponding strain are given as a function of dry density. Results from unconfined compression tests on specimens of Calcigel. The result put in brackets represents a deviating failure surface in that only the outer surface was involved in the rupture.

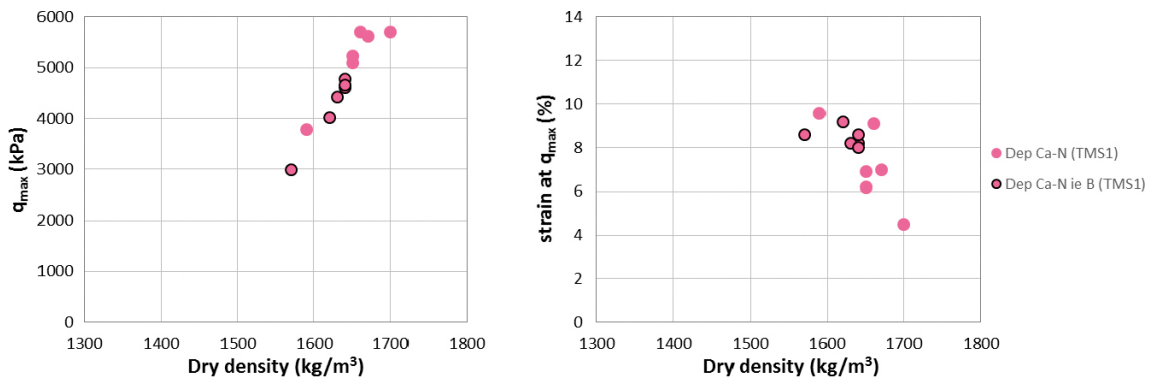


Figure 4-2. Maximum deviator stress and corresponding strain are given as a function of dry density. Results from unconfined compression tests on specimens of Deponit Ca-N (without marker lines) and on specimens of ion-exchanged Ca-dominated material (with black marker lines and the label Deponit Ca-N ie B) are shown.

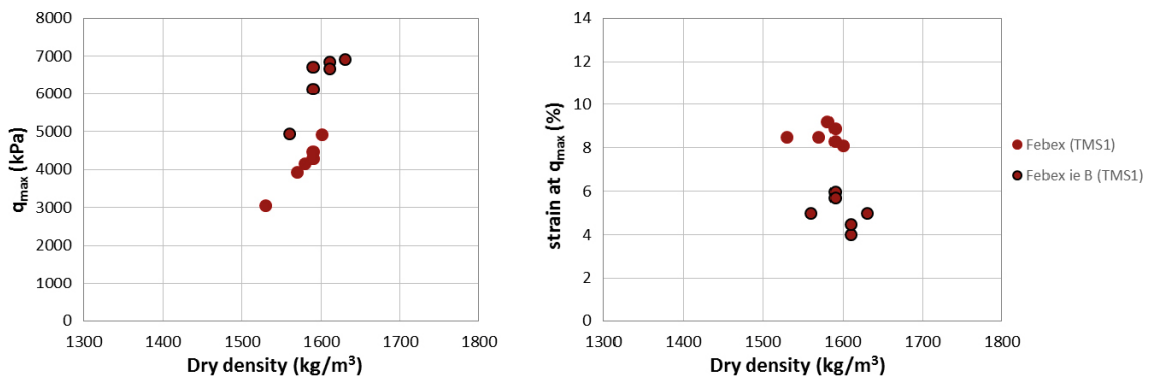


Figure 4-3. Maximum deviator stress and corresponding strain are given as a function of dry density. Results from unconfined compression tests on specimens of Febex (without marker lines) and on specimens of ion-exchanged Ca-dominated material (with black marker lines and the label Febex ie B) are shown.

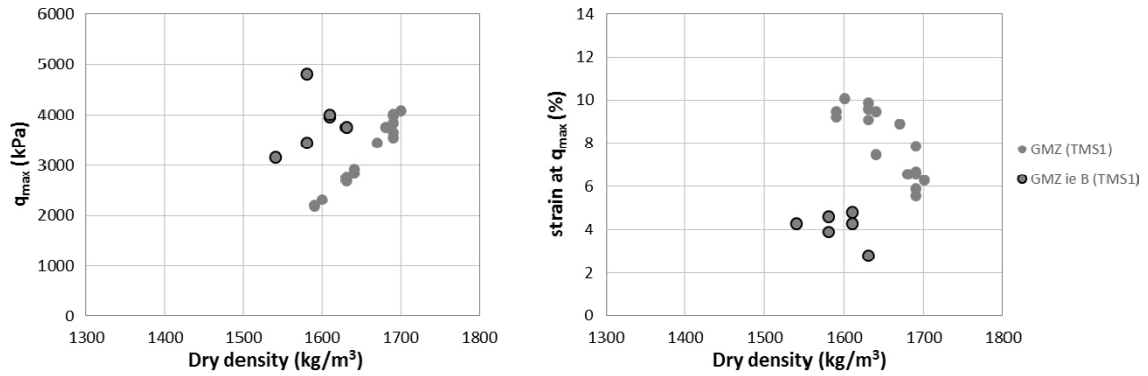


Figure 4-4. Maximum deviator stress and corresponding strain are given as a function of dry density. Results from unconfined compression tests on specimens of GMZ (without marker lines) and on specimens of ion-exchanged Ca-dominated material (with black marker lines and the label GMZ ie B) are shown.

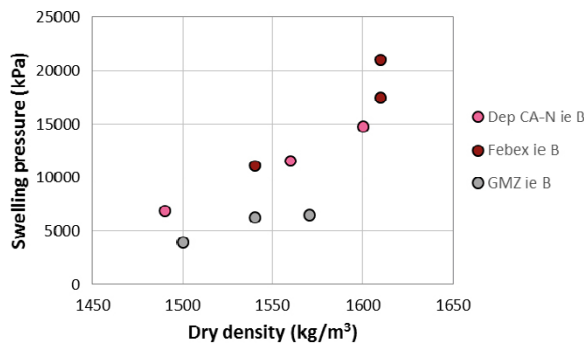


Figure 4-5. Results from swelling pressure measurements in the series TMS1.

4.2.4 Comments

Although the swelling pressure was not measured directly on the ion-exchanged specimens used for the unconfined compression tests the actual swelling pressure can be estimated from the measurements made cf. Figure 4-5. In Figure 4-6 the maximum deviator stress (left) and the estimated swelling pressure (right) are shown as a function of dry density. None of the specimens were used for measurements of both swelling pressure and unconfined compressive strength and the estimations of swelling pressure at the actual dry densities were made according to the equations given in Appendix 1 based on measurements within this project (Deponit Ca-N ie B, Febex ie B, GMZ ie B and GMZ) and based on results from other projects (Deponit Ca-N and Febex).

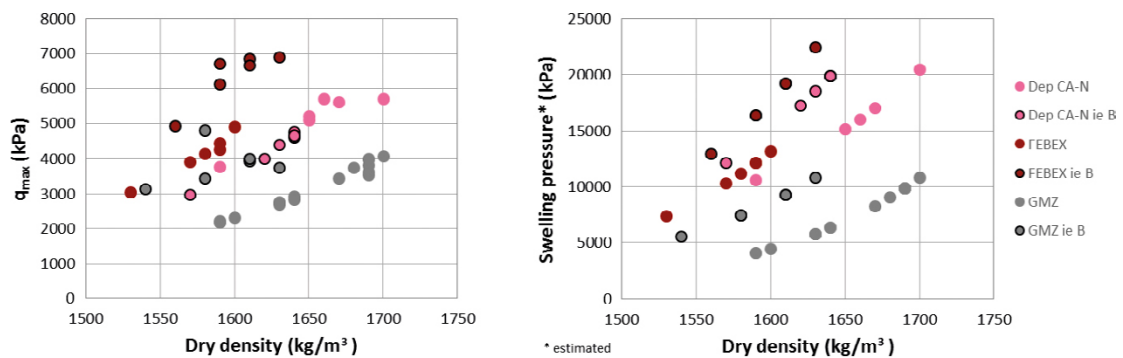


Figure 4-6. Unconfined compressive strength (left) and estimated swelling pressure (right) as a function of dry density in test series in the study TMS1.

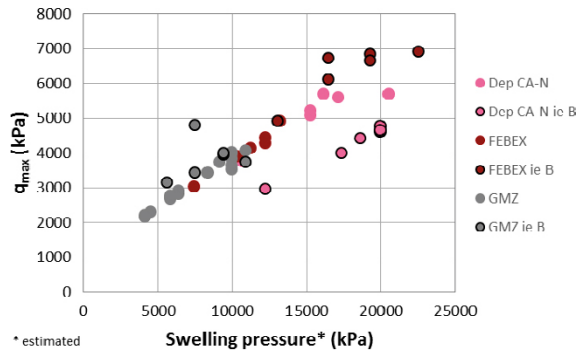


Figure 4-7. Unconfined compressive strength as a function of estimated swelling pressures.

4.2.5 Concluding remarks

In the study TMS1 the unconfined compression tests were run on four materials (Calcigel, Deponit Ca-N, Febex and GMZ). Tests were also run on ion-exchanged Ca-dominated samples of three of the materials (Deponit Ca-N, Febex and GMZ). Some extra series on two of the materials (Calcigel, GMZ) were made to estimate the variability of the test type. Swelling pressure was determined separately on ion-exchanged Ca-dominated specimens of Deponit Ca-N, Febex and GMZ.

In this part of the project the ion-exchange to Ca²⁺ dominated materials were made on powder samples with excess salt washed out (methodology ie B). From the results the observations below could be made.

Compared to each reference material at the same dry density the results from the Ca²⁺ dominated materials showed

- a maximum deviator stress that was
 - higher in Febex and GMZ,
 - approximately the same in Deponit Ca-N,
- and a corresponding strain that was
 - lower in Febex and GMZ,
 - approximately the same in Deponit Ca-N.

In addition, the following general observations have also been made:

- The repeatability was tested with two extra test series and it was found that the scatter was small in the determined maximum deviator stress and corresponding strain as a function of dry density.
- The degree of saturation for a majority of the specimens were between 97 and 103 %. However, Calcigel deviates from this which indicates that a slightly different, higher, value of the particle density is valid for this material; 2 740 kg/m³ instead of 2 695 kg/m³ could be used to get 100 % saturation.
- It was noticed that deviating values of the liquid limit of Febex were determined within this project compared to previous published values.

Regarding the relations between maximum deviator stress and estimated swelling pressure:

- It can be observed that the results of reference materials and of the ion-exchanged materials (ie B) of Deponit Ca-N, Febex and GMZ follow the same trend, however, with some scatter and some deviation from the ion-exchanged material of Deponit Ca-N.

4.3 Test series TMS2

4.3.1 General

In the second series TMS2 the materials Asha505, Ikosorb and Kunigel were tested in two types of series; series with swelling pressure measurements during saturation and series without swelling pressure measurement where three to ten specimens were prepared at a time. Samples of Asha505, Ikosorb and Kunigel were ion-exchanged and the methodology used in these test series was the methodology C (ie C) where the ion-exchange was made on compacted specimens at confined conditions and with excess salt left in the specimens, see Section 3.6.2. In addition to the results presented below additional results are shown in Appendix 3.

4.3.2 Unconfined compression tests

In Figure 4-8 to Figure 4-10 the results are presented in diagrams with maximum deviator stress and corresponding strain as a function of dry density. In the diagrams the colours green, red and yellow denote the materials Asha505, Ikosorb and Kunigel, respectively. Black marker lines are used for the ion-exchanged specimens (with labels ie C).

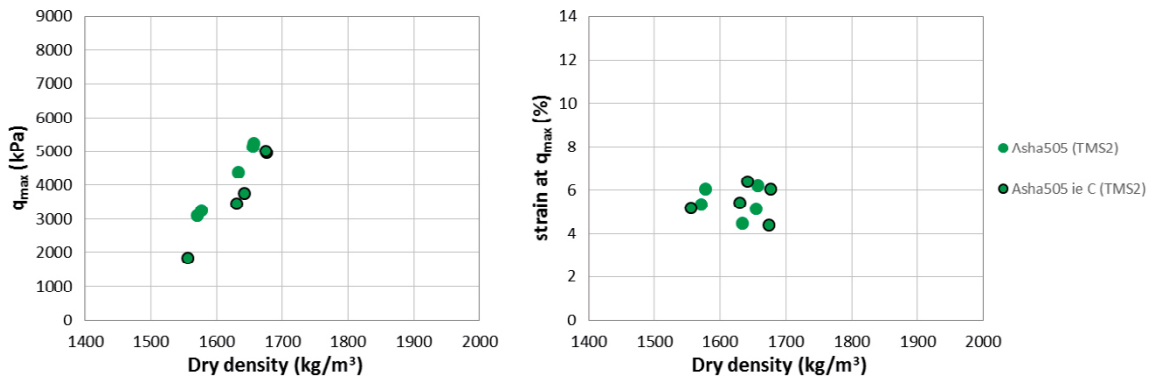


Figure 4-8. Maximum deviator stress and corresponding strain are given as a function of dry density. Results from unconfined compression tests on specimens of Asha505 (TMS2) and on ion-exchanged specimens Asha505 ie C (TMS2).

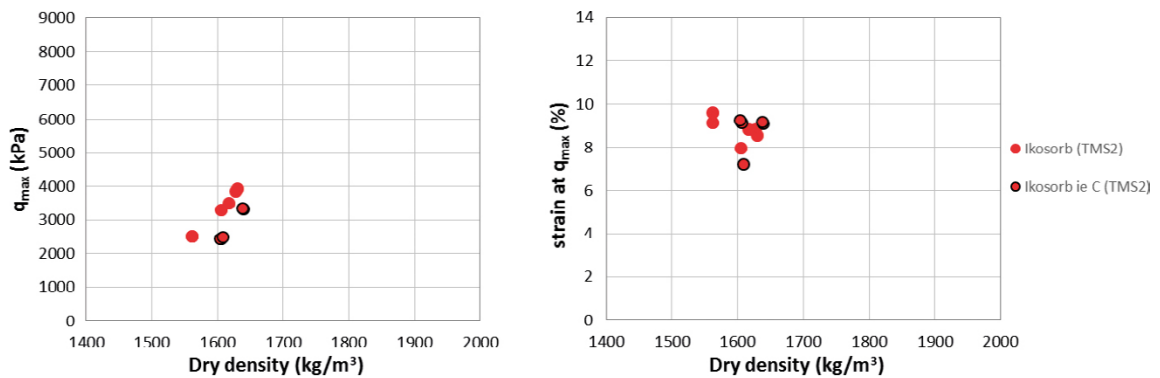


Figure 4-9. Maximum deviator stress and corresponding strain are given as a function of dry density. Results from unconfined compression tests on specimens of Ikosorb (TMS2) and on ion-exchanged specimens Ikosorb ie C (TMS2).

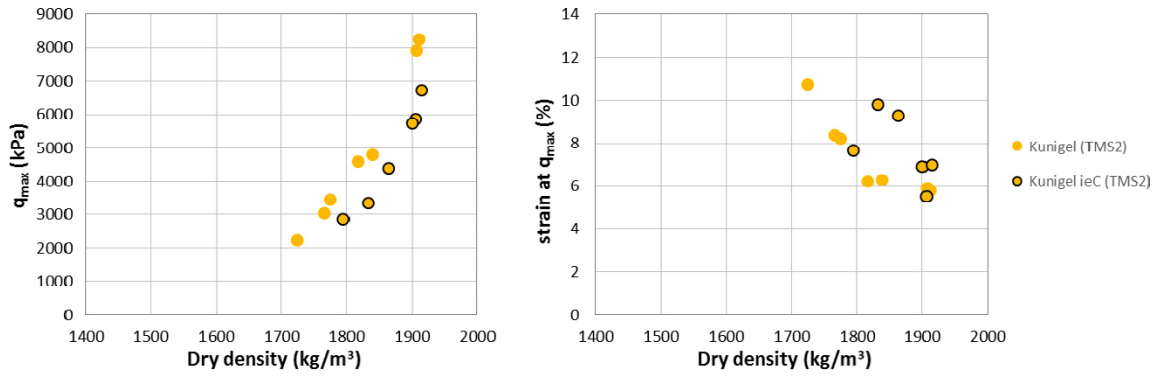


Figure 4-10. Maximum deviator stress and corresponding strain are given as a function of dry density. Results from unconfined compression tests on specimens of Kunigel (TMS2) and on ion-exchanged specimens Kunigel ie C (TMS2).

4.3.3 Swelling pressure tests

In Figure 4-11 the results from swelling pressure measurements on samples of the reference materials of Asha505, Ikosorb and Kunigel are shown. No measurement was made on ion-exchanged specimens. In Figure 4-12 the measured maximum deviator stress is plotted as a function of the swelling pressures measured on the same specimens during preparation.

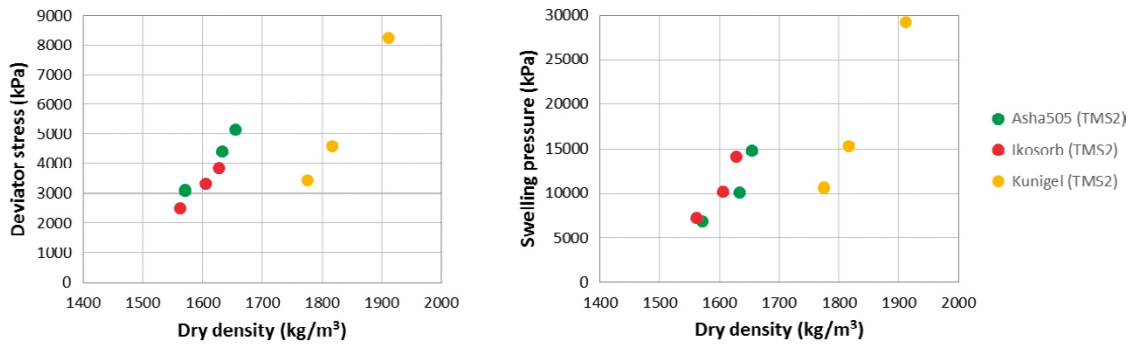


Figure 4-11. Results from unconfined compression tests (left) and swelling pressure measurements (right) made on the same specimens. The results to the left were shown in Figure 4-8, Figure 4-9 and Figure 4-10.

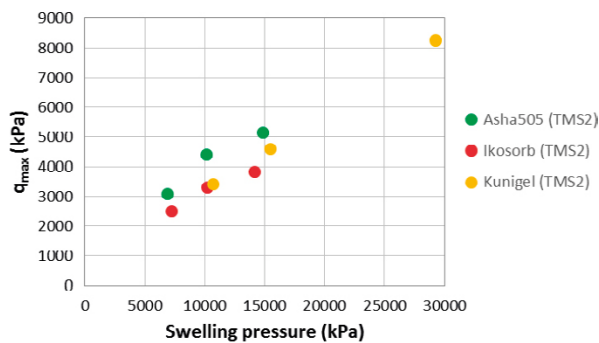


Figure 4-12. Measured deviator stress as a function of swelling pressure measured before the unconfined compression test but on the same specimens, see Figure 4-11.

4.3.4 Comments

After ion-exchange with the methodology ie C the specimens contained excess salt in the interlayer water from the final equilibrium with 1M CaCl₂ before the dismantling. In an attempt to adjust the final dry density for this, the salt concentration of the interlayer water of the specimens was estimated to be the same as in the external solution and from the mass and the water content of the actual specimen the mass of the dissolved salt was calculated. The estimated mass of the dissolved salt was then removed from the total dry mass of the specimen and the dry density of the actual specimen was re-calculated, see Figure 4-13. Further details are given in Appendix 1.

4.3.5 Concluding remarks

In study TMS2 the unconfined compression tests were run on three materials (Asha505, Ikosorb and Kunigel). Tests were also run on ion-exchanged Ca-dominated samples of the three materials. Swelling pressure was determined on the specimens of the reference materials which were also used for unconfined compression tests. In this part of the project the ion-exchange to get Ca²⁺ dominated materials were made on compacted specimens at confined conditions with excess salt left (methodology ie C). From the corrected results (the dry densities corrected for excess salt) the observations below could be made.

Compared to each reference material and as a function of dry density the results from the Ca²⁺ dominated materials showed

- a maximum deviator stress that was
 - approximately the same in Asha505, Ikosorb and Kunigel,
- and a corresponding strain that was
 - approximately the same in Asha505, Ikosorb and Kunigel.

In addition, the following was observed from the test results:

- The degree of saturation was for all specimens between 97 and 103 % calculated without correcting for excess salt.
- Some deviating value was seen in the liquid limit of Asha505 determined within this project compared to previous published values, see Table 2-1 and Table 4-1. Due to shortage of material further tests were not possible to do.

Regarding the relation between maximum deviator stress and swelling pressure:

- The relationship is almost the same for the three reference materials although the relationship deviates when the maximum deviator stress is plotted as a function of dry density, especially regarding Kunigel.

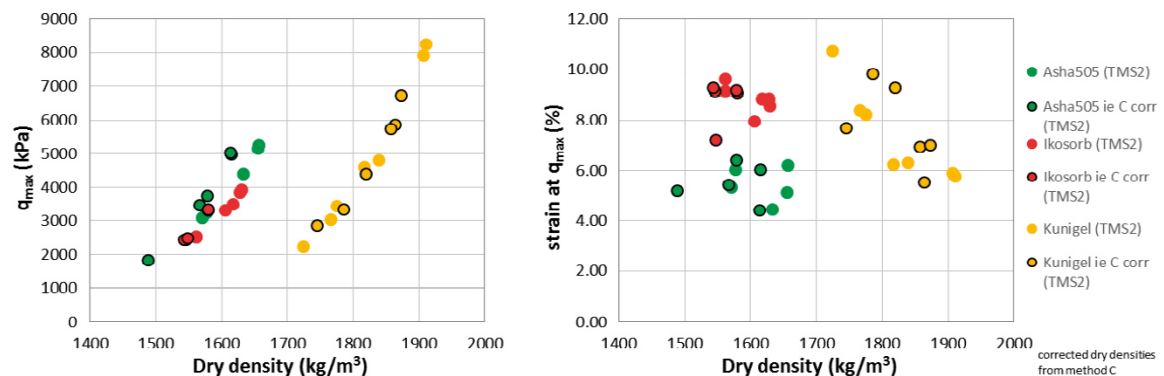


Figure 4-13. Unconfined compressive strength from tests in series TMS2; Asha, Ikosorb, Kunigel (Figure 4-8, Figure 4-9 and Figure 4-10). Dry density corrected for excess salt in specimens, ion-exchanged with the method ieC.

4.4 Test series TMS3

4.4.1 General

In the third series TMS3 series the materials MX-80, Ikosorb and GMZ were tested. The materials were ion-exchanged with all four methodologies A–D (ie A to ie D), see Section 3.6.2. Swelling pressure was measured during preparation of some of the specimen ion-exchange according to methodology D (ie D). Detailed results are shown in Appendix 4.

4.4.2 Unconfined compression tests

The results are shown in Figure 4-14 to Figure 4-16. In the diagrams the colours (blue, red, grey) denote specimens of the different materials (MX-80, Ikosorb, GMZ). In the diagrams the markers (circle, triangle) indicate on which type of sample the ion-exchange was made (powder sample, confined specimen) and the marker lines (no lines, black marker lines) indicate the presence or not of excess salt in the specimens at testing (excess salt still present, excess salt washed out). Diamonds are used for the not ion-exchanged reference specimens. The markers are tabulated in Table 4-2.

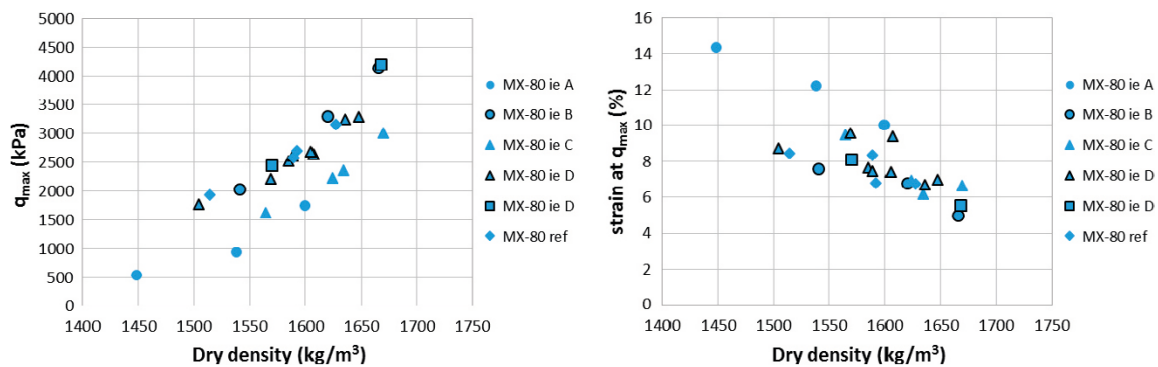


Figure 4-14. Results from unconfined compression tests on MX-80. Maximum deviator stress (left) and corresponding strain (right) as a function of dry density.

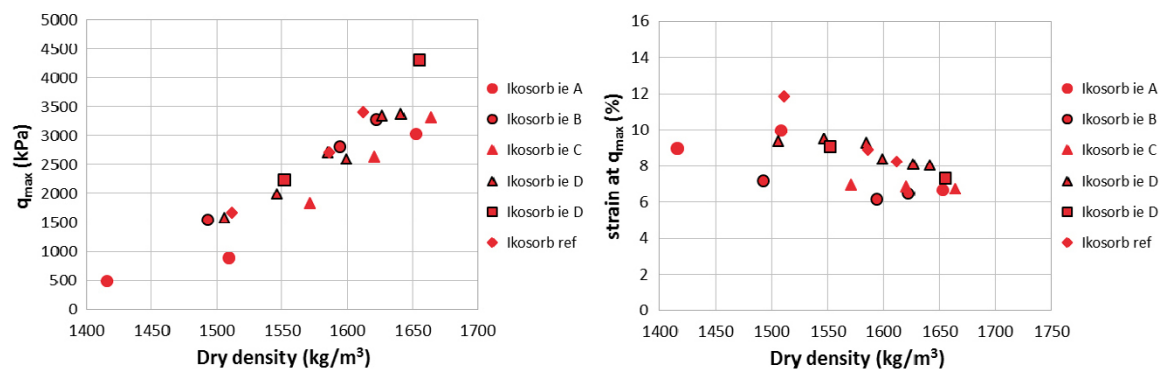


Figure 4-15. Results from unconfined compression tests on Ikosorb. Maximum deviator stress (left) and corresponding strain (right) as a function of dry density.

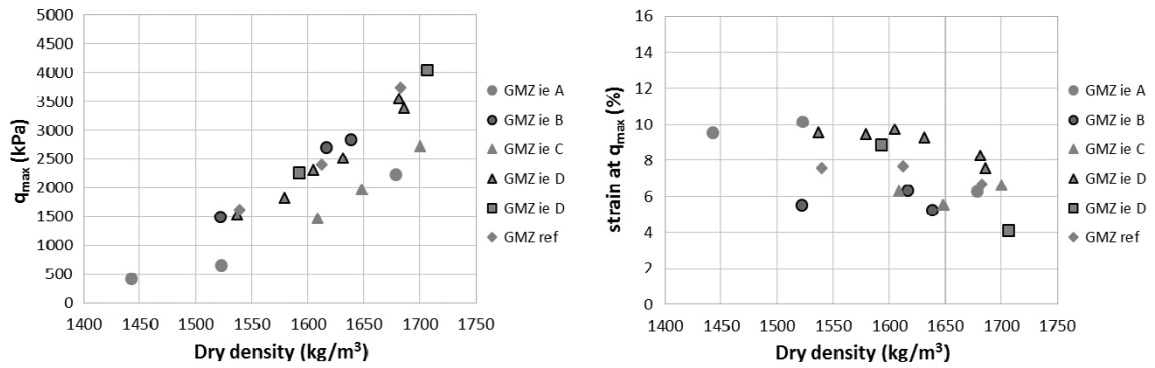


Figure 4-16. Results from unconfined compression tests on GMZ. Maximum deviator stress (left) and corresponding strain (right) as a function of dry density.

Table 4-2. Markers and marker lines used in the diagrams denoting different types of ion-exchange.

Type of specimens and ion-exchange	Type of ion-exchange	Marker used	Marker lines used
Ion-exchange of powder sample with excess salt left	A	circle	-
Ion-exchange of powder sample and excess salt washed out	B	circle	marker line
Ion-exchange of confined spec. with excess salt left	C	triangle	-
Ion-exchange of confined spec. and excess salt washed out	D	triangle	marker line
Ion-exchange of confined spec. with excess salt washed out and with measurement of P_s	D	square	marker line
Reference specimens	no ion-exchange	diamond	-

4.4.3 Swelling pressure tests

In Figure 4-17 the measured swelling pressure at different steps of the ion-exchange (ie D) are shown for 6 specimens. The three values resulting from each specimen represent the initial saturation with DI-water, the equilibrium with 1M CaCl_2 -solution, and finally the equilibrium with DI-water after the ion-exchange. In Figure 4-18 the maximum deviator stress has been plotted as a function of the final swelling pressure measured at equilibrium with DI-water after the ion-exchange but before the unconfined compression tests.

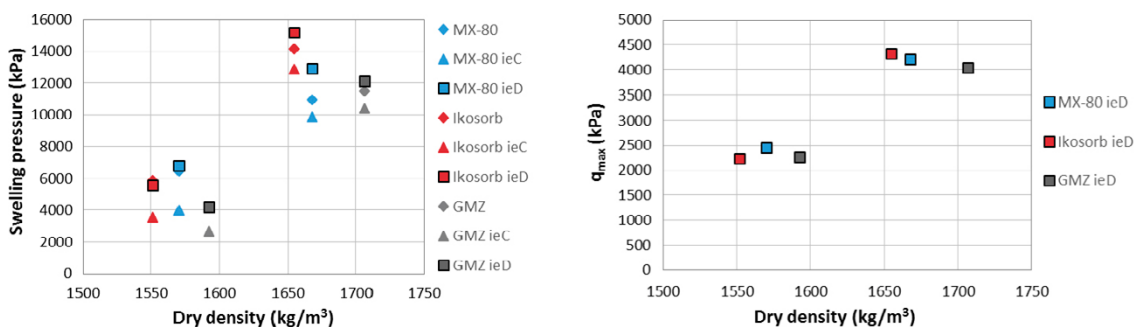


Figure 4-17. Measured swelling pressure (left) and maximum deviator stress (right) as a function of dry density of 6 specimens. The swelling pressure was measured at different stages of the ion-exchange (ie D); the initial saturation with DI-water (diamond), the equilibrium with 1M CaCl_2 -solution (triangle) and the final equilibrium with DI-water after the ion-exchange (square). After dismantling the maximum deviator stress was measured on the same specimens, the results were also shown in Figure 4-14, Figure 4-15 and Figure 4-16.

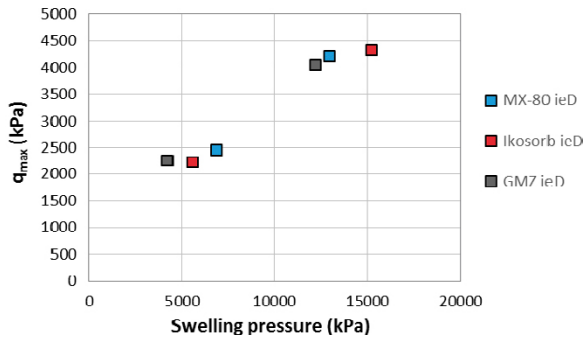


Figure 4-18. Measured deviator stress on ion-exchanged specimens (ie D) as a function of swelling pressure measured before the unconfined compression test but on the same specimens, see Figure 4-17.

4.4.4 Comments

After ion-exchange with the methodology A and C the specimens contained excess salt in the interlayer water from the final equilibrium with 1M CaCl₂ before the dismantling. In an attempt to adjust the final dry density for this, the salt concentration of the interlayer water of the specimens was estimated to be the same as in the external solution. From the mass and the water content of the actual specimen the mass of the dissolved salt was calculated. The estimated mass of the dissolved salt was then removed from the total dry mass of the specimen and the dry density of the actual specimen was re-calculated. The results from Figure 4-14, Figure 4-15 and Figure 4-16 are re-plotted in Figure 4-19, Figure 4-20 and Figure 4-21 with adjusted dry densities of the specimens ion-exchanged according to the methodologies A and C. Further details are given in Appendix 1.

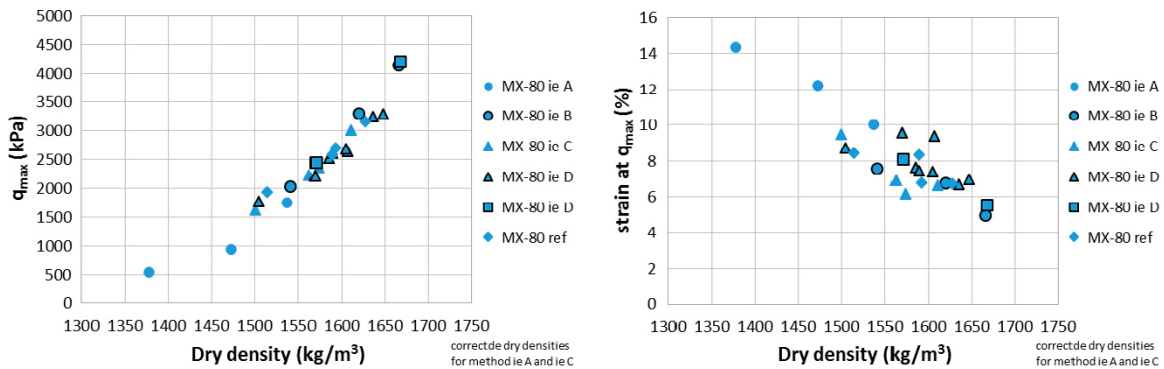


Figure 4-19. Unconfined compressive strength from tests on MX-80 with the dry density adjusted for excess salt after ion-exchange with the methodologies A and C (cf. Figure 4-14).

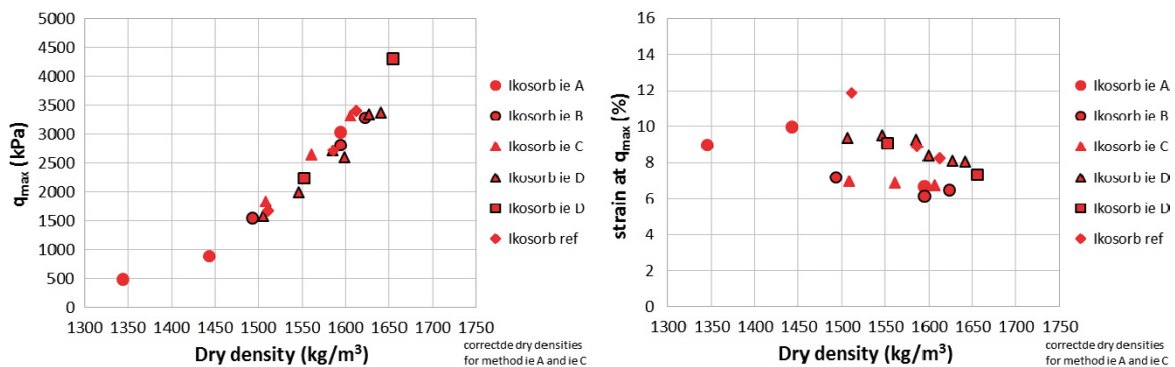


Figure 4-20. Unconfined compressive strength from tests on Ikosorb with the dry density adjusted for excess salt after ion-exchange with the methodologies A and C (cf. Figure 4-15).

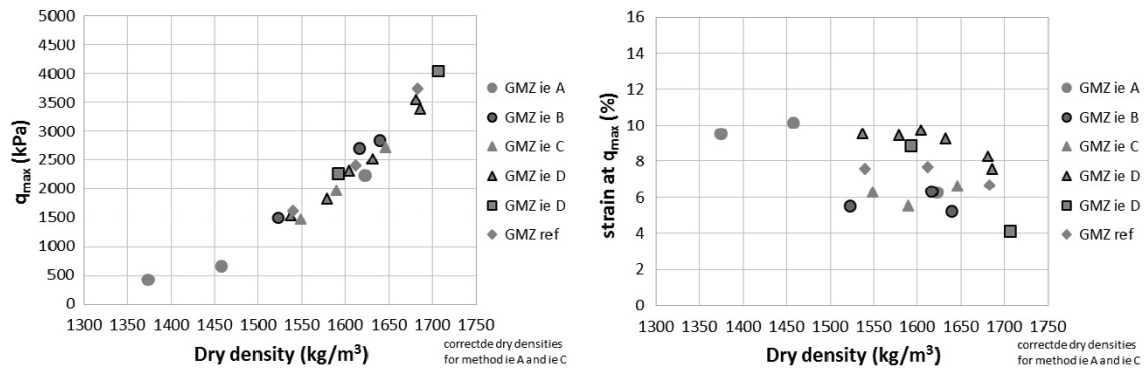


Figure 4-21. Unconfined compressive strength from tests on GMZ with the dry density adjusted for excess salt after ion-exchange with the methodologies A and C (cf. Figure 4-16).

The results from the different methodologies of ion-exchange and with the dry density adjusted for any excess salt show that the unconfined compressive strength agrees well with the results from the reference specimens, for all three materials.

The effect of ion-exchange should not depend on the methodology, i.e. if the ion-exchange is made on powder samples or on compacted specimens. This is also the case for the maximum deviator stress. However, regarding the strain at failure a slight difference can be noticed in that lower strain at failure was observed if the ion-exchange was made on powder (circle with black marker line) compared to if the ion-exchanged was made on the compacted specimens, at least regarding Ikosorb and GMZ (cf. Figure 4-20 and Figure 4-21).

From the measured swelling pressure in Figure 4-17 estimations of swelling pressure can be made for all specimens used for the unconfined compression tests. In Figure 4-22, Figure 4-23, Figure 4-24 the deviator stress is plotted as a function of swelling pressure (left) and the used estimated or measured swelling pressure is plotted as a function of dry density (right). Two points of each material represent measured values (squares) of both q_{max} and swelling pressure from the same specimen.

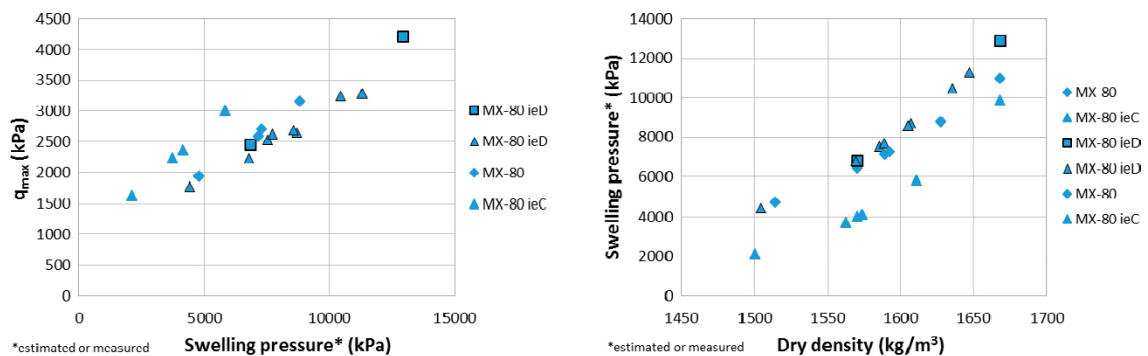


Figure 4-22. MX-80, deviator stress as a function of estimated swelling pressure (left) and the estimated swelling pressure as a function of dry density (right).

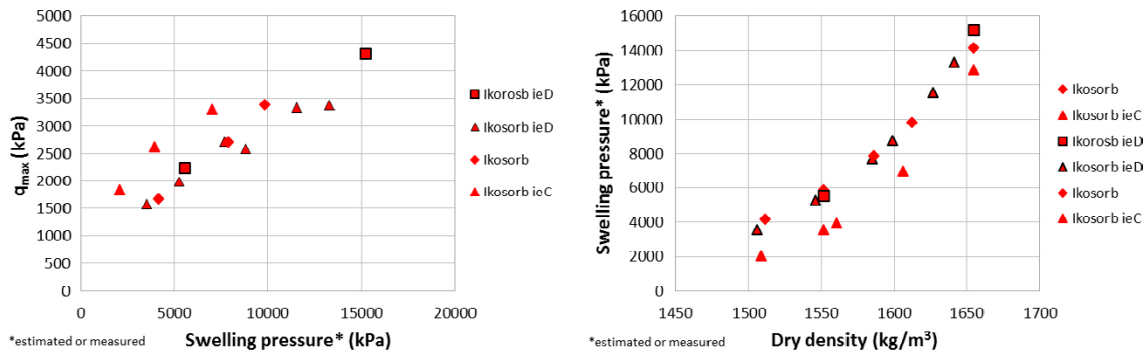


Figure 4-23. Ikosorb, deviator stress as a function of estimated swelling pressure (left) and the estimated swelling pressure as a function of dry density (right).

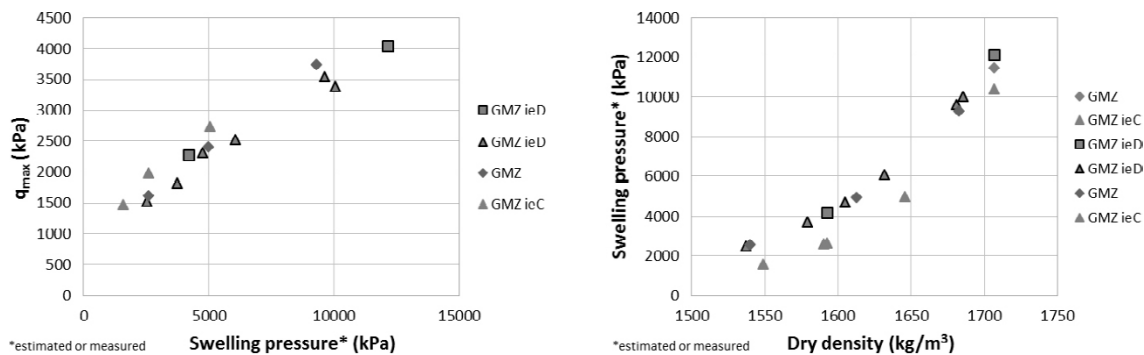


Figure 4-24. GMZ, deviator stress as a function of estimated swelling pressure (left) and the estimated swelling pressure as a function of dry density (right).

From the results in Figure 4-22, Figure 4-23 and Figure 4-24 it can be seen that specimens ion-exchanged with the excess salt left (triangles without marker lines) show q_{max} (maximum deviator stress) above the references when plotted as a function of swelling pressure. However, when the resulting q_{max} is related to the dry density no deviation is seen, c.f. Figure 4-19, Figure 4-20 and Figure 4-21.

4.4.5 Concluding remarks

The test series on MX-80, Ikosorb and GMZ resulted in the following observations on the unconfined compressive strength and the corresponding strain regarding the effects of an ion-exchange (where the exchangeable ions were exchanged to Ca^{2+} -ions).

Regarding the effects of the different methodologies used for the ion-exchange the results showed that

- the dry density has to be corrected for excess salt after the ion-exchange,
- the unconfined compressive strength seemed to be independent of the methodology used for the ion-exchange, however, a scatter was observed,
- there was a scatter in the strain at failure but also a tendency that lower strain was observed on specimens, ion-exchanged as powder compared to those ion-exchange as confined specimens.

Plotted as a function of dry density, the ion-exchanged specimens (without excess salt) showed, in comparison with the references,

- no large deviations in the unconfined compressive strength,
- a scatter in strain at failure but also a tendency that the materials MX-80 and GMZ followed the references while Ikosorb showed lower strain than the reference.

In addition,

- the degree of saturation was between 97 % and 103 % evaluated on specimens without excess salt.

Regarding the relationship between maximum deviator stress and swelling pressure

- approximately the same trend is followed by the three materials tested (MX-80, Ikosorb and GMZ) both regarding the original material and the ion-exchanged material without excess salt.
- somewhat higher deviator stress was observed from specimens containing excess salt even though this was not seen when plotted as a function of corrected dry density.

4.5 Test series SC-OE

4.5.1 General

In the fourth series SC-OE the material MX-80 was used and no ion-exchange was made. Different types of preparation described in Section 3.6.3 were used to introduce different stress paths during saturation before the unconfined compression tests. The results are presented in separate sections, below. Detailed results are shown in Appendix 5.

The results are presented together with a model of MX-80 (label TR-95-20) calculated from Equation 4-1 and Equation 4-2 originally presented by Börgesson et al. (1995) and based on results from triaxial tests. The reference line relates to the average stress p (kPa), the deviator stress q (kPa) and the void ratio e , which in the diagrams below has been exchanged for dry density (according to Section 3.2).

$$e = 1.1 \cdot (p/1000)^{-0.19} \quad (4-1)$$

$$q = 500 \cdot (p/1000)^{0.77} \quad (4-2)$$

4.5.2 Series with constant axial stress and no radial deformation

Data from the preparation (stress as a function of dry density) of specimens exposed to constant axial stress and no radial deformation is shown in Figure 4-25. The colours (yellow, red, purple) represent the constant axial stresses aimed at (1 750 kPa, 3 500 kPa, 7 000 kPa) and the markers (diamond, triangle) represent the type of volume change during the preparation (consolidation, swelling). The bars show the measured axial and radial stresses. At the final stress and dry density the volume changes were 3 %, 10 %, and 19 % for the specimens that swelled and -5 %, -10 % and -15 %, for the consolidated specimens, see also Appendix 5.

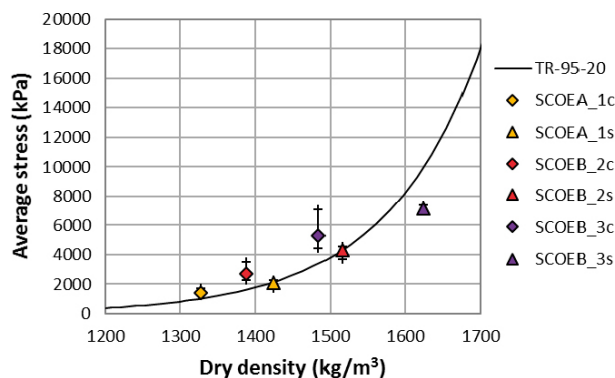


Figure 4-25. Measured average stress as a function of dry density after preparation involving constant axial stress before the unconfined compression tests. The solid line represents the model of strength presented by Börgesson et al. (1995).

The results from the unconfined compression tests on the specimens in this series are presented in Figure 4-26. The results are presented with the same colours and markers as in Figure 4-25. Regarding the deviator stress the results follow the model from Börgesson et al. (1985) and regarding the strain slightly larger strain is seen on specimens that swelled during preparation compared to those that consolidated.

In Figure 4-27 the maximum deviator stress from the unconfined compression tests is shown as a function of the average stress measured during preparation.

4.5.3 Series with constant volume conditions

Only two specimens were prepared with constant or almost constant volume conditions. The results from the preparation, i.e. swelling pressure measurements before shear, are shown in Figure 4-28 where the bars show the axially and radially measured stresses, respectively. The results from the unconfined compression tests are presented in Figure 4-29 and the agreement with the model (Börgesson et al. 1995) is good. The increase in strain in Figure 4-29 (to the right) should be regarded as a measure of the scatter in these results due to the ductile behaviour of the specimens not showing any drop in deviator stress at failure, see Appendix 5.

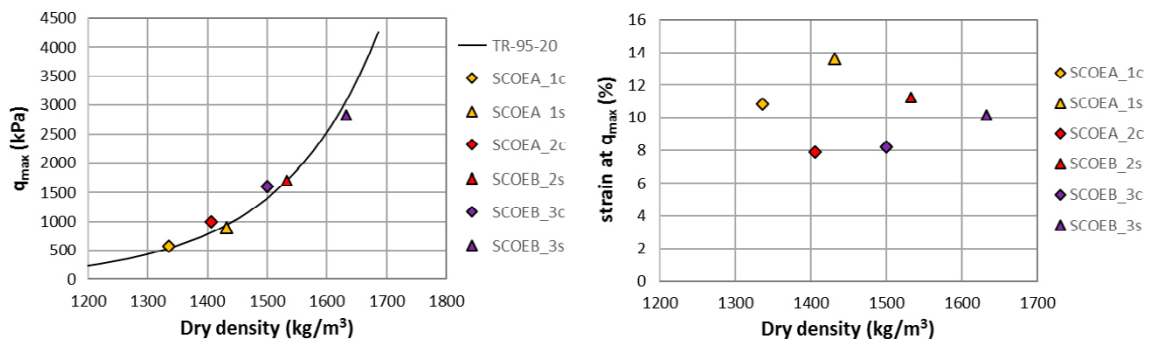


Figure 4-26. Results from unconfined compression tests on specimens prepared by saturation at constant axial stress and no radial deformation. Maximum deviator stress and corresponding strain are given as a function of dry density. The solid line represents the model of strength presented by Börgesson et al. (1995).

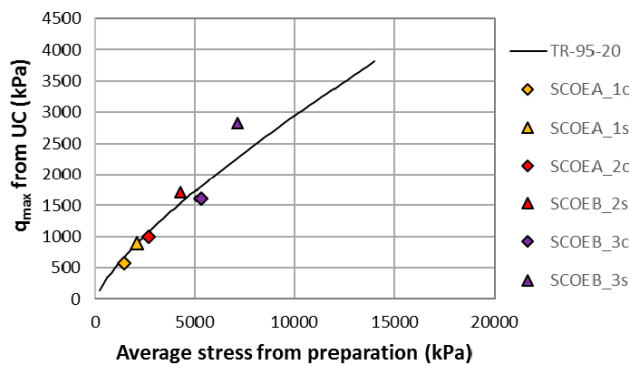


Figure 4-27. Resulting maximum deviator stress q_{max} from the unconfined compression tests plotted as a function of average stress from the preparation. The solid line represents Equation 4-2 originally presented by Börgesson et al. (1995).

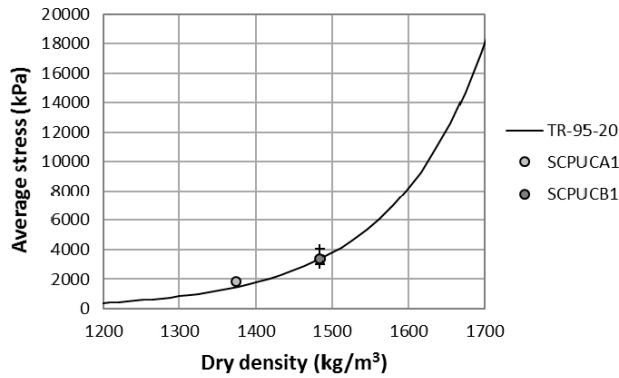


Figure 4-28. Measured average stresses as a function of dry density after preparation, before shear, with constant volume conditions. The solid line represents the model of strength presented by Börgesson et al. (1995).

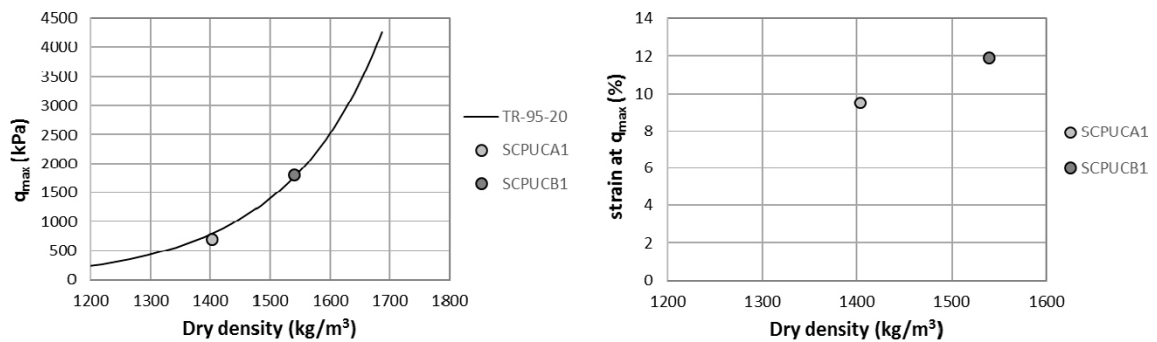


Figure 4-29. Results from unconfined compression tests on specimens prepared by saturation at constant volume conditions. Maximum deviator stress and corresponding strain are given as a function of dry density. The solid line represents the model of strength presented by Börgesson et al. (1995).

In Figure 4-30 the maximum deviator stress from the unconfined compression tests are plotted as a function of the average stress during preparation. Even though the results follow the model from TR-95-20 (Börgesson et al. 1985) in Figure 4-28 and Figure 4-29 this is not the case in Figure 4-30 due to an unexpected change in density between the preparation and the unconfined compression test. Generally, in this study the difference in dry density between the preparation and the UC-tests was usually less than 1 % but the actual specimen increased its density 4 % and it is not clear why. In Figure 4-30 the deviating density is corrected for by plotting the results from the UC-tests at an average stress corresponding to the dry density after the UC-test and calculated stress from the model.

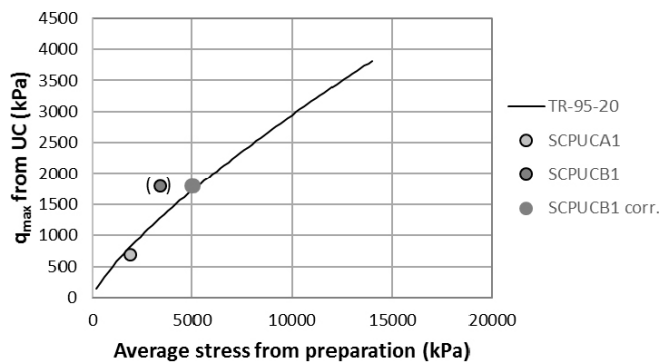


Figure 4-30. Resulting maximum deviator stress q_{max} from the unconfined compression tests plotted as a function of average stress from the preparation. The solid line represents Equation 4-2 originally presented by Börgesson et al. (1995). Since the dry density increased during the handling of specimen B1 the average stress was corrected (legend SCPUCB1 corr.).

4.5.4 Series with controlled final volume

The results from the specimens prepared with a controlled final volume without stress measurements are presented in Figure 4-31 to Figure 4-33. Three different types of preparation were used; large swelling from high degree of saturation (SCUC1, SCUC2), minimized swelling from a high degree of saturation (SCUC4) or applied water pressure during and after saturation (SCUC3).

The specimens in series SCUC1 and SCUC2 swelled either axially or radially during saturation and the main part of the specimens had a high initial degree of saturation, $S_{r,ini} = 95-97\%$ (two specimens started from slightly lower degree of saturation; SCUC1 1 $S_{r,ini} = 92\%$ and SCUC2 6 $S_{r,ini} = 90\%$). While the specimens in series SCUC1 started from approximately the same water content and dry density ($w = 19.6\%$ and $\rho_d = 1760 \pm 20 \text{ kg/m}^3$) and ended up at different final dry density the specimens in series SCUC2 started from different initial water contents and different dry densities ($w = 16.7-21.9\%$ and $\rho_d = 1705-1875 \text{ kg/m}^3$) and ended up at approximately the same dry density ($\rho_d = 1455 \pm 30 \text{ kg/m}^3$). In series SCUC4 the initial degree of saturation at preparation was also high $S_{r,ini} = 89-98\%$ but with this series the aim was to avoid or minimize swelling during the saturation. In series SCUC3 a water pressure of 1 000–4 000 kPa was applied after saturation but before the unconfined compression tests.

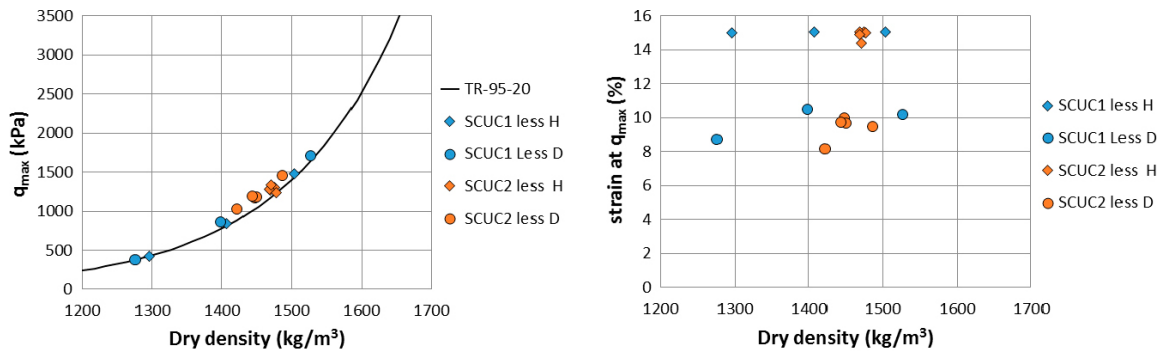


Figure 4-31. Deviator stress as a function of dry density from test series SCUC1 and SCUC2 where the specimens swelled radially (initially less D) or axially (initially less H) during saturation. The solid line represents the model of strength presented by Börgesson et al. (1995).

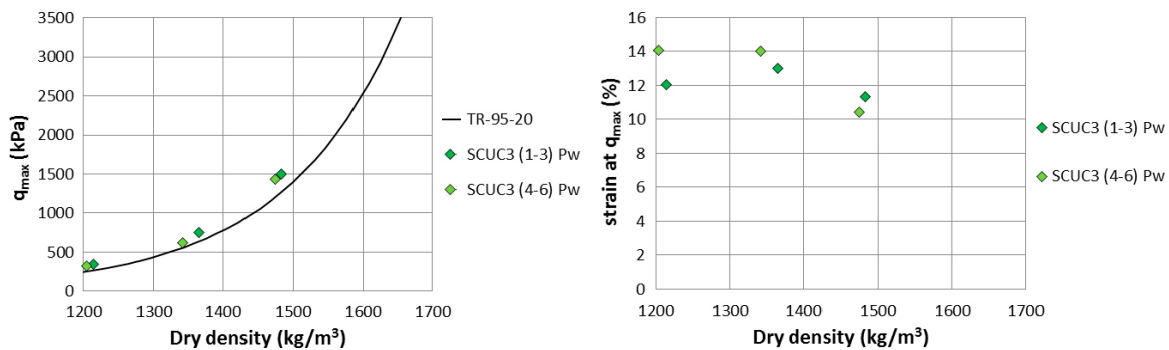


Figure 4-32. Deviator stress as a function of dry density from test series SCUC3 where water pressure (1 000–3 000 kPa) was applied after saturation but before the UC tests.

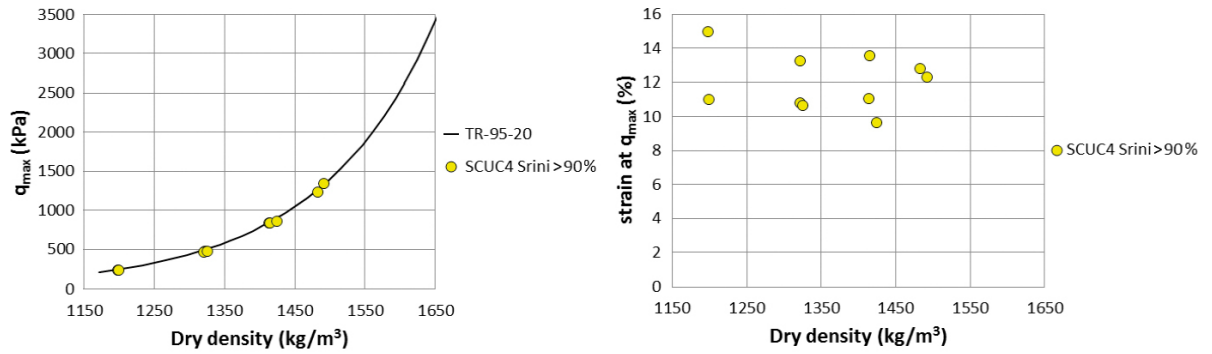


Figure 4-33. Deviator stress as a function of dry density from test series SCUC4.

No large deviations of deviator stress at failure from the reference line (TR-95-20) can be seen in the test results in Figure 4-31, Figure 4-32 or Figure 4-33. Slightly larger maximum deviator stress is seen from the specimens exposed to water pressure during preparation while the results from the series SCUC4 show no deviation from the model at all. No large difference in strain was seen but both the largest and smallest strain at failure was seen on specimens that swelled deliberately during saturation, SCUC1 and SCUC2. The one that swelled axially showed the largest strain at failure while the specimens that swelled radially, with mainly no axially swelling, showed the smallest strain at failure.

4.5.5 Comments

The results from the series with different stress paths and stress measurements during the preparation are plotted in Figure 4-34 to Figure 4-36, slightly different from above. In Figure 4-34 the average stress, calculated according to Equation 3-5, is plotted as a function of the dry density at preparation and the paths are marked with dotted lines and arrows. The swelling pressures at the initial state are here estimated from the model presented by Börgesson et al. (1995), from the initial dry density and the fact that the specimens were compacted to almost saturated conditions. In Figure 4-35 the measured deviator stress at preparation is plotted as a function of average stress from Figure 4-34. In Figure 4-36 the stress states shown in Figure 4-35 are plotted with a final step for each specimen representing the deviator stress from the unconfined compression tests and the average stress from Figure 4-34. In Figure 4-36 the average stress after the unconfined compression test was calculated taking the deviator stress from the test into account. The final density is assumed to be homogeneously distributed although different amounts of swelling took place.

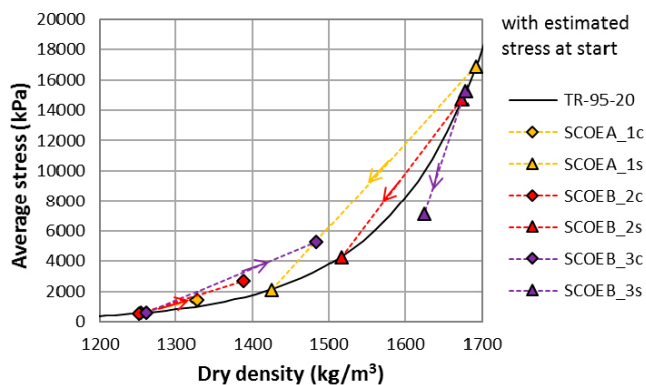


Figure 4-34. Measured average stresses as a function of dry density at preparation with dotted lines for the assumed stress paths (cf. Figure 4-25).

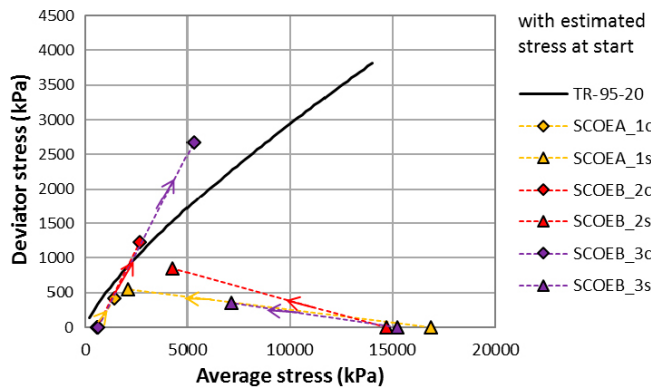


Figure 4-35. Measured average stresses as a function of deviator stress at preparation with dotted lines for the assumed stress paths (cf. Figure 4-25).

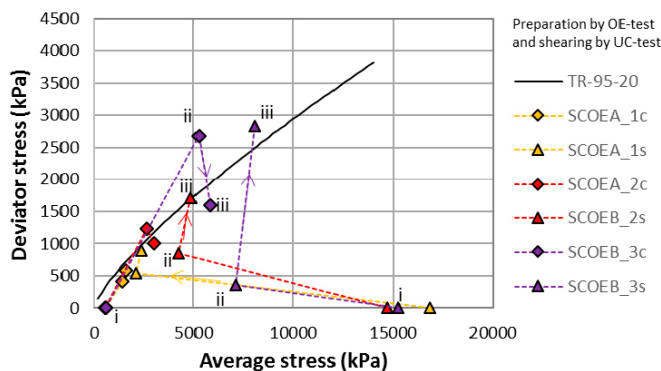


Figure 4-36. Stress paths of specimens with measured stresses during the preparation (i.e. the SCOE-series). The stress path of each specimen includes: i. The initial state with an estimated average stress from the measured dry density; ii. The measured stress state after preparation; iii. The maximum deviator stress from the unconfined compression test plotted with an average stress based on the isotropic stress from the preparation. See also Figure 4-27 and Figure 4-35.

The stresses measured after volume change at constant axial stress deviates from the model of swelling pressure which illustrates that the model is based on constant volume tests. Based on the measurements in this study consolidation overestimates and swelling underestimates the stresses when plotting as a function of dry density. At consolidation different stresses were measured radially and axially and the deviation from the model depends on which stress is used for the comparison; the radially measured, the axially measured or the average stress, cf. Figure 4-25. At swelling no large difference was seen between the axially and radially measured stresses. Since a deviation from the actual model of swelling pressure is seen both after consolidation and swelling the deviation cannot be correlated to the size of the deviator stress, i.e. the difference between the axially and radially measured stresses, but rather to the size of volume change since larger deviations were measured at densities where larger volume changes were present during the preparation, see Section 4.5.2.

During preparation by consolidation different stresses were measured axially and radially as mentioned above, i.e. a deviator stress was present. The deviator stress measured at the unconfined compression tests was in these three tests lower than the value measured after preparation. The specimens that swelled during preparation had low deviator stress after the swelling and the stress state after the unconfined compression tests ended up above the model. The results are plotted as a function of the average stress measured before the unconfined compression test. Since the dismantling from the saturation device is made without any water uptake the stress state before dismantling is assumed to be kept. In Figure 4-36 the deviator stress was added to the average stress, as commented above.

4.5.6 Concluding remarks

The objective of test series SC-OE was to investigate the relation between the swelling pressure and the evaluated shear strength with the main focus on how the stress path influences the strength. The test results presented are results from tests aiming at studying this relation. The specimens were exposed to different types of stress states and the effect on the deviator stress at failure was studied with unconfined compression tests.

The influence of stress paths on the maximum deviator stress was studied on specimens of MX-80. The specimens were saturated at different stress paths with either: constant axial stress and no radial deformation, constant volume conditions or large swelling. The results are compared with a model presented by Börgesson et al. (1995). The average of the degree of saturation of the 40 specimens was 101 %.

After consolidation or swelling with constant axial load and no radial deformation during saturation the resulting measured stresses showed that

- the radial and axial stresses were different after consolidation but not after swelling (i.e. a deviator stress was introduced during consolidation).
- after consolidation with a constant axial load the final dry density was lower than the dry density after swelling with the same axial load, cf. Figure 4-25,
- compared to the model presented by Börgesson et al. (1995) the final stress state after consolidation was larger than predicted by the model while the final stress state after swelling was lower.

Regarding the unconfined compression tests

- the deviator stress as a function of dry density showed
 - correspondence between the results from specimens prepared at different stress paths, irrespective of consolidation or swelling,
 - correspondence between the model and the test results, irrespective of the stress paths at preparation.
- the corresponding strain at failure as a function of dry density showed
 - a tendency to lower strain measured after consolidation compared to after swelling.

Regarding the relationship between maximum deviator stress and swelling pressure:

- the specimens that consolidated resulted in lower strength compared to the specimens that swelled which follows from the observation above that at constant axial load the final dry density is lower after consolidation than after swelling (cf. Figure 4-25),
- the model (Börgesson et al. 1995) shows values between the results of the swelled and consolidated specimens.

4.6 Test series DS1

4.6.1 General

The preparation of specimens in these test series was described in Section 3.6.4, Table 3-4. The main results are presented in this chapter, but additional details are shown in Appendix 6. The test series were focused on:

- the combined effect of content of chloride salts and drying at 90 °C (32 tests),
- the effect of content of calcium oxide (20 tests).

The results consist of unconfined compressive strength and the basic parameters water content and density. In addition, swelling pressure was measured during preparation of 6 of the specimens. Some of the results are shown with a reference line presented by Dueck et al. (2011).

4.6.2 Combined effect of content of chloride salts and drying at 90 °C

All specimens were prepared from samples of MX-80 and all specimens were influenced by drying at 90 °C for 48 hours and subsequently saturated with 1M salt solution of CaCl₂ or NaCl. The resulting unconfined compressive strength and the corresponding strains are presented in Figure 4-37 and Figure 4-38. Detailed results can be found in Appendix 6.

The results from the series with specimens being ion-exchanged in-situ (as a compacted specimen during or after saturation) are shown in Figure 4-37 (PUC1, PUC2, UC1). In the series PUC1 and PUC2 all specimens were ion-exchanged to be Ca²⁺ dominated. In series UC1 the specimens were ion-exchanged to be either Ca²⁺ or Na⁺ dominated. The specimens were exposed to drying at 90 °C and had excess salt left at dismantling.

The results from the series UC2 and UC4 are shown in Figure 4-38. In these series the specimens were prepared from ion-exchanged MX-80 powder (circles), from MX-80 powder with added salt crystals (triangles) or from MX-80 powder (diamonds). The difference between the series is that the specimens in series UC2 were in equilibrium with 1 M CaCl₂ solution at dismantling while the specimens in the series UC4 were saturated with a stagnant solution with an increasing concentration from the initial 1M CaCl₂.

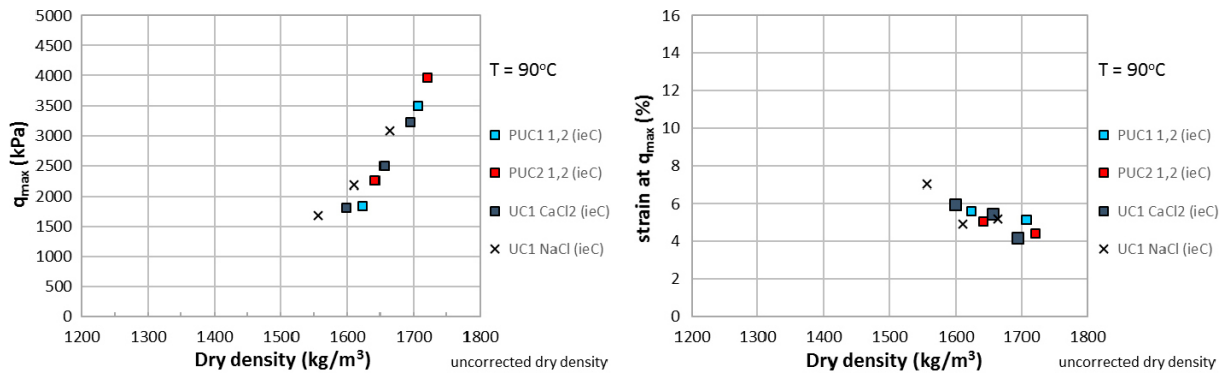


Figure 4-37. Results from unconfined compression tests on ion-exchanged specimens exposed to 90 °C and with excess salt left at testing. The ion-exchange was made in-situ (ie C) and the markers (squares, crosses) show the dominating ion (Ca²⁺, Na⁺). The dry densities have not been corrected for excess salt.

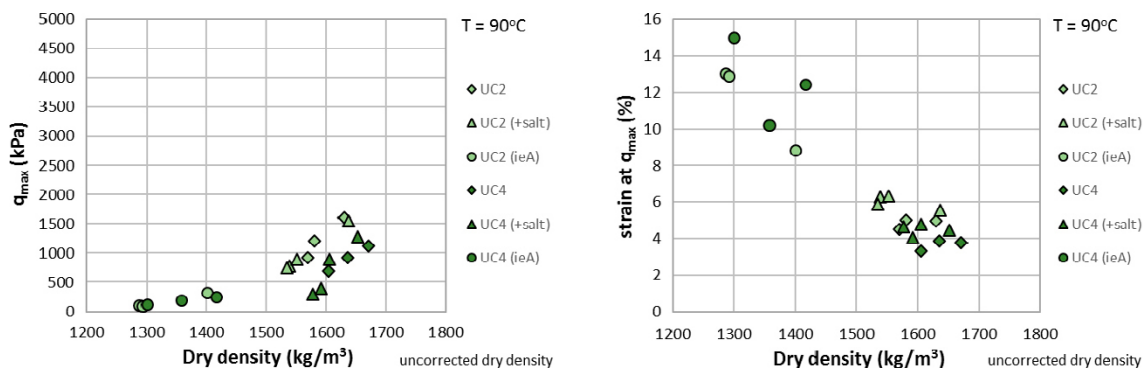


Figure 4-38. Results from unconfined compression tests on specimens influenced by salt (CaCl₂) in different ways. The specimens in the two series were prepared in similar ways but in series UC2 (light green) the specimens were in equilibrium with 1M CaCl₂ solution at dismantling while the specimens in series UC4 (dark green) were saturated with a solution having higher concentration than 1M CaCl₂. The dry densities have not been corrected for excess salt.

The results to the left of Figure 4-37 and Figure 4-38 show deviating compressive strength compared to the reference tests in previous test series. This is to a large extent caused by the fact that the dry densities presented have not been corrected for the presence of excess salt in the specimens after dismantling. The amount of excess salt was larger in series UC4 compared to series UC2 which gave that the results from series UC4 are located furthest away to the right in Figure 4-38. The content of excess salt also influenced the calculated degree of saturation which was lower than 100 % in all specimens. Measurement of swelling pressure was made in series PUC1 and PUC2 and the resulting unconfined compressive strength is plotted as a function of the measured swelling pressure in Figure 4-39.

4.6.3 Effect of content of calcium oxide

The results from the specimens with added contents of CaO and Ca(OH)₂ are shown in Figure 4-40. Detailed results are shown in Appendix 6. The content of CaO seems to influence the compressive strength markedly while the content of Ca(OH)₂ seems not to influence the results. However, both salts seem to influence the corresponding strain at failure. The results are shown with a previous reference line.

The specimens having added contents of CaO showed a behaviour expected after cementation i.e. high unconfined compressive strength in combination with small strain at failure, see also the stress-strain curves in Appendix 6. Measurement of pH in the water after saturation showed higher values than expected from pure water which also indicates some kind of cementation.

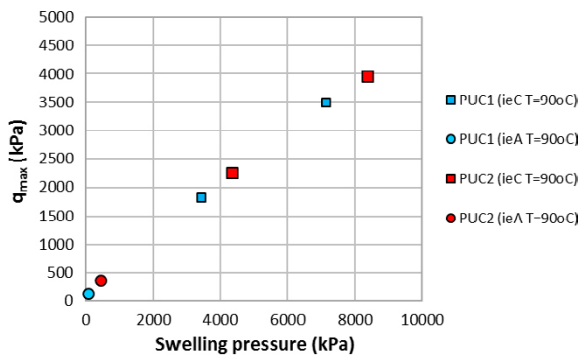


Figure 4-39. Test results from unconfined compression tests and swelling pressure measurements during the preparation of specimens. Results from series PUC1 and PUC2 are shown as compressive strength as a function of measured swelling pressure.

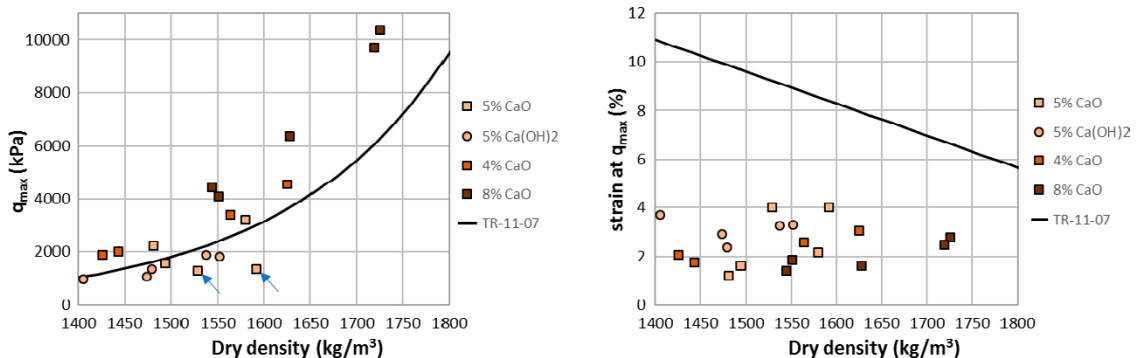


Figure 4-40. Results from specimens having added contents of CaO or Ca(OH)₂. Two specimens were in pieces but were still sheared (marked with arrows). The results are shown with a previous reference line.

4.6.4 Comments

The main part of the specimens in this series was exposed to ion-exchange, presence of excess salt and a temperature of 90 °C. The results in Figure 4-41 and Figure 4-42 have been corrected for excess salt by a simplified empirical equation based on an assumption of 1M CaCl₂ in the interlayer water, see Appendix 1. The excess salt also influences the water content which has not been further analysed.

Figure 4-41 shows the results from all specimens influenced by CaCl₂ solutions from Figure 4-37 and Figure 4-38 but with the dry density corrected for excess salt. Higher concentration of salt was present in the external salt solution used in UC4 but since the same correction for excess salt was used for all specimens the results from UC4 specimens are located furthest away from the strength-reference line in Figure 4-41 (left) due to additional excess salt still not corrected for.

In Figure 4-42 the results from Figure 4-39 (from specimens where both unconfined compressive strength and swelling pressure were measured) are plotted with a model presented by Börgesson et al. (1995). In the diagram to the right the dry densities have been corrected for excess salt. The diagrams illustrate that deviating swelling pressure as a function of dry density will give deviating results when strength is plotted as a function of the swelling pressure even if the strength does not deviate that much from the expected relationship between strength and dry density, cf. Figure 4-41 especially at high dry density.

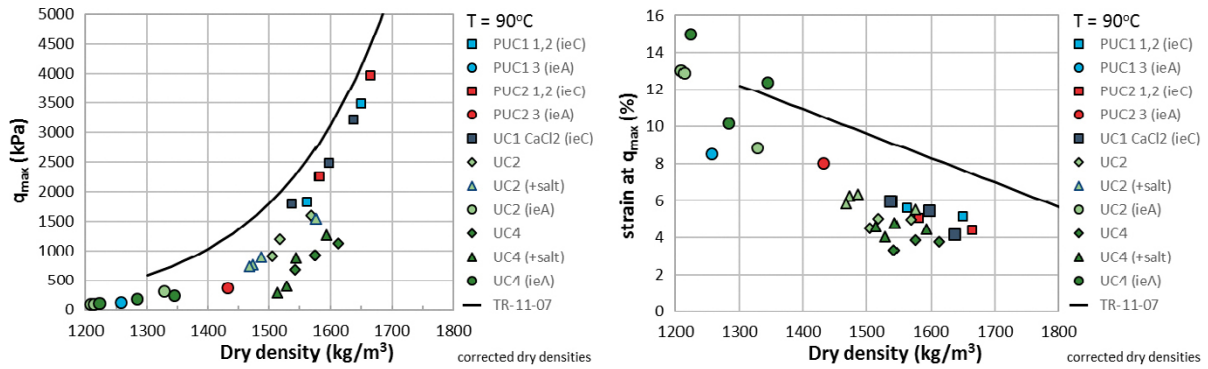


Figure 4-41. Results from all specimens dried at 90 °C and subsequently saturated by CaCl₂. Corresponding results from Figure 4-37 and all results from Figure 4-38 are shown. The markers (square, circle, triangle, diamond) show the type of preparation of the MX-80 powder (ion-exchanged in-situ (ie C), ion-exchanged powder (ie A), powder with added salt, original powder). The dry densities have been corrected for excess salt.

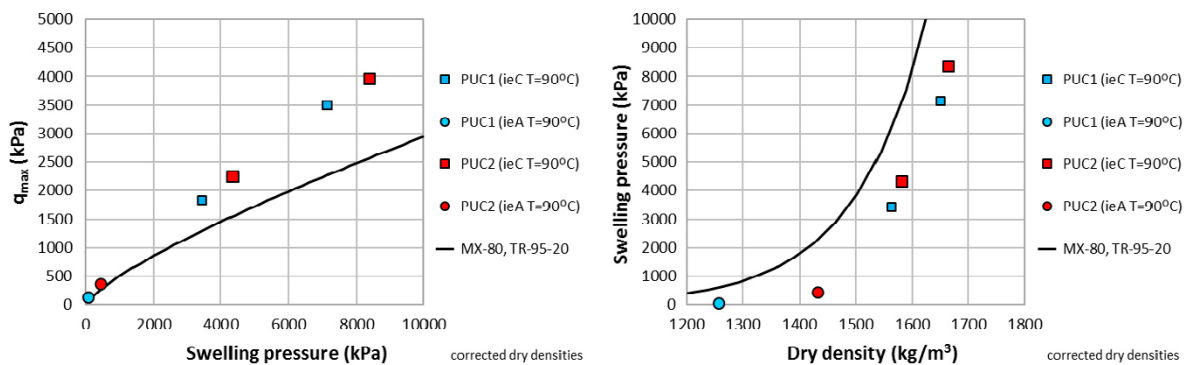


Figure 4-42. Test results from unconfined compression tests and swelling pressure measurements during the preparation of the specimens. Results from Figure 4-39 (left) and swelling pressure as a function of corrected dry density (right).

4.6.5 Concluding remarks

The results of test series DS1, regarding the combined effect of content of chloride salts and drying at 90 °C (where the dry densities have been corrected of excess salt) show that

- the combination of heating and ion-exchange gave small deviations compared to a reference line of MX-80 at corrected dry densities above 1 500 kg/m³,
- the corresponding strain was in general lower than the reference,
- in the series with different amount of excess salt, the strength and the strain decreased with increasing salt, cf. Figure 4-41, however, the largest amount of salt was probably not fully compensated for, which gave too high dry densities.

The swelling pressure measured during the preparation (measured during the saturation before the unconfined compression test but after the ion-exchange and heating) and compared to previous references shows that

- while the strength deviates when related to the swelling pressure it does not when related to the dry density (corrected for excess salt) in most tests.

In addition, the results of exposure to the combined effect of salt and heating show that

- the same results were observed on specimens prepared from ion-exchanged powder and from powder with added salt crystals,
- no large difference was seen on the compressive strength determined on specimens, ion-exchanged with NaCl or CaCl₂,
- the degree of saturation was less than 100 % in all specimens and was lower the higher content of excess salt. In the calculation neither the dry density nor the water content was corrected for excess salt.

In the series concentrated on the effect of content of calcium oxide cemented specimens were prepared and the resulting stress-strain-strength behaviour showed an expected stiff and brittle behaviour.

4.7 Test series DS2

4.7.1 General

The preparation of specimens in these test series was described in Section 3.6.4, Table 3-5. The test series were focused on the following:

- drying and testing unsaturated specimens (36 tests),
- saturated specimens (16 tests),
- determinations of swelling pressure, water retention properties and compressive strength (6 tests).

The results consist of unconfined compressive strength, water content and dry density for all specimens. In some series swelling pressure and retention curves were also determined. The results from this study are presented in this section and additional data and details are shown in Appendix 7. A reference relation representing saturated specimens of MX-80 from Dueck et al. (2011) is also shown.

4.7.2 Drying and testing unsaturated specimens

All specimens were prepared from MX-80 and all specimens were exposed to a relative humidity of either 75 % (75.4 % ± 0.1 %) or 85 % (85.1 % ± 0.1 %) at 25 °C (25 °C ± 0.1 °C) for approximately three weeks. The resulting unconfined compressive strength and the corresponding strain are presented in Figure 4-43 and Figure 4-44. In Figure 4-44 the dry density is corrected for the content of 5 % salt, i.e. 95 % of the dry density determined at dismantling, since salt was added to these specimens.

The labels in Figure 4-43 and Figure 4-44 show the series (A1, A2, B1), the actual *RH* the specimens were exposed to (75 %, 85 %) and the water contents (initial water content – final water content).

In series A1 and B1 the colours of the circles (blue, yellow, grey, green) show the different initial water contents (18 %, 20 %, 31 %, 35 %) and the use of marker lines (marker line, no marker line) shows the *RH* in the climate chamber (75 %, 85 %). The results from series A2 with ion-exchanged specimens are shown with red circles and labels with corresponding information as series A1, in Figure 4-43. The labels show thus which specimens hydrated or dehydrated during the preparation in the climate chamber.

The specimens in series UCA (A1, A2) that dried, i.e. grey, green and red circles in Figure 4-43, showed higher strength compared to the reference relation (Dueck et al. 2011a) while the specimens with water uptake (blue circles) showed lower strength. In series UCA, the strain measured after exposure to *RH* = 85 % were in general lower than the strain after exposure to *RH* = 75 % although the former had lower dry density.

In series UCB (B1) with salt added to the specimens the strength is lower than the reference for all specimens and lower the more hydrated. The strain in series UCB seems to follow the reference line. Specimens having approximately the same dry density and being exposed to the same *RH* did not reach the same strength. They also did not reach the same water content which might have influenced the results.

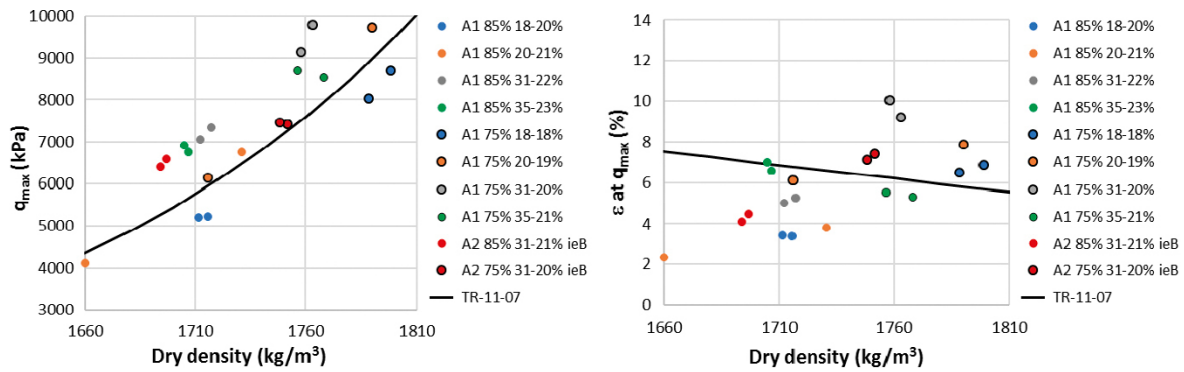


Figure 4-43. Results from unconfined compression tests on specimens exposed to dehydration (drying) or hydration (water uptake) at 25 °C in series UCA. The specimens were prepared of MX-80 or of Ca-dominated ion-exchanged MX-80 (labels include the method used for the ion-exchange, ie B). The labels show the series (A1, A2), the actual *RH* (75 %, 85 %) and water contents (initial water content – final water content). A reference line of saturated MX-80 from TR-11-07 (Dueck et al. 2011a) is also shown.

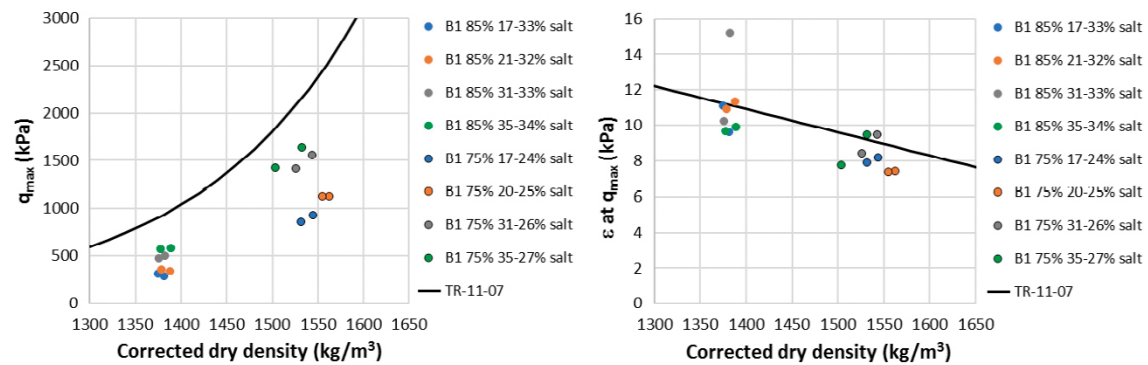


Figure 4-44. Results from unconfined compression tests on specimens of MX-80 with added amounts of CaCl_2 (labels include the word salt) exposed to dehydration (drying) or hydration (water uptake) at 25 °C in series UCB. The labels show the series (B1), the actual *RH* (75 %, 85 %) and water contents (initial water content – final water content). The dry densities have been corrected for the salt content. A reference line of saturated MX-80 from TR-11-07 (Dueck et al. 2011a) is also shown.

4.7.3 Saturated specimens

This series with complementary specimens was made to repeat previous tests but instead of adding a solution of 1M CaCl₂, de-ionized water was used for saturation. In series UCC both ion-exchanged MX-80 and MX-80 mixed with CaCl₂ were used. In addition, series UCD was performed in order to study the repeatability of the method. The time used for the saturation and washing out excess salt was 30 days which is approximately double the time compared to the ordinary time used for saturation. The test results are shown in Figure 4-45.

The results from both test series agree well with the reference line (label TR-11-07) although the specimens in series UCC were either ion-exchanged or had salt added initially. No correction of dry density was made since these specimens were saturated with circulating DI-water removing a large part or all of the excess salt.

4.7.4 Determinations of characterizing properties

The test results from this series characterize ion-exchanged (ieB or ieD) MX-80 hydro-mechanically in terms of swelling pressure measured at preparation, unconfined compressive strength and water retention properties. The results from the unconfined compression tests are shown in Figure 4-46. The strength of the ion-exchanged Ca-dominated material follows the same trend as MX-80 (TR-11-07). The swelling pressure is shown as a function of dry density in Figure 4-47 (right) where some difference between the specimens ion-exchanged as powder (PUCB ieB) and the specimens ion-exchanged in-situ (PUCA ieD) are seen. The difference is seen as a scatter when the strength is related to the swelling pressure in Figure 4-47 (left) while almost no deviation from the previous reference is seen when the strength is plotted as a function of dry density, cf. Figure 4-46.

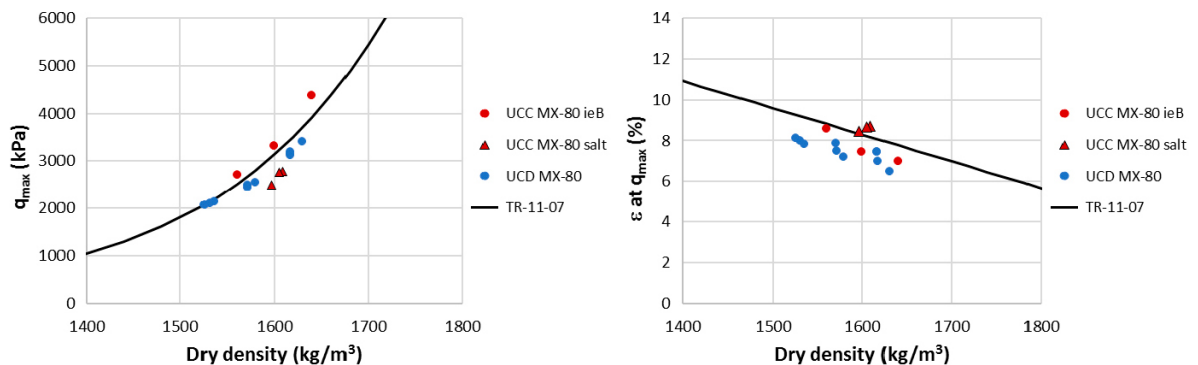


Figure 4-45. Deviator stress and corresponding strain as a function of dry density resulting from test series UCC and UCD. The type of ion-exchange of MX-80 (ieB) or addition of CaCl₂ (salt) are indicated in the labels. A reference line of saturated MX-80 from TR-11-07 ((Dueck et al. 2011a)) is also shown.

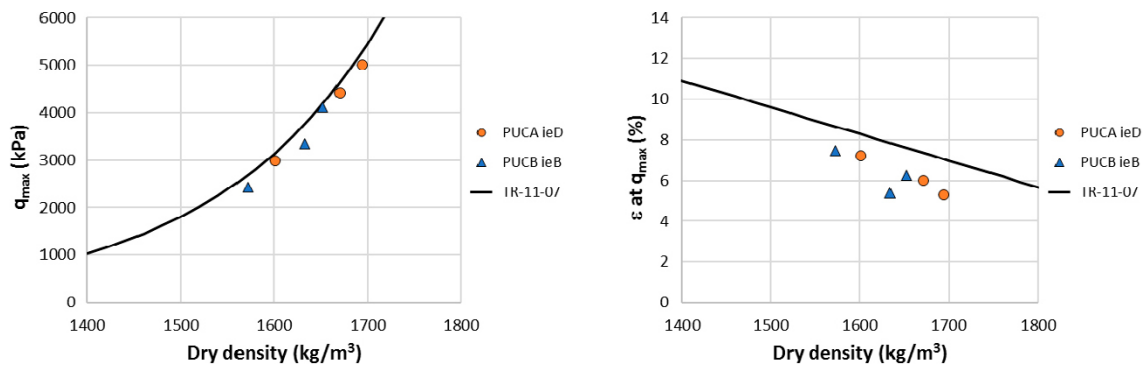


Figure 4-46. Deviator stress and corresponding strain as a function of dry density in series PUCA and PUCB. In the labels the test series and the type of ion-exchange used are shown. A reference line of saturated MX-80 from TR-11-07 ((Dueck et al. 2011a)) is also shown.

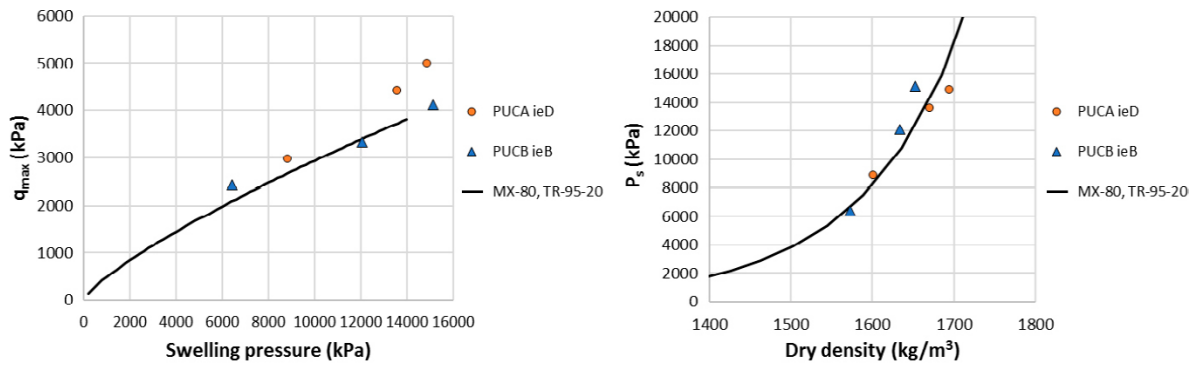


Figure 4-47. Deviator stress as a function of swelling pressure and swelling pressure as a function of dry density in series PUCA and PUCB. In the labels the test series and the type of ion-exchange used are shown. A model introduced by Börjesson et al. (1995) is shown.

As a complement, retention curves of the ion-exchanged Ca-dominated materials used in the actual test series were determined, Figure 4-48. In the diagram, the label MX-80Ca refers to the same material as used for the specimen PUCB ieB in Figure 4-47. Less hysteresis is seen compared to previous retention curves of MX-80.

4.7.5 Comments

A study on the influence of degree of saturation on strength was presented by Dueck (2010). Specimens of MX-80 with dry densities above 1 500 kg/m³ and degree of saturation higher than 70 % were used for the study and no influence of degree of saturation on strength was seen. In this actual study no obvious influence of degree of saturation can be seen in Figure 4-49 where the degree of saturation of specimens in series A1 and A2 are shown, cf. Figure 4-43. However, the results from the unsaturated specimens do not agree with results from saturated references in this actual study. It seems as the difference is rather an effect of drying and wetting. In Figure 4-50 the water uptake in the climate chamber is shown together with previous retention curves of MX-80.

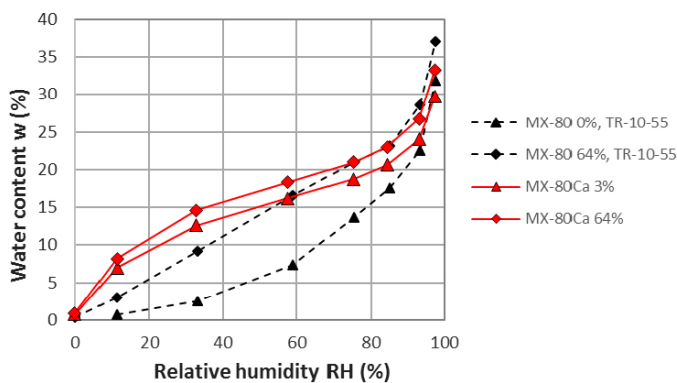


Figure 4-48. Water retention curves of the ion-exchanged material MX-80Ca (the same as used for PUCB ieB in Figure 4-47) shown as the resulting water content after equilibrium at different RH. Water retention curves of MX-80 are also shown (Dueck and Nilsson 2010).

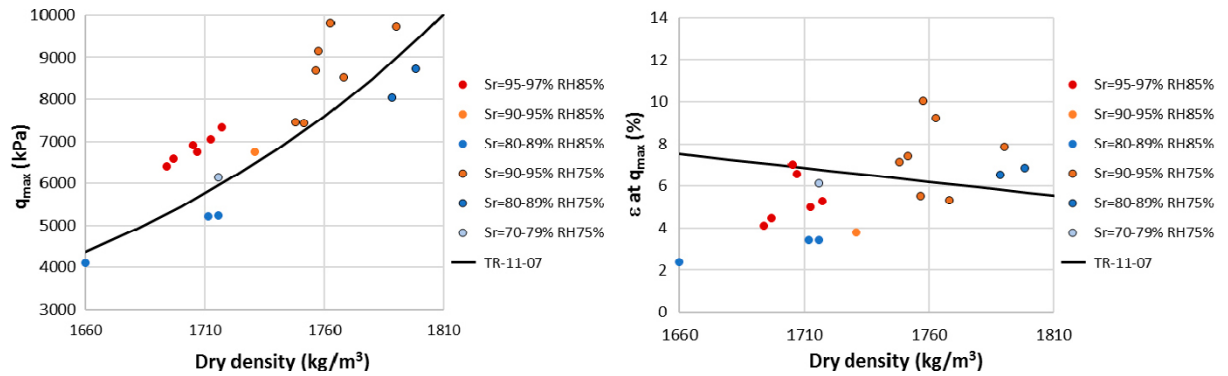


Figure 4-49. Results from Figure 4-43 (series A1 and A2) on MX-80 specimens where the final degree of saturation is indicated in the labels together with the actual relative humidity, e.g. RH75 %. A previous reference line valid for saturated specimens is shown.

The final water contents after hydration or dehydration (water uptake or drying) are plotted as a function of RH in Figure 4-50 to Figure 4-52, where previous retention curves of MX-80 (Dueck and Nilsson 2010) are shown. The different test series A1, A2 and B1 are shown in separate diagrams where the specimens consist of powder of MX-80, of ion-exchanged (Ca-dominated) MX-80 and of MX-80 mixed with $CaCl_2$, respectively. The different colours (blue, yellow, grey, green) denote the initial water contents (18 %, 20 %, 30 %, 35 %). Red circles denote results from ion-exchanged materials. The corresponding change in volume, and dry density, is illustrated in Appendix 7.

Thus, the final water content after exposure in the climate chamber differs and depends on the initial water content of the specimens. The results from Figure 4-50 and Figure 4-43 can be compared since the same legends are used, i.e. the colours blue, orange, grey and green denote the amount of drying from almost no drying (blue) to a decrease in water content of more than 10 % (green). The different water uptake seems to influence the compressive strength.

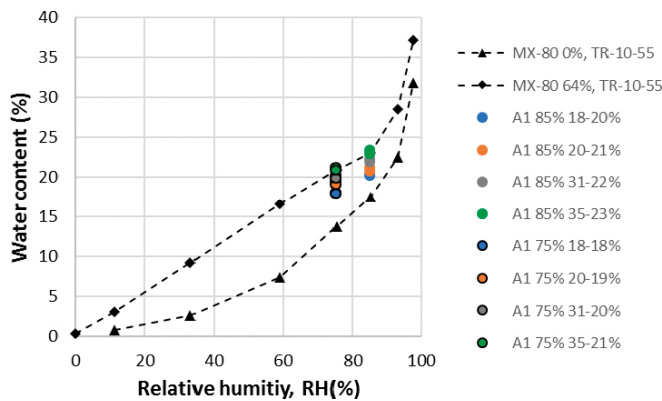


Figure 4-50. Series A1 with specimens of MX-80 exposed to relative humidity of 75 % and 85 %. The labels show information about the specimens, e.g. (A1, 85 %, 18–20 %) shows results from the series A1, the relative humidity RH=85 % and a water content interval 18–20 % with the initial water content and the final water content at equilibrium. Each result is an average of two tests. Results from previous results on MX-80 from Dueck and Nilsson (2010) are also shown.

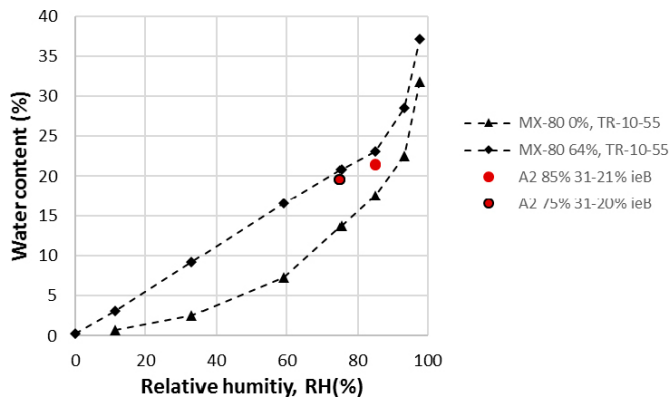


Figure 4-51. Series A2 with specimens of MX-80Ca, ion-exchanged with the method B, exposed to relative humidity of 75 % and 85 %. The labels show information about the specimens, e.g. (A2, 85 %, 31–21 %, ieB) shows results from the series A2, the relative humidity RH=85 %, an interval of water contents 31–21 % with the initial water content and the final water content at equilibrium and the method used for the ion-exchange ieB. Each result is an average of two tests. Results from previous results on MX-80 from Dueck and Nilsson (2010) are also shown.

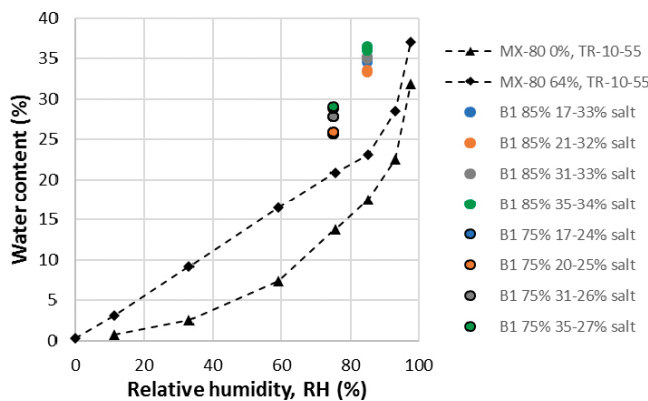


Figure 4-52. Series B1 with specimens of MX-80 with added amounts of CaCl₂ exposed to relative humidity of 75 % and 85 %. The labels show information about the specimens, e.g. (B1, 85 %, 17–33 %, salt) shows results from series B1 where the specimens were exposed to relative humidity RH=85 %, an interval of water contents 17–33 % where the initial water content was 17 % and the final water content was 33 % at equilibrium and the word salt indicates added amount of CaCl₂. An attempt was made to correct the water contents for the excess salt. Each result is an average of two tests. Results from previous results on MX-80 from Dueck and Nilsson (2010) are also shown.

4.7.6 Concluding remarks

Considering strength as a function of dry density and compared to reference tests on saturated specimens of MX-80 (Dueck et al. 2011a) the results show that

- the strength increased for unsaturated specimens exposed to drying at a dry density between $\rho_d = 1\,600\text{--}1\,800\text{ kg/m}^3$,
- the strength was slightly lower for unsaturated specimens exposed to hydration at dry density between $\rho_d = 1\,600\text{--}1\,800\text{ kg/m}^3$,
- the strength was clearly lower for unsaturated specimens containing excess salt although an attempt was made to correct the dry density which was between $\rho_d = 1\,350\text{--}1\,550\text{ kg/m}^3$.

The unsaturated specimens in this study had a degree of saturation higher than 80 % and should according to a previous study (Dueck 2010) follow the reference line of saturated specimens referred to above. However, the results from the unsaturated specimens in the actual study deviate from the reference line and thus, it seems as drying has had an influence.

Subsequent characterizing properties of ion-exchanged Ca-dominated MX-80 were determined in a final test series. The test series included a set of standard tests with ion-exchanged specimens; swelling pressure tests and subsequent unconfined compression tests and, in addition, determination of retention curves. In the tests no excess salt was present and consequently no correction of the dry density was needed. A scatter was observed when the strength was considered a function of the determined swelling pressure but not when plotted as a function of dry density.

4.8 Test series UCT

4.8.1 General

The possibility to have elevated strength after exposure to high temperature was studied with this test series. A limited number of specimens of different bentonites were exposed to short-term heating to 240 °C and then sheared with the unconfined compression test. The high temperature was used to accelerate any slow process and thus, the temperature was higher than expected in a KBS-3 repository. The preparation of the specimens was described in Section 3.6.5 and results are presented in this chapter. Additional details are shown in Appendix 8. All specimens were saturated before the unconfined compression tests in this series.

4.8.2 Exposure to high temperature

The specimens in these test series were exposed to 240 °C. In the main three series (UCT1–UCT3) the specimens of three different bentonites were exposed to 240 °C at saturated conditions. In an additional series (UCT4) some of the specimens were exposed to 240 °C at unsaturated and drying conditions while some specimens were kept at room temperature. The resulting unconfined compressive strength and the corresponding strain are presented in Figure 4-53 to Figure 4-55.

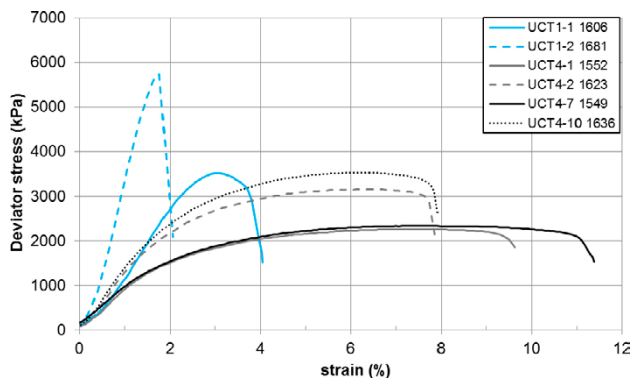


Figure 4-53. Deviator stress as a function of strain from the tests on MX-80. Specimens exposed to 240 °C at saturated conditions (blue lines) and at unsaturated conditions (grey lines) together with two reference tests (black lines). The labels show test ID and dry density (kg/m^3).

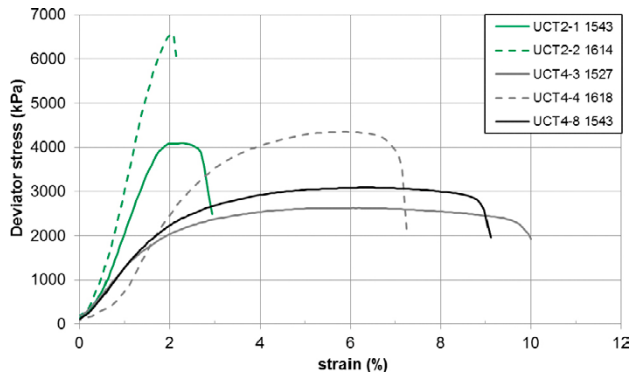


Figure 4-54. Deviator stress as a function of strain from the tests on Asha505. Specimens exposed to 240 °C at saturated conditions (green lines) and at unsaturated conditions (grey lines) together with one reference test (black line). The labels show test ID and dry density (kg/m^3).

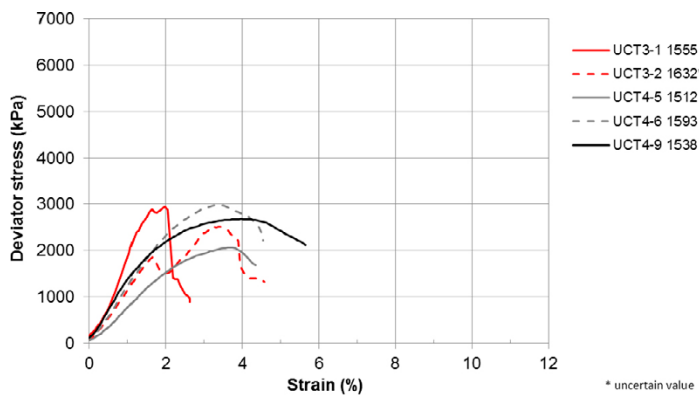


Figure 4-55. Deviator stress as a function of strain from the tests on Calcigel. Specimens exposed to 240 °C at saturated conditions (red lines) and at unsaturated conditions (grey lines) together with one reference test (black line). The labels show test ID and dry density (kg/m^3).

In Figure 4-56, Figure 4-57 and Figure 4-58 the results of MX-80, Asha505 and Calcigel, respectively, are presented as the maximum deviator stress and corresponding strain as a function of dry density. In each diagram the markers (circles with black marker line, circles without marker line, diamonds) denote the different preparation used for the specimens (heated at saturated conditions, heated at unsaturated drying conditions, not heated at all).

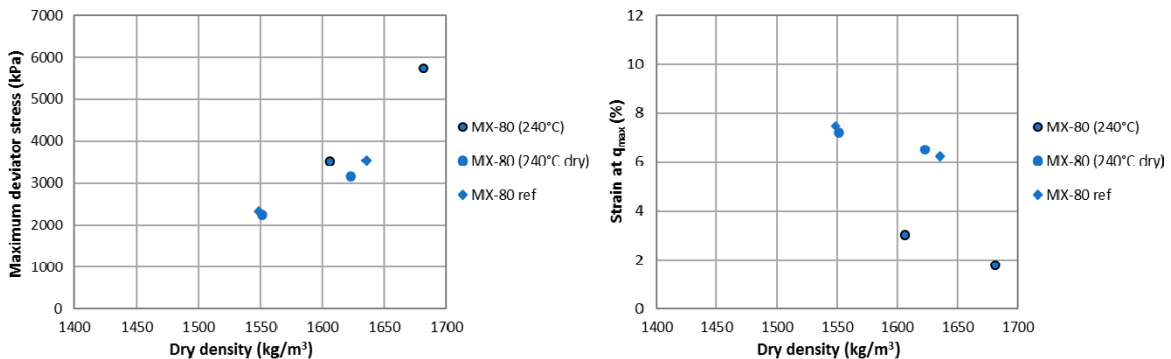


Figure 4-56. Results from unconfined compression tests on specimens of MX-80. Specimens exposed to 240 °C at saturated conditions (blue circles with marker lines) and unsaturated conditions (blue circles). Two reference tests from the actual series (blue diamonds) are shown.

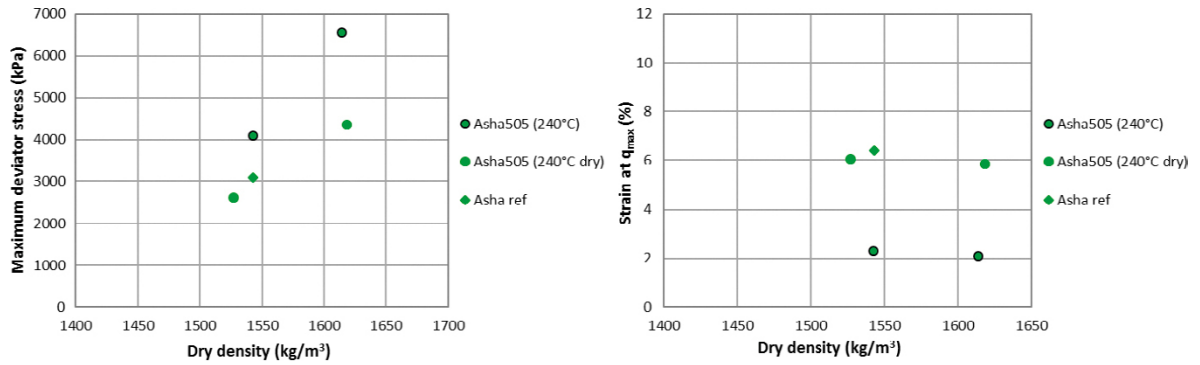


Figure 4-57. Results from unconfined compression tests on specimens of Asha505. Specimens exposed to 240 °C at saturated conditions (green circles with marker lines) and unsaturated conditions (green circles). One reference test from the actual series (green diamond) is shown.

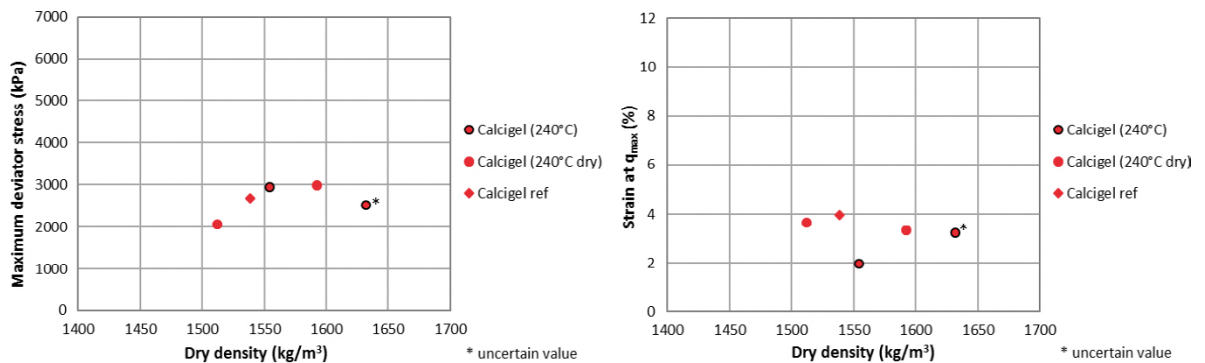


Figure 4-58. Results from unconfined compression tests on specimens of Calcigel. Specimens exposed to 240 °C at saturated conditions (red circles with marker lines) and unsaturated conditions (red circles). One reference test from the actual series (red diamond) is shown.

4.8.3 Comments

The results of specimens exposed to heating to 240 °C at saturated conditions showed brittle behaviour, for almost all specimens, with rapidly decreasing stress at low strain. However, increased strength and stiffness were seen for the specimens of MX-80 and Asha505 but not for the specimens of Calcigel.

In Figure 4-59 to Figure 4-61 photos with examples of failure surfaces of each material are shown. The first photo in each figure shows the failure surface of a specimen heated at saturated conditions and the second photo corresponds to a specimen heated and dried and then saturated. The stress-strain curves corresponding to the photos in Figure 4-59 to Figure 4-61 are the dashed lines in Figure 4-53 to Figure 4-55, respectively. Additional photos can be found in Appendix 8.



Figure 4-59. Specimens of MX-80. To the left heated at saturated conditions (UCT1-2) and to the right from the reference series (UCT4-2).



Figure 4-60. Specimens of Asha505. To the left heated at saturated conditions (UCT2-2) and to the right from the reference series (UCT4-4).



Figure 4-61. Specimens of Calcigel. To the left heated at saturated conditions (UCT3-2) and to the right specimen from the reference series (UCT4-6).

The unconfined compressive strength is determined according to Equation 3-6. When the shear strength is evaluated as one half of the unconfined compressive strength a shear failure is assumed to take place along a plane inclined 45° to the horizontal plane. Often the inclination is larger, but the equation is still used. In the actual test series failure along a shear plane inclined 45° to the horizontal was the common type of failure but the specimens exposed to 240 °C at saturated conditions showed almost vertical failure surfaces. Regarding Calcigel, the failure surface was almost vertical in all specimens, irrespective of the preparation. The vertical failure planes indicate another type of failure (e.g. a tensile failure instead of the shear failure).

Vertical failure surfaces in specimens of MX-80 have previously been reported by e.g. Karland et al. (2009) and Dueck (2010) where this type of failure surface was observed in combination with an abrupt decrease in stress after failure at low strain. The brittle behaviour was defined and the strength at brittle failures was found to agree or be lower than the references (Dueck 2010). This is in contrast to the results from the actual tests series where the brittle failure also includes higher strength, see e.g. Figure 4-56.

In the test methodology, relatively short time was used for cooling the specimens, which may have caused an uneven pore pressure in the specimens and it cannot be excluded that this influenced the results.

4.8.4 Concluding remarks

A limited number of specimens exposed to short-term heating to 240 °C at saturated conditions were tested. Unfortunately, it cannot be excluded that the test methodology influenced the results but compared to references of each material the following were found:

- Increased strength and stiffness were found for specimens of MX-80 and Asha505.
- No increase in strength and no clear increase in stiffness was seen for the specimens of Calcigel.
- Failure at reduced strain was seen for the specimens of MX-80, Asha505 and Calcigel.
- A rapid decrease in stress at low strain, i.e. brittle failure, was seen for almost all specimens.

The results for the specimens heated to 240 °C at unsaturated drying conditions and subsequently saturated, agreed well with the single references of each material.

5 Additional analyses

In this chapter further analyses are made of some of the results shown in Chapter 4. The results are compared to a model presented by Börgesson et al. (1995) and Dueck et al. (2010) and a reference line for MX-80 derived by Dueck et al. (2011).

5.1 Strength as a function of dry density

5.1.1 Different materials

Strength is a function of dry density and the type of bentonite. All results from the tests in series TMS1–3 (not ion-exchanged) are shown in Figure 5-1 where the unconfined compressive strength is plotted as a function of dry density. Febex bentonite has the highest strength in relation to density and Kunigel the lowest.

5.1.2 Ion-exchanged material

Results of the ion-exchanged and the references of the materials MX-80, Deponit Ca-N and Ikosorb are shown in Figure 5-2 to Figure 5-4. Only tests where no excess salt was present at dismantling are shown (i.e. ion-exchanged with the methodology ieB and ieD).

Regarding the results of MX-80 in Figure 5-2 the diagram includes results both from the original material and ion-exchanged material. The diagram also includes the results from the specimens prepared with different stress paths presented in Section 4.5. Results from previous studies are also included in the diagram. Good repeatability is seen. Influence of the different treatments cannot be seen. Results of Deponit Ca-N are also shown together with results from a previous study, Figure 5-3. Results of Ikosorb are shown in Figure 5-4.

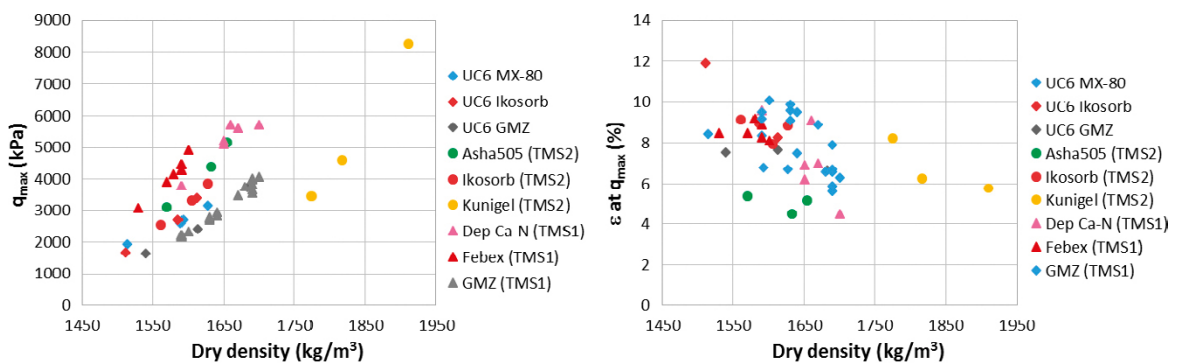


Figure 5-1. Results from all specimens from TMS1-3 not being ion-exchanged.

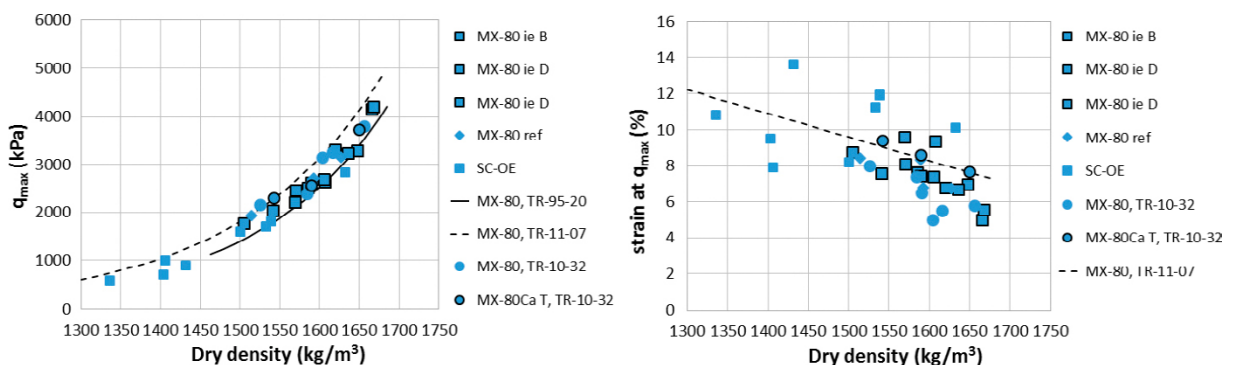


Figure 5-2. Results of MX-80 specimens from this and previous studies.

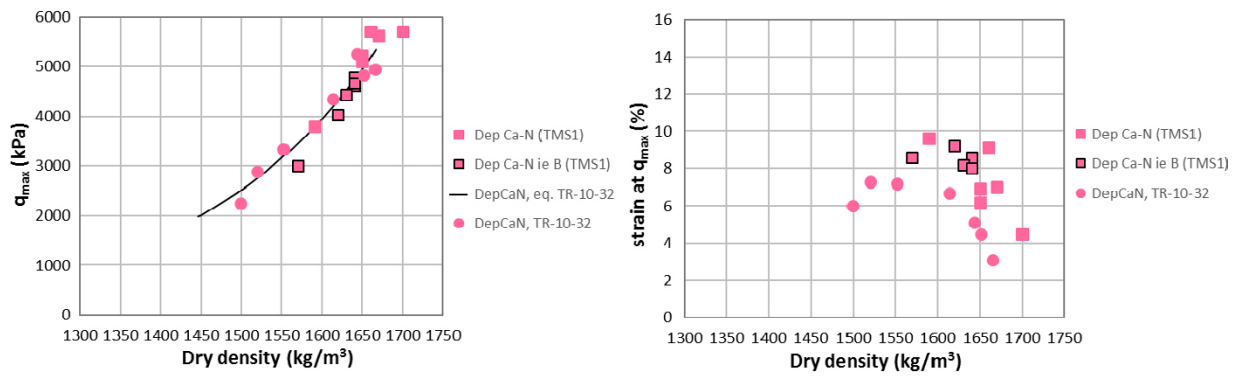


Figure 5-3. Results of Deponit Ca-N specimens from this and previous studies.

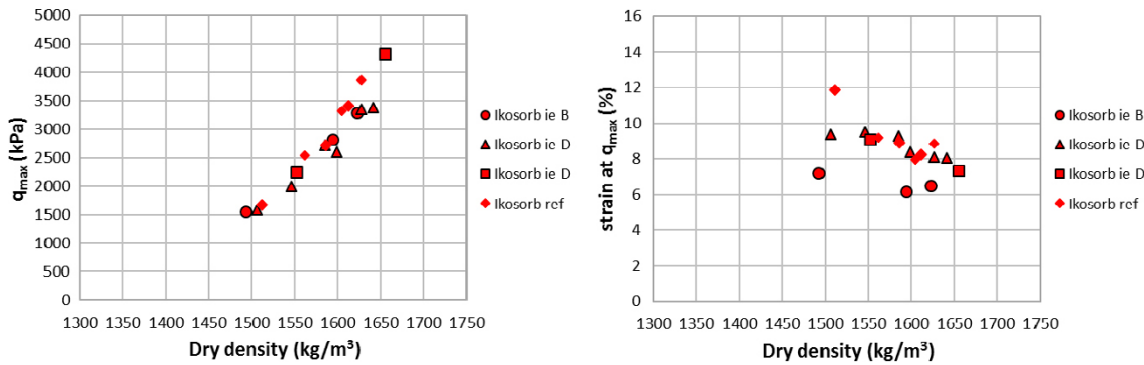


Figure 5-4. Results of Ikosorb from this study.

The results from some of the ion-exchanged material show deviating results compared to the original material, Figure 5-5 and Figure 5-6. Regarding the deviating results of MX-80 (crosses in Figure 5-5) the ion-exchange was made without accessory minerals. Regarding the methodologies of ion-exchange the accessory minerals were, in general, left in the specimens. Regarding one of the series with ion-exchanged specimens of GMZ powder, it was unclear if the accessory minerals was left or not. The results from these specimens were deviating (light grey circles with marker lines in Figure 5-6) compared to other ion-exchanged specimens of GMZ. An additional test series, with three specimens, was run where the presence of accessory minerals was ensured and the results from this additional series (dark grey circles with marker lines in Figure 5-6) followed the trend from the previous tests on ion-exchanged materials, i.e. the deviating results were not repeated. Thus, the accessory minerals were probably removed in the first series of ion-exchanged specimens, mentioned above.

The conclusion from the test results in Figure 5-5 and Figure 5-6 is that the strength is a function of the dry density and the material and the ion-exchange is not influencing the results in the actual range of dry densities unless the accessory minerals are removed since then a new material seems to be created.

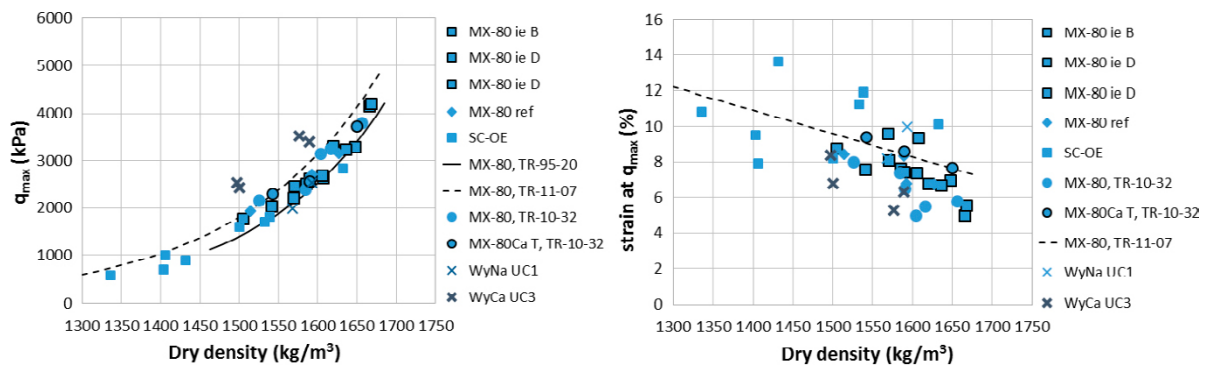


Figure 5-5. Results from Figure 5-2 but with additional results on MX-80 specimens with the accessory minerals removed. WyNa and WyCa were published by Dueck et al. (2010).

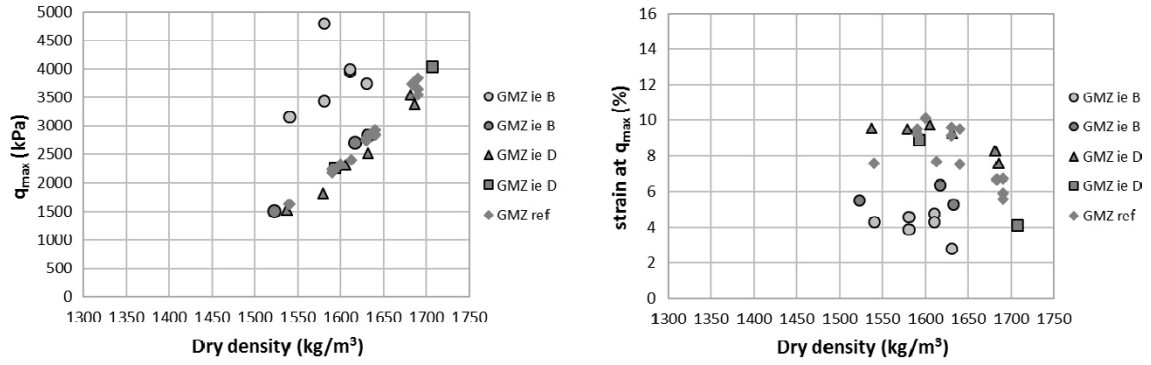


Figure 5-6. Results of GMZ from Figure 4-4 and Figure 4-21.

5.1.3 Strength as a function of clay dry density

To have a more general expression of sealing properties the montmorillonite dry density, i.e. the ratio between the mass and volume of montmorillonite, has been used by e.g. Karnland (2010) and Man and Martino (2009). By using such variable, the accessory minerals are only considered as filler material without significance. In this section the montmorillonite dry density ρ_{dm} and the montmorillonite void ratio e_m according to Equations 5-1 and 5-2, respectively, are used with X as the ratio between the mass of the montmorillonite to the dry mass. The variables m_m , m_a , m_s , are the mass of the montmorillonite, the accessory minerals and the solid, respectively, and V , V_a , V_m , V_p and V_s are the total volume and the volume of the accessory minerals, the montmorillonite, the pores and the solid, respectively. In the equations below the particle density of the bentonite is assumed to be equal to the particle density of the accessory minerals, $\rho_a = \rho_s$.

$$\rho_{dm} = \frac{m_m}{V - V_a} = \frac{m_m}{\frac{m_s}{\rho_d} - \frac{m_a}{\rho_a}} = \frac{Xm_s}{\frac{m_s}{\rho_d} - \frac{m_s - Xm_s}{\rho_s}} = \frac{X}{\frac{1}{\rho_d} - \frac{(1-X)}{\rho_s}} \quad (5-1)$$

$$e_m = \frac{V_p}{V_m} = \frac{V_p}{V_s - V_a} = \frac{\frac{V_p}{V_s}}{\frac{V_s - V_a}{V_s}} = \frac{e}{1 - \frac{m_a/\rho_a}{m_s/\rho_s}} = \frac{e}{1 - \frac{(m_s - m_sX)/\rho_s}{m_s/\rho_s}} = \frac{e}{X} \quad (5-2)$$

In Figure 5-7 results of MX-80 and Deponit CaN are plotted as a function of void ratio e to the left and as a function of the montmorillonite void ratio ($1/e_m^3$) to the right and data from Table 5-1 was used for the calculation. The scatter to the right in Figure 5-7 is in general small along a linear trend but results from specimens of ion-exchanged pure montmorillonite without accessory minerals, WyNa and WyCa, are clearly deviating.

Table 5-1. Amount of montmorillonite X and particle density ρ_s of different materials.

Material	X %	ρ_s kg/m ³
MX-80	80	2780
Dep-CaN	82	2750
WyCa	100	2780
WyNa	100	2780

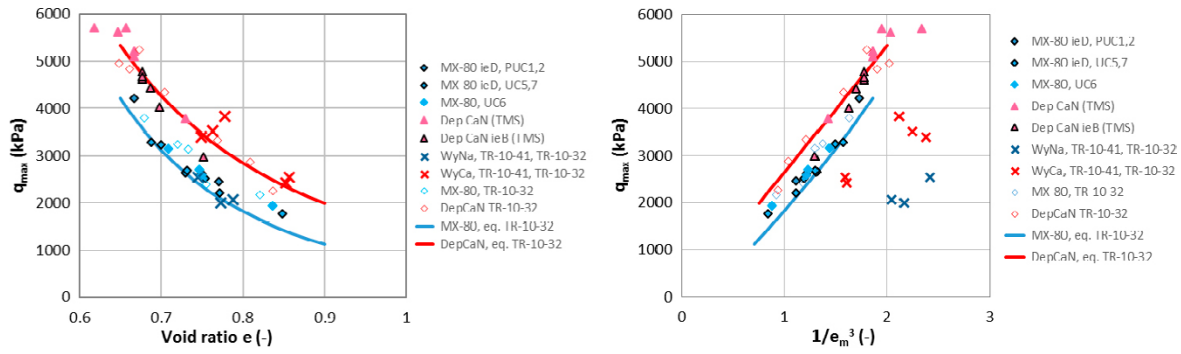


Figure 5-7. Resulting maximum deviator stress as a function of dry density (left) and $1/e_m^3$ (right) of different bentonites.

To further interpret the strength, an attempt was made to correlate the shear stress in the failure surface after unconfined compression tests to a physical attractive force between the particles in the montmorillonite. The van der Waals force is mentioned as an attractive force causing clay aggregates to keep together (Marshall et al. 1996, Chapter 9.2) and it also describes the interaction between molecules in colloidal systems of montmorillonite (Hedström et al. 2016). The van der Waals force F_{vdw} describes the interaction between clay layers in a bentonite according to Equation 5-3 (e.g. Russel et al. 1992, Hedström et al. 2016) where δ is the thickness of the clay layer (~ 0.93 nm), h is the separation between the clay layers and A_H the effective Hamaker constant (with typical values in the vicinity of 2×10^{-20} J for smectite-smectite interactions across aqueous interlayers).

Assuming that the ratio of the clay layer thickness δ to the repeat distance ($h + \delta$) is the same as the volume of solids to the total volume according to Equation 5-4 the separation between the clay layers h can be estimated from the montmorillonite void ratio e_m according to Equation 5-5.

The shear stress in the failure surface after unconfined compression tests can be calculated by Equation 5-6 from the difference between the principal stresses σ_1 and σ_3 . Generally, the angle from the failure surface to the major principal stress plane is $\theta = 45^\circ$ which gives the shear stress $\tau_f = q/2$ where q is the deviator stress, cf. Section 3.7.

$$\frac{F_{vdw}}{area} = -\frac{A_H}{6 \cdot \pi} \cdot \left(\frac{1}{h^3} + \frac{1}{(h + 2 \cdot \delta)^3} - \frac{2}{(h + \delta)^3} \right) \quad (5-3)$$

$$\frac{\delta}{h + \delta} = \frac{V_s}{V} \quad (5-4)$$

$$h = \delta \cdot e_m \quad (5-5)$$

$$\tau_f = \frac{1}{2} \cdot (\sigma_1 - \sigma_3) \cdot \sin 2\theta \quad (5-6)$$

In Figure 5-8 the results from Figure 5-7 are re-plotted with the shear stress as a function of part of Equation 5-3. The best fitted linear relations through origin are shown in the diagram. From the given slopes the Hamaker constant A_H are calculated for the materials MX-80 & DepCaN, WyCa and WyNa as $2.2 \cdot 10^{-20}$ J, $1.3 \cdot 10^{-20}$ J and $0.9 \cdot 10^{-20}$ J, respectively. Based on the approximation to the right in Figure 5-7 ($F_{vdw}(1/h^3)$) the values of A_H were calculated to $1.9 \cdot 10^{-20}$ J, $1.1 \cdot 10^{-20}$ J and $0.8 \cdot 10^{-20}$ J. Further analyses could give valuable information about the origin and limits of strength and influence of accessory minerals.

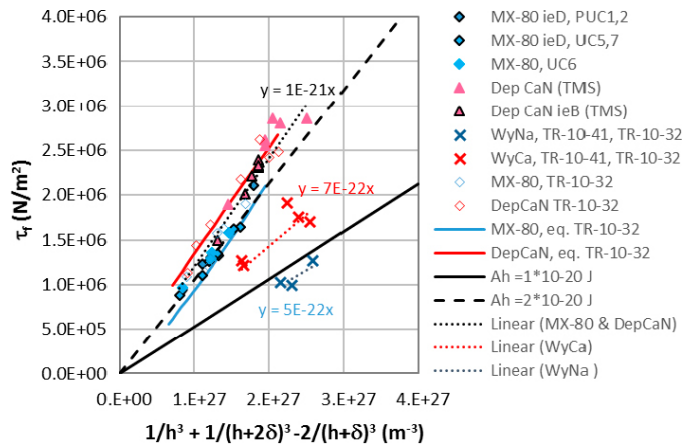


Figure 5-8. The calculated shear stress at the failure surface after unconfined compression tests plotted as a function of an expression of the interlayer distance. Test results (markers) and models (solid lines) are shown with the best fit linear relationships through origin of the test results (dashed lines).

5.2 Strength as a function of stress

5.2.1 Different materials

The results from all tested materials, but not ion-exchanged, in the test series TMS1-3 are shown in Figure 5-9. Similar results were shown by Svensson et al. (2019).

The content of montmorillonite can be taken into account by plotting the strength as a function of the swelling pressure. This relationship is almost the same for different materials although large scatter is seen between the materials when plotted as a function of dry density.

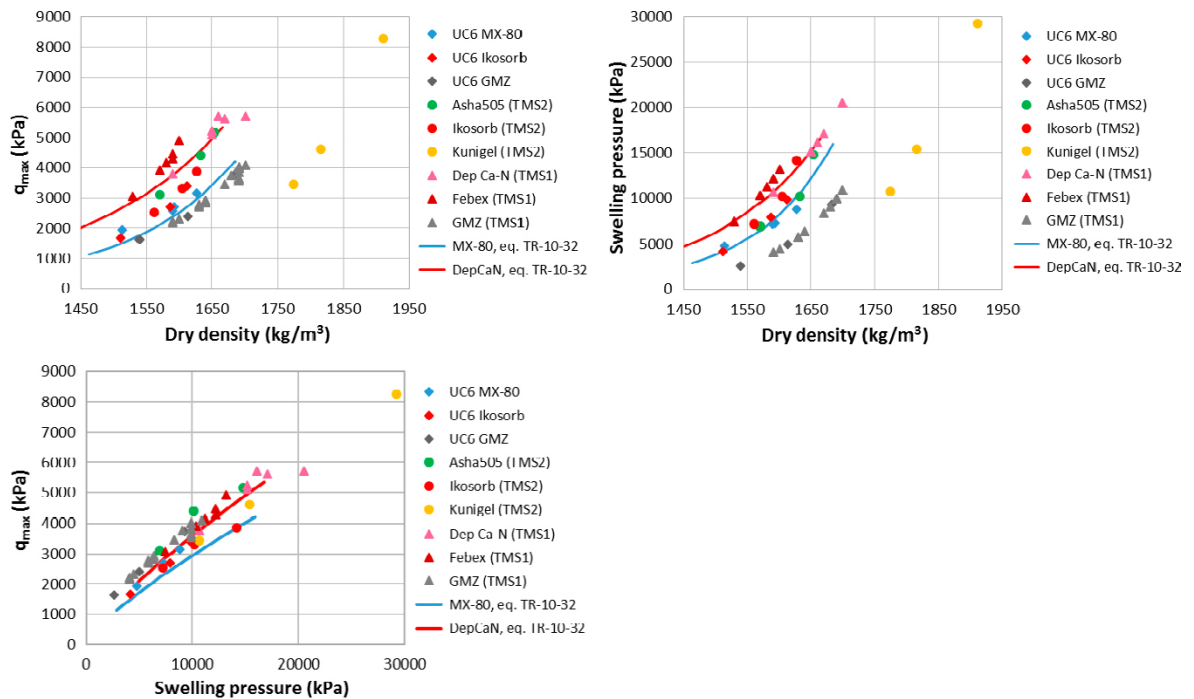


Figure 5-9. Results from test series TMS 1-3 with results from previous models in terms of swelling pressure, unconfined compressive strength and dry density. The swelling pressure was in some cases estimated, see Appendix 1.

5.2.2 Ion-exchanged materials

After ion-exchange some of the materials show no large variation in strength and swelling pressure which gives that they fit into the same relationships as shown in Figure 5-9. In Figure 5-10 the results from Figure 5-9 are plotted together with results from tests on specimens of the same but ion-exchanged materials (however, only specimens without excess salt). As in Figure 5-9 the relationships for the different bentonites deviate less from each other when the unconfined compressive strength is plotted as a function of swelling pressure compared to when plotted as a function of dry density.

5.2.3 Influence of salt solution and other factors on the strength of MX-80

In Figure 5-11 results from tests where the dry density, the strength and the swelling pressure are available for the same specimens are shown. The strength does not deviate from the previous reference when plotted as function of the dry density (above 1500 kg/m³) while when plotted as a function of swelling pressure the influence of salt on the swelling pressure will be visible, see series MX-80 ieC and MX-80 ieC 90 °C. Some of the results were shown in Figure 4-42 where the specimens were exposed to the combined effect of salt and heating.

Additional conditions where similar behaviour can be observed involve volume change as illustrated in Figure 4-26 together with Figure 4-27 or at complicated field conditions involving high temperature discussed by Åkesson et al. (2012).

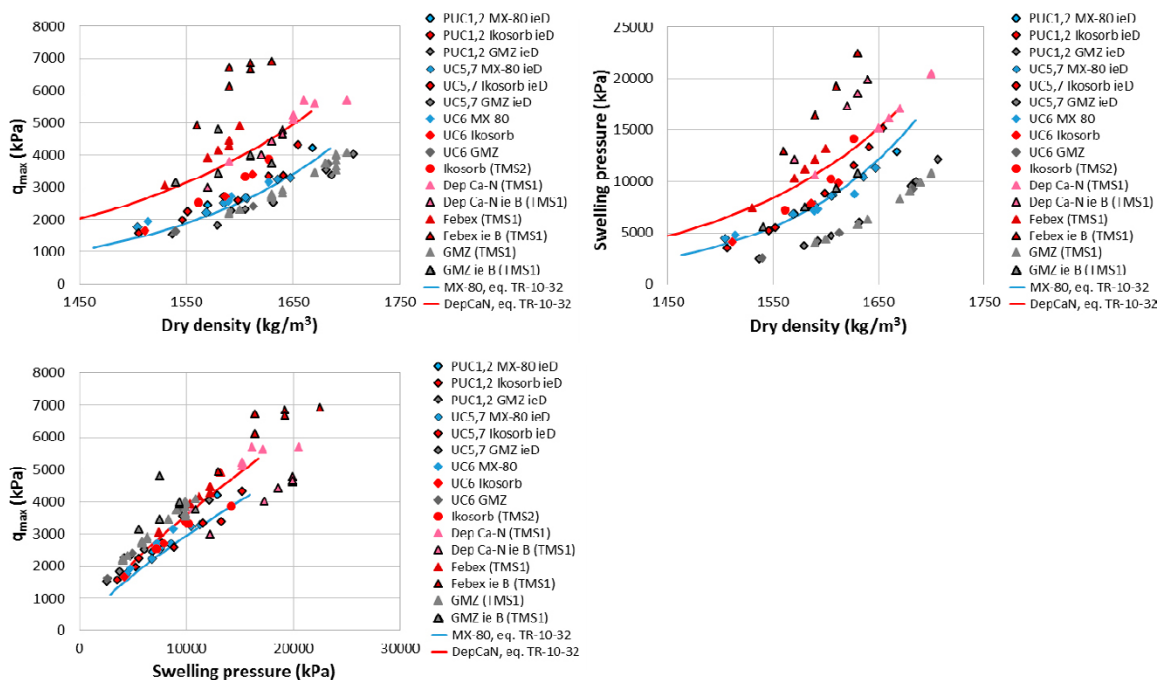


Figure 5-10. Results from Figure 5-9 and results of specimens of the same but ion-exchanged materials (except Asha and Ikosorb, due to lack of swelling pressure data). The results are shown in terms of swelling pressure, unconfined compressive strength and dry density. The swelling pressure was in some cases estimated, see Appendix 1.

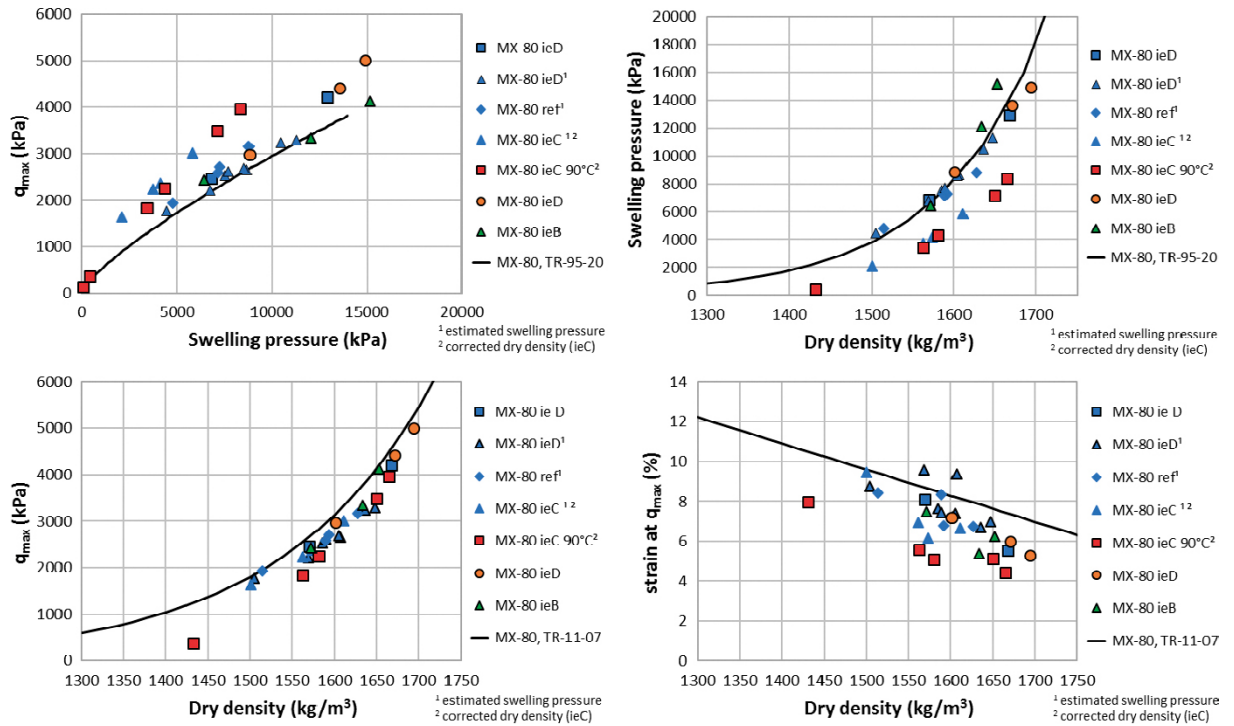


Figure 5-11. Illustration of results which deviate when the unconfined compressive strength is plotted as a function of swelling pressure but not when plotted as a function of dry density.

5.3 Influence of drying

To estimate the influence of the combination of salt and exposure to 90 °C some of the results from Figure 4-41 are plotted in Figure 5-12 with results of ion-exchanged MX-80 from Section 4.4.4. In addition, the reference line from Dueck et al. (2011a) is shown. The results show that the combination of heating and ion-exchange only caused small deviations in stress from the reference tests and also that only small deviations appear when compared to the previous reference of MX-80. This is mainly valid at dry densities higher than 1 500 kg/m³. The strain shown in Figure 5-12 was, however, somewhat lower for the specimens exposed to both ion-exchange and 90 °C.

The results are also compared to results from previous test results presented by Dueck (2014), Figure 5-13, where results of tests on specimens of MX-80 exposed to increased temperature either before or after saturation are shown. No large difference was seen in results from the different specimens although still the strain at failure was small for the specimens exposed to both ion-exchange and 90 °C.

Regarding unsaturated specimens exposed to drying, the results from Figure 4-43 are shown again in Figure 5-14 where the degree of drying is marked in the legend. Increased strength is observed after drying (shrinkage) while decreased strength is seen after wetting (swelling) compared to the reference at densities between 1 600 kg/m³ and 1 800 kg/m³. Small strain at failure was mainly seen for the specimens placed at RH=85 % and especially where no drying (rather a small water uptake, i.e. swelling) took place. However, according to the results on specimens re-saturated after drying (Figure 5-13) increased strength is not expected after saturation.

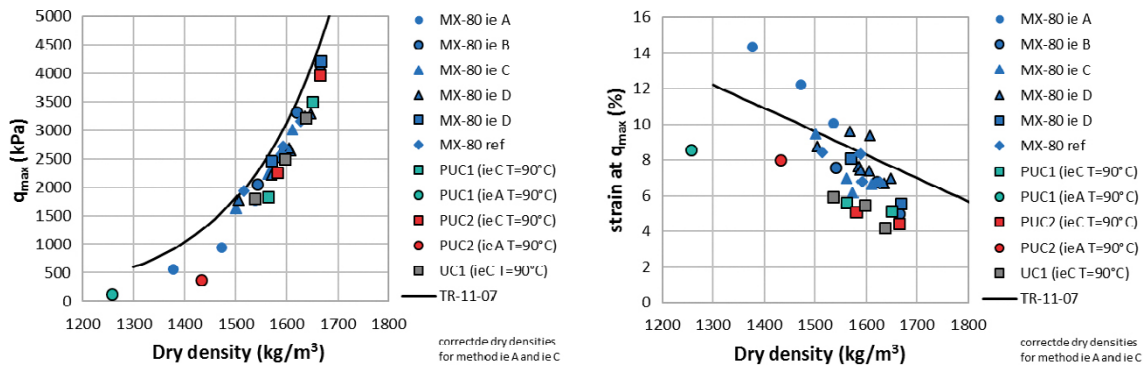


Figure 5-12. Comparison with ion-exchanged specimens from Figure 4-19 and some results from Figure 4-41. The same markers are used.

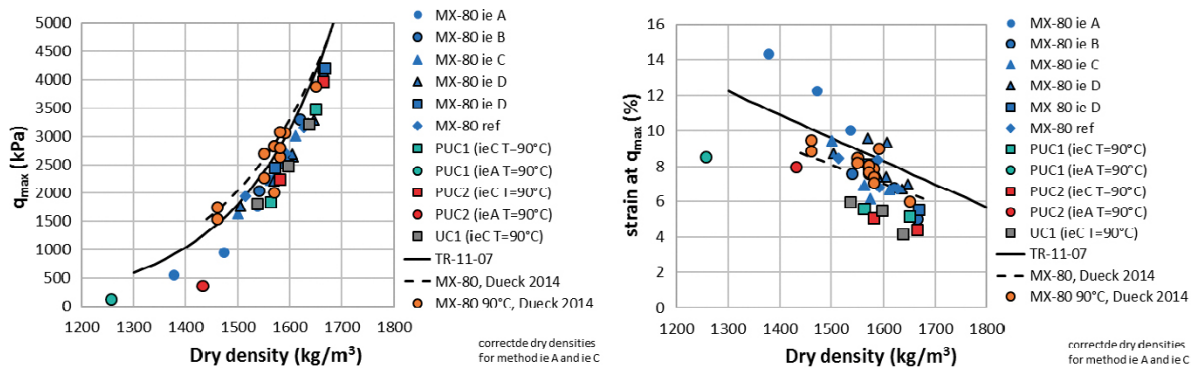


Figure 5-13. Results from Figure 5-12 compared to results from previous test series where MX-80 specimen were exposed to 90 °C (Dueck 2014).

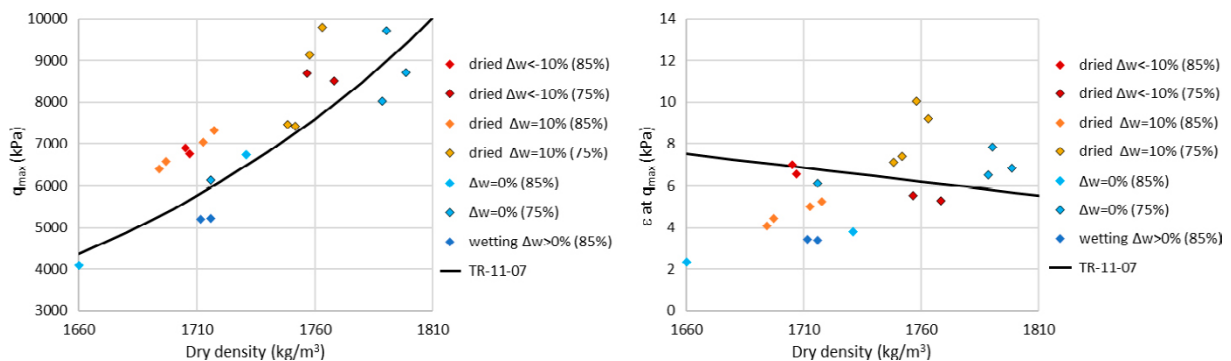


Figure 5-14. Results from Figure 4-43 on MX-80 specimens where drying or wetting are indicated in the labels together with the actual relative humidity in brackets. A previous reference line from Dueck et al. (2011) is shown.

5.4 Influence of exposure to a temperature of 240 °C

In Figure 5-15 to Figure 5-17 results from unconfined compression tests on specimens of MX-80, Asha505 and Calcigel exposed to short-term heating at 240 °C are shown. Results for each material are presented in separate diagrams where the results from Figure 4-56 to Figure 4-58 are plotted together with references from previous parts of this project (TMS1-3). In Figure 5-15 the test results for MX-80 are shown together with the reference line related to saturated MX-80 derived from Dueck et al. (2011a) (label TR-11-07) and used above.

The previously noted increase in strength of MX-80 and Asha505 specimens exposed to increased temperature at saturated conditions, cf. Section 4.8.4, are further confirmed in Figure 5-15 to Figure 5-16. The results for Calcigel are, however, ambiguous since the results of the exposed specimens do not

clearly deviate from the references in Figure 5-17 while still somewhat brittle behaviour is seen. From the results it was also observed that when exposed to increased temperature at unsaturated conditions and subsequently saturated, the results agreed well with the actual references, although the temperature was 240 °C.

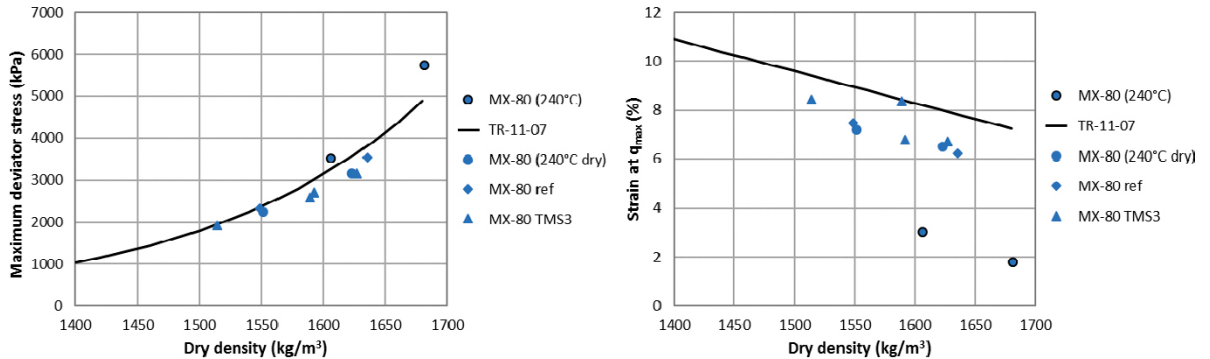


Figure 5-15. Results from unconfined compression tests on specimens of MX-80. The results from Figure 4-56 (with specimens exposed to 240 °C at saturated conditions, exposed at unsaturated conditions and references marked with circles with marker lines, circles without marker lines and diamonds) are shown together with reference tests from a previous part of the project (TMS3) (triangles) and a reference line related to saturated MX-80 derived from the report SKB TR-11-07 (Dueck et al. 2011a).

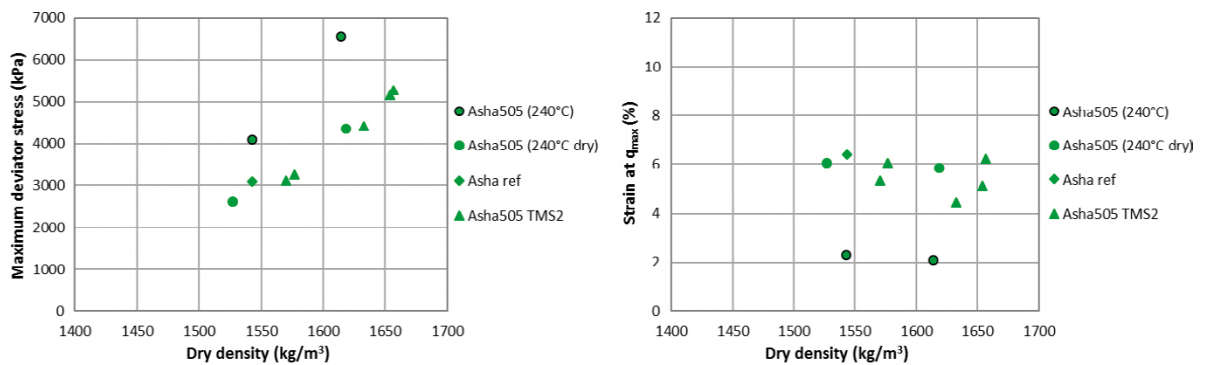


Figure 5-16. Results from unconfined compression tests on specimens of Asha505. The results from Figure 4-57 (with specimens exposed to 240 °C at saturated conditions, exposed at unsaturated conditions and one reference marked with circles with marker lines, circles without marker lines and a diamond) are shown together with reference tests from a previous part of the project (TMS2) (triangles).

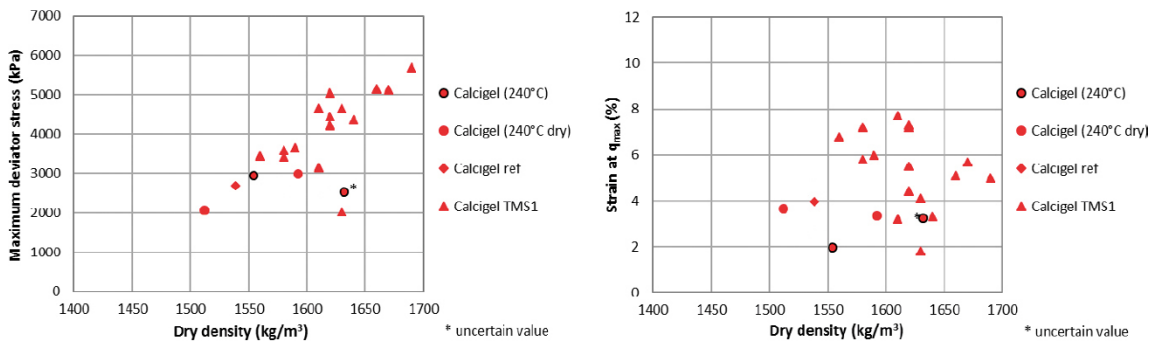


Figure 5-17. Results from unconfined compression tests on specimens of Calcigel. The results from Figure 4-58 (with specimens exposed to 240 °C at saturated conditions, exposed at unsaturated conditions and one reference marked with circles with marker lines, circles without marker lines and a diamond) are shown together with reference tests from a previous part of the project (TMS1) (triangles).

In Figure 5-18 test results of MX-80 from this study (diamonds) are plotted together with results from comparable short-term laboratory heated specimens presented by Karnland et al. (2009) (circles), Dueck (2010) (squares) and Dueck (2014) (triangles). In Karnland et al. (2009) several specimens at the same dry density (1500 kg/m^3) were tested and a small but significant increase in strength and decrease in the corresponding strain were seen when the temperature was increased from 20°C to 150°C . The different colours (blue, green, yellow, orange, red) show the different temperatures (20°C , 90°C , 120°C , 150°C , $\geq 200^\circ\text{C}$).

The specimens tested by Dueck (2010) were exposed to 150°C and 200°C . At low dry density ($\sim 1420 \text{ kg/m}^3$) the trend with increased strength and decreased corresponding strain was confirmed with these tests. At higher density the impact of temperature on strength was more ambiguous but the strain was clearly decreasing with temperature. The specimens deviating the most from the trend in Figure 5-18, red square and blue square, showed no clear and continuous failure surface through the specimen at failure, but showed a propagation of more local fractures (Dueck 2010). An example of such failure is shown in Figure 5-19a which is the specimen corresponding to the deviating square in Figure 5-18. The cause of such failure surface is however not clear. The failure surface should be continuous through the specimen to represent the strength of it.

In the third mentioned test series (Dueck, 2014) specimens at saturated conditions were exposed to 90°C , 120°C and 150°C . In these series no large deviations from the references were seen but increased strength and decreased strain at temperatures above 120°C were observed.

Thus, increased strength as a consequence of increased temperature may occur. However, in the performed tests it cannot be excluded that uneven pore pressure was present which may have influenced the results. The majority of the specimens exposed to short-term heating at 150°C , 200°C and 240°C at saturated and laboratory-controlled conditions showed somewhat increased strength at decreased strain. The specimens deviating from this also deviated from having a continuous failure surface through the actual specimen.

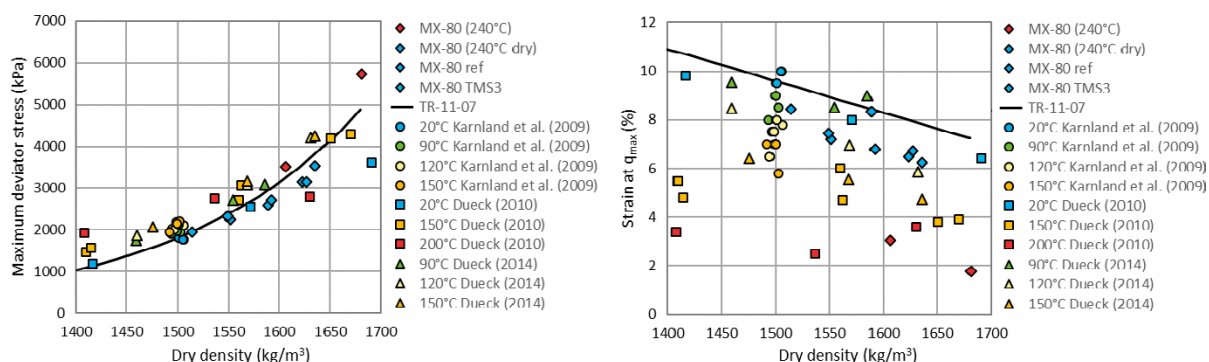


Figure 5-18. Test results from Figure 5-15(diamonds) are plotted together with results from Karnland et al. (2009) (circles), Dueck (2010) (squares) and Dueck (2014) (triangles).



Figure 5-19. Examples of failure without continuous surfaces going through the specimen, but rather with local fractures: a. MX-80 (specimen F124 exposed to 20°C , Dueck 2010), b. Calcigel, (TMS A2 exposed to 20°C , this study), c. Calcigel (UCT3-2 exposed to 240°C , this study).

The results for Calcigel are ambiguous, partly due to the scatter of the results, also in the references. Photos of the failure of the two specimens deviating the most from the maximum deviator stress in Figure 5-17 are shown in Figure 5-19b and c. Thus, the scatter in the results for Calcigel is to some extent caused by local fractures at failure but the cause of this is unclear. Specimens of Ca-dominated bentonites do not always behave as the Calcigel specimens above. In a previous study on the Ca dominated DepCaN (Dueck 2010) an increase in strength was shown after short-term heating at saturated conditions.

5.5 Additional observations and comments

Repeatability of the results from the unconfined compression tests was investigated by some test series and a relative low scatter was seen (Section 4.2.5 (Calcigel and GMZ) and Section 4.7.3 (MX-80)). From these test series the accuracy was evaluated. The evaluation was done by determination of a best fit line and then subtracting values according to the adopted line from the original data and analysing the residuals. The analysis was done by calculation of average and standard deviation. Similar evaluation of accuracy has been reported by e.g. Dueck (2014) and Svensson et al. (2019).

In Appendix 9 the accuracy is calculated and for MX-80 the average and standard deviation from the residual deviator stress at failure was -1 kPa and 48 kPa, respectively. When using the previously determined reference line TR-11-07 (Dueck et al. 2011a) the values were about 200 kPa which is logical since the reference line was determined on another batch of the material.

The degree of saturation is an important base variable. All specimens in this project, except two series in the study DS2, were saturated before the unconfined compression test. However, in some test series with saturated specimens excess salt was present and the degree of saturation was calculated to be less than 100 %. In specimens with excess salt the dry density was corrected for excess salt with an empirical relation directly applied to the determined dry density, see e.g. Appendix 1. However, the water content was not corrected. The influence of the content of salt on the water content is more complicated and relates to the dry mass and the water uptake caused by the salt. In this report the degree of saturation of specimens with excess salt was mainly calculated from the uncorrected water content and corrected dry density.

The evaluated shear strength is often related to mean stress or swelling pressure for modelling purposes and such relation has also been verified by triaxial tests. The unconfined compression test does not replace the more controlled triaxial test, but it gives a good estimate of the maximum deviator stress at failure. While the specimens used for the unconfined compression tests can be slightly influenced by dismantling from the saturation device before the tests the specimens used for the triaxial tests are tested at hydraulic and chemical equilibrium. However, stress paths and ion-exchange, mentioned in Section 5.2 above, will most probably influence the results from triaxial tests in the same way as indicated above.

The measured stresses after saturation have, in this project, been used as a measure of the swelling pressure irrespective of e.g. ion equilibrium or stress paths. To have a useful relationship between swelling pressure and strength (and avoid ambiguous results indicated in Section 5.2.3), a swelling pressure that refers to a specific condition is required. According to Birgersson and Karnland (2015) the swelling pressure should refer to a specific condition of a saturated specimen at a given set of exchangeable cations and given density, contacted at room-temperature with non-pressurized de-ionized water. In this context the given density implies a homogeneously distributed density and constant volume conditions. When stresses, determined at conditions deviating from these specific conditions, are correlated to strength, factors are introduced into the relationship although these do not influence the strength as a function of dry density.

6 Conclusions

6.1 General

In this project the unconfined compressive strength of different bentonites has been studied. The effect of ion-exchange, the effect of different stress paths and the combined effect of drying and heating of saturated specimens have been studied. A series with unsaturated specimens exposed to drying has also been included in the study. In this section the unconfined compressive strength is generalized to strength.

Concluding remarks were given after each section with results in Chapter 4. In Section 6.2, below, the most important concluding remarks regarding the unconfined compressive strength (strength) are compiled. In Section 6.3 some additional remarks regarding the results from this project are presented. All specimens, except those in the two unsaturated series, were considered to be saturated before the unconfined compression tests. The dry density of the specimens tested was between 1 300 and 1 800 kg/m³.

Regarding ion-exchanged specimens only Ca²⁺ dominated bentonites are considered. The conclusions regarding effects of ion-exchange are, in general, based on results from specimens without excess salt (ion-exchanged with the methodologies B or D, see Section 3.6.2).

6.2 Conclusions from each different test series

Test series TMS1

The *influence of ion-exchange (methodology B)* on the unconfined compressive strength was studied on the four materials *Calcigel, Deponit CaN, Febex and GMZ*.

Compared to each reference material at the same dry density the results from the tests on ion-exchanged Ca²⁺ dominated materials showed the following:

- The strength was
 - higher for Febex and GMZ,
 - approximately the same for Deponit Ca-N.
- The corresponding strain was
 - lower for Febex and GMZ,
 - approximately the same for Deponit Ca-N.

Regarding the relations between strength and estimated swelling pressure for each material it was observed that the results of the reference materials and of the ion-exchanged materials of Deponit Ca-N, Febex and GMZ followed the same trend, however, with some scatter and some deviation of the results from ion-exchanged Deponit Ca-N.

Test series TMS2

The influence of *ion-exchange (methodology C)* on the unconfined compressive strength was studied on the three bentonites *Asha505, Ikosorb and Kunigel*. The actual method for the ion-exchange, to get Ca²⁺ dominated materials, involved compacted specimens at confined conditions with excess salt left. The dry density was corrected for excess salt, when relevant.

Compared to each reference material and as a function of dry density the results from tests on the Ca²⁺ dominated materials showed

- a strength that was approximately the same for Asha505, Ikosorb and Kunigel
- a corresponding strain that was approximately the same for Asha505, Ikosorb and Kunigel.

Regarding the relation between strength and swelling pressure the relationship is almost the same for the three reference materials although the relationship deviates when the strength is plotted as a function of dry density, especially regarding Kunigel.

Test series TMS3

The influence of *ion-exchange (methodology A–D)* on the unconfined compressive strength was studied on the three bentonites *MX-80, Ikosorb and GMZ*. The ion-exchange to get Ca^{2+} dominated materials was made on both powder samples and compacted specimens and both with and without excess salt left. The dry density was corrected for excess salt when relevant.

Regarding the effects of the different methodologies used for the ion-exchange the results showed that

- dry density has to be corrected for excess salt after the ion-exchange
- unconfined compressive strength seemed to be independent of the methodology used for the ion-exchange, however, a scatter was observed
- there was a scatter in the strain at failure but also a tendency that lower strain was observed on specimens ion-exchanged as powder compared to those ion-exchange as confined specimens.

Compared to the references of each material and plotted as a function of dry density, the ion-exchanged specimens (without excess salt) showed

- no large deviations in the unconfined compressive strength
- a scatter in the strain at failure but also a tendency that the materials MX-80 and GMZ followed the references while Ikosorb showed lower strain than the reference.

Regarding the relationship between strength and swelling pressure:

- Approximately the same relationship is followed by the three materials tested (MX-80, Ikosorb and GMZ) both regarding the original material and the ion-exchanged material without excess salt.
- Somewhat higher strength was observed in the test results on specimens containing excess salt when plotted as a function of swelling pressure although this was not seen when the strength is plotted as a function of corrected dry density.

Test series SC-OEOC

The influence of *stress path* on the unconfined compressive strength was studied on the bentonite *MX-80*. After consolidation or swelling with constant axial load and no radial deformation during saturation the resulting measured stresses showed that

- the radial and axial stresses were different after consolidation but not after swelling (i.e. a deviator stress was introduced during consolidation)
- after consolidation with a constant axial load the final dry density was lower than the dry density after swelling with the same axial load, cf. Figure 4-25
- compared to the model presented by Börgesson et al. (1995) the final stress state after consolidation was higher than predicted by the model while the final stress state after swelling was lower.

Regarding the unconfined compression tests:

- The strength as a function of dry density showed
 - correspondence between the results from specimens prepared at different stress paths, irrespective of consolidation or swelling
 - correspondence between the model presented by Börgesson et al. (1995) and the test results, irrespective of the stress paths at preparation.
- The corresponding strain as a function of dry density showed
 - a tendency to lower strain measured after consolidation compared to after swelling.

Regarding the relationship between strength and swelling pressure:

- There is a trend that the consolidated specimens showed lower strength compared to the specimens that swelled, which follows from the observation that at constant axial load the final dry density is lower after consolidation than after swelling (cf. Figure 4-25).
- The model (Börgesson et al. 1995) shows values between the results of the swelled and consolidated specimens.

Test series DS1

The *combined effect of content of CaCl₂ and drying at 90 °C* on the strength was studied on the bentonite MX-80. The dry densities used for the analyses have been corrected for excess salt, when relevant.

Regarding the unconfined compression tests:

- The strength as a function of dry density indicated that
 - the combination of heating and ion-exchange gave small deviations compared to the reference of MX-80 at a corrected dry density above 1 500 kg/m³, cf. Figure 4-41.
- The corresponding strain as a function of dry density was
 - somewhat lower for the specimens exposed to a combination of heat and ion-exchange, cf. Figure 4-41.

Based on the swelling pressure measured during the preparation (measured during the saturation before the unconfined compression test but after the ion-exchange and heating) it was observed that while the strength deviates from the reference when related to the swelling pressure it does not deviate that much when related to the dry density (corrected for excess salt), cf. Figure 4-42 and above.

Test series DS2

The effect of *drying* at room temperature on the strength of *unsaturated MX-80* was studied. Considering strength as a function of dry density of $\rho_d = 1\ 600\text{--}1\ 800\ \text{kg/m}^3$ and compared to reference tests on saturated specimens of MX-80

- increased strength was observed on unsaturated specimens exposed to drying
- slightly lower strength was observed on unsaturated specimens exposed to hydration.

Test series UCT

A limited number of specimens *exposed to short-term heating to 240 °C at saturated conditions* were tested. Unfortunately, it cannot be excluded that the test methodology influenced the results but compared to the references of each material the following were found:

- Increased strength and stiffness were found for specimens of MX-80 and Asha505.
- No increase in strength and no clear increase in stiffness was seen for the specimens of Calcigel.
- Failure at reduced strain was seen for the specimens of MX-80, Asha505 and Calcigel.
- A rapid decrease in stress at low strain, i.e. brittle failure, was seen for almost all specimens.

The results of the specimens heated to 240 °C at unsaturated drying conditions and subsequently saturated, agreed well with references of each material.

6.3 Concluding remarks

Strength as a function of dry density and influence of ion-exchange

Strength is dependent on the dry density and the type of bentonite. There are no indications that equilibrium with an external salt solution (CaCl₂) will influence the strength, however, any excess salt at dismantling should be corrected for. In the main part of the materials tested no large influence of ion-exchange (to Ca-dominated material) on strength was seen (Figure 5-2 to Figure 5-4). However, removal of the accessory minerals will influence the strength (Figure 5-5 and Figure 5-6).

Strength as a function of stress

When strength is plotted as a function of swelling pressure and the influence of e.g. the montmorillonite content is taken into account the scatter between the results from materials with different montmorillonite contents will decrease. This seems also to be the case for ion-exchanged materials (Ca-dominated).

However, to have a useful relationship between swelling pressure and strength the swelling pressure should refer to a specific condition (cf. Section 5.5) including e.g. saturation at constant volume condition and equilibrium with de-ionized water. When average stresses at deviating conditions are correlated to strength, factors can be introduced into the relationship although these do not influence the strength as a function of dry density. Two examples are given here:

- The stress paths (swelling or consolidation) will influence the final density at a certain value of average stress. Since the actual dry density seems to be directly coupled to the strength, a certain value of average stress may result in different strengths (Figure 4-27).
- Saline solution in equilibrium with the specimens will influence the average stress. However, it seems not to influence the strength so the strength at a certain dry density may be coupled to different average stresses depending on the external salt solution (Figure 5-11).

Influence of drying

The effect of drying by exposure to a combination of CaCl_2 (including ion-exchange) and heating ($T=90\text{ }^\circ\text{C}$) was studied on specimens of MX-80. Compared to references the drying caused no or small deviations for the saturated specimens of MX-80, cf. Figure 5-13. However, the strain was somewhat lower compared to specimens that were only ion-exchanged.

Unsaturated specimens exposed to drying resulted in an increase in strength, the increased dry density taken into account. This deviated from previous results of MX-80 where no influence of the degree of saturation was seen in the actual range of dry density ($1\ 600\text{--}1\ 800\ \text{kg/m}^3$) and degree of saturation ($S_r > 70\%$). Thus, it seems as the drying has an influence. Small strain at failure was mainly seen for the specimens placed at $RH=85\%$ and especially where no drying took place. However, according to results on specimens re-saturated after drying increased strength is not expected after saturation.

Any increased strength at a temperature of $240\text{ }^\circ\text{C}$

A limited number of specimens of different bentonites were exposed to accelerating conditions with short time heating to $240\text{ }^\circ\text{C}$ in order to study the influence on strength. The results of the heating at saturated conditions showed that in almost all specimens a brittle behaviour developed with a rapidly decreasing stress at low strain. However, somewhat different behaviour was seen in the three tested materials (MX-80, Asha505 and Calcigel) since the increased strength and stiffness in the specimens of MX-80 and Asha505 were not observed in the specimens of Calcigel. The results of the specimens heated to $240\text{ }^\circ\text{C}$ at unsaturated drying conditions and subsequently saturated, agreed well with the references of each material.

Thus, increased strength as a consequence of increased temperature may occur. The majority of the specimens exposed to short-term heating to $240\text{ }^\circ\text{C}$ at saturated and laboratory-controlled conditions showed increase strength and decreased strain at failure. However, in the performed tests it cannot be excluded that the test methodology influenced the results.

References

SKB's (Svensk Kärnbränslehantering AB) publications can be found at www.skb.com/publications.

- Birgersson M, Karnland O, 2015.** Flow and pressure response in compacted bentonite due to external fluid pressure. SKB TR-14-28, Svensk Kärnbränslehantering AB.
- Birgersson M, Karnland O, Nilsson U, 2008.** Freezing in saturated bentonite – A thermodynamic approach. *Physics and Chemistry of the Earth* 33, S527–S530.
- Börgesson L, Johannesson L-E, Sandén T, Hernelind J, 1995.** Modelling of the physical behavior of water saturated clay barriers. Laboratory test, material models and finite element application. SKB TR 95-20, Svensk Kärnbränslehantering AB.
- Börgesson L, Johannesson L-E, Hernelind J, 2004.** Earthquake induced rock shear through a deposition hole. Effect on the canister and the buffer. SKB TR-04-02, Svensk Kärnbränslehantering AB.
- Börgesson L, Dueck A, Johannesson L-E, 2010.** Material model for shear of the buffer – evaluation of laboratory test results. SKB TR-10-31, Svensk Kärnbränslehantering AB.
- Clarke E C W, Glew D N, 1985.** Evaluation of the thermodynamic functions for aqueous sodium chloride from equilibrium and calorimetric measurements below 154 °C. *Journal of Physical and Chemical Reference Data* 14, 489–610.
- Craig R F, 1974.** *Soil mechanics*. London: Chapman & Hall.
- Dueck A, 2010.** Thermo-mechanical cementation effects in bentonite investigated by unconfined compression tests. SKB TR-10-41, Svensk Kärnbränslehantering AB.
- Dueck A, 2014.** Laboratory studies on stress-strain behavior (Deliverable D2.2-12). Long-term Performance of Engineered Barrier Systems PEBS. European Commission.
- Dueck A, Börgesson L, 2015.** Thermo-mechanically induced brittleness in compacted bentonite investigated by unconfined compression tests. *Engineering Geology* 193, 305–309.
- Dueck A, Nilsson U, 2010.** Thermo-hydro-mechanical properties of MX-80. Results from advanced laboratory tests. SKB TR-10-55, Svensk Kärnbränslehantering AB.
- Dueck A, Börgesson L, Johannesson L-E, 2010.** Stress-strain relation of bentonite at undrained shear. Laboratory tests to investigate the influence of material composition and test technique. SKB TR-10-32, Svensk Kärnbränslehantering AB.
- Dueck A, Johannesson L-E, Kristensson O, Olsson S, 2011a.** Report on hydro-mechanical and chemical-mineralogical analyses of the bentonite buffer in Canister Retrieval Test. SKB TR-11-07, Svensk Kärnbränslehantering AB.
- Dueck A, Johannesson L-E, Kristensson O, Olsson S, Sjöland A, 2011b.** Hydro-mechanical and chemical-mineralogical analyses of the bentonite buffer from a full-scale field experiment simulating a high-level waste repository. *Clay and Clay Minerals* 59, 595–607.
- Dueck A, Goudarzi R, Börgesson L, 2018.** Buffer homogenisation – status report 4. SKB TR-17-04, Svensk Kärnbränslehantering AB.
- Greenspan L, 1977.** Humidity fixed points of binary saturated aqueous solutions. *Journal of Research of the National Bureau of Standards, A. Physics and Chemistry* 81A, 89–96.
- Hedström M, Ekvy Hansen E, Nilsson U, 2016.** Montmorillonite phase behaviour. Relevance for buffer erosion in dilute groundwater. SKB TR-15-07, Svensk Kärnbränslehantering AB.
- Johannesson L-E, 2008.** Backfilling and closure of deep repository. Phase 3 – pilot tests to verify engineering feasibility. Geotechnical investigations made on unsaturated backfill materials. SKB R-08-131, Svensk Kärnbränslehantering AB.
- Karnland O, 2010.** Chemical and mineralogical characterization of the bentonite buffer for the acceptance control procedure in a KBS-3 repository. SKB TR-10-60, Svensk Kärnbränslehantering AB.

- Karnland O, Olsson S, Nilsson U, 2006.** Mineralogy and sealing properties of various bentonites and smectite-rich clay materials. SKB TR-06-30, Svensk Kärnbränslehantering AB.
- Karnland O, Olsson S, Dueck A, Birgersson M, Nilsson U, Hernan-Håkansson T, Pedersen K, Nilsson S, Eriksen T, Rosborg B, 2009.** Long term test of buffer material at the Äspö Hard Rock Laboratory, LOT project. Final report on the A2 test parcel. SKB TR-09-29, Svensk Kärnbränslehantering AB.
- Kozaki T, Fujishima A, Sato S, Ohashi H, 1998.** Self-diffusion of sodium ions in compacted montmorillonite. Nuclear Technology 121, 63–69.
- Man A, Martino J B, 2009.** Thermal, hydraulic and mechanical properties of sealing materials. NWMO TR-2009-20, Nuclear Waste Management Organization, Canada.
- Marshall T J, Holmes J W, Rose C W, 1996.** Soil physics. 3rd ed. Cambridge: Cambridge University press.
- Muurinen A, 1994.** Diffusion of anions and cations in compacted sodium bentonite. PhD thesis. Helsinki University of Technology. (VTT publications 168)
- Posiva SKB, 2017.** Safety functions, performance targets and technical design requirements for a KBS-3V repository. Conclusions and recommendations from a joint SKB and Posiva working group. Posiva SKB Report 01, Posiva Oy, Svensk Kärnbränslehantering AB.
- Russel W B, Saville D A, Schowalter W R, 1992.** Colloidal dispersions. Cambridge: Cambridge University Press.
- Sandén T, Nilsson U, Andersson L, Svensson D, 2018.** ABM45 experiment at Äspö Hard Rock Laboratory. Installation report. SKB P-18-20, Svensk Kärnbränslehantering AB.
- SIS, 2007.** SIS-CEN ISO/TS 17892-12:2007: Geotekniska undersökning och provning – Laboratorieundersökning av jord – Del 12: Bestämning av Atterbergs konsistensgränser. Geotechnical investigation and testing – Laboratory testing of soils – Part 12: Determination of Atterberg limits. Stockholm: Swedish Institute for Standards.
- Svensson D, Dueck A, Nilsson U, Olsson S, Sandén T, Lydmark S, Jägerwall S, Pedersen K, Hansen S, 2011.** Alternative buffer material. Status of the ongoing laboratory investigation of reference materials and test package 1. SKB TR-11-06, Svensk Kärnbränslehantering AB.
- Svensson D, Eriksson P, Johannesson L-E, Lundgren C, Bladström T, 2019.** Development and testing of methods suitable for quality control of bentonites as KBS-3 buffer and backfill. SKB TR-19-25, Svensk Kärnbränslehantering AB.
- Wadsö L, Svennberg K, Dueck A, 2004.** An experimentally simple method for measuring sorption isotherms. Drying Technology 22, 2427–2440.
- Åkesson M, Olsson S, Dueck A, Nilsson U, Karnland O, Kiviranta L, Kumpulainen S, Lindén J, 2012.** Temperature buffer test. Hydro-mechanical and chemical/mineralogical characterizations. SKB P-12-06, Svensk Kärnbränslehantering AB.

Tables

A1.1 Materials used

Table A1-1. Materials and batches of these used in the different parts of this study.

Material	Reference	Batches
Asha505	TMS2	Asha505 2006#1 (ABM45) crushed
Calcigel	TMS	Calcigel 2006#2 (ABM)
Deponit Ca-N	TMS	(ABM)
Febex	TMS	Febex 2012#01 (ABM45) crushed
GMZ	TMS, TMS3	GMZ 2011#03 (ABM45)
Ikosorb	TMS2, TMS3	Ikosorb 2011#6 (AMB45) crushed
Kunigel	TMS2	Kunigel 2012#4 (ABM45)
MX-80	TMS3, DS1, DS2, UCT	CT MX-80 2012#5
MX-80	SC-OE	CT MX-80 2015

A1.2 Estimations of swelling pressure

Equations used for estimations of swelling pressure Ps(1) or Ps(2)

$$P_s(1) = C \cdot \exp(D \cdot \rho_d) \tag{A1-1}$$

Table A1-2. Constants for determination of swelling pressure with Equation A1-1.

Material	Constants		Dry density interval		Reference
	C	D	Min kg/m ³	Max kg/m ³	
Deponit Ca-N ie B	0.197	0.0070	1490	1600	Dueck (2014)
Febex ie B	0.0643	0.0078	1540	1610	
GMZ ie B	0.0652	0.0074	1500	1570	
Febex ref	0.0244	0.0083	1420	1650	
MX-80 ref	1.306	0.0054	1570	1668	
MX-80 ie C	0.00215	0.0092	1570	1668	
MX-80 ie D	0.245	0.0065	1570	1668	
Ikosorb ref	0.0102	0.0085	1552	1655	
Ikosorb ie C	1.29E-05	0.013	1552	1655	
Ikosorb ie D	0.00150	0.010	1552	1655	
GMZ ref	0.00282	0.0089	1592	1707	
GMZ ie C	1.45E-05	0.012	1592	1707	
GMZ ie D	0.00151	0.0093	1592	1707	

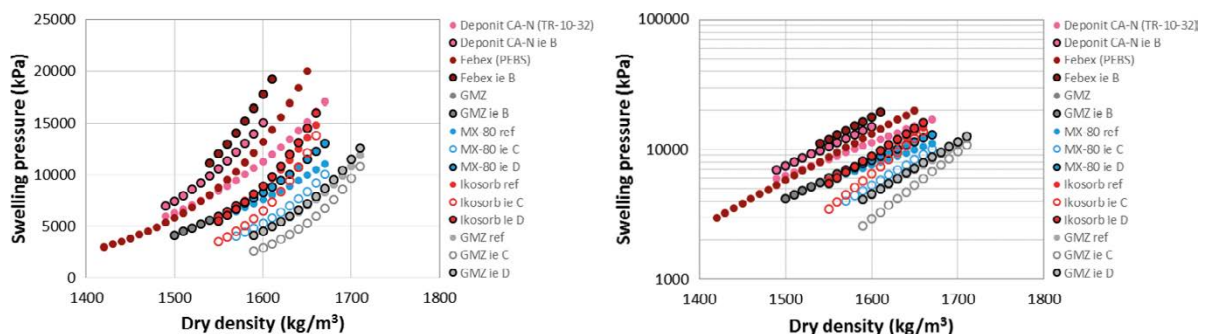


Figure A1-1. Calculated swelling pressure, Equation A1-1, used as estimated values from measured dry densities.

For Deponit Ca-N the swelling pressure was estimated from Equation A1-2 which is a relation expressed as a function of void ratio e with $p_0 = 1\,000$ kPa, $e_0 = 1.33$ and $\beta = -0.254$ according to Dueck et al. (2010). The valid interval of void ratio (dry density) is 0.65 to 0.85 ($1\,490$ kg/m³ to $1\,670$ kg/m³).

$$P_s(2) = p_0 \cdot \left(\frac{e}{e_0}\right)^{1/\beta} \quad (\text{A1-2})$$

A1.3 Correction of dry density due to excess salt

After ion-exchange with the methodology C the specimens contained excess salt in the interlayer water from the final equilibrium with 1M CaCl₂ before the dismantling. In an attempt to adjust the final dry density for this, the salt concentration of the specimen water was estimated to be the same as in the external solution and from the mass and the water content of the actual specimen the mass of the dissolved salt was calculated. The estimated mass of the dissolved salt was then removed from the total dry mass of the specimen and the dry density of the actual specimen was re-calculated, $\rho_{d,corrected}$, according to Equation A1-3 and the values A and B in Table A1-3.

$$\rho_{d,corrected} = A \cdot (\rho_d) + B \quad (\text{A1-3})$$

Table A1-3. Constants used for correcting dry density for excess salt with an external solution of 1M CaCl₂ with the Equation A1-3.

Material	A	B
MX-80	1.0529	-147
Ikosorb	1.0536	-147
GMZ	1.0542	-147
Asha505	1.0512	-147
Kunigel	1.0548	-147

A1.4 Influence of using small instead of tall specimens in the unconfined compression tests

The unconfined compression test can be used for determination of strength and then the specimens should have a height which is double the size of the diameter (tall specimens) to admit the failure surface to fully develop without end effects. However, specimens with the height equal to the diameter (small specimens) have often been used when aiming at comparison of the mechanical behaviour between different specimens. In this report small specimens with lubricated end surfaces have been used in all test series. In a previous project, hydro-mechanical analyses of material from the Canister Retrieval Test (Dueck et al. 2011a), the difference in results from small and tall specimens were analysed. From ten small and four tall specimens the best fit lines according to Figure A1-2 were found. Thus, (based on results from Dueck et al. 2011a) no large difference is expected on the strength when small specimens are used instead of tall but somewhat larger strain at failure.

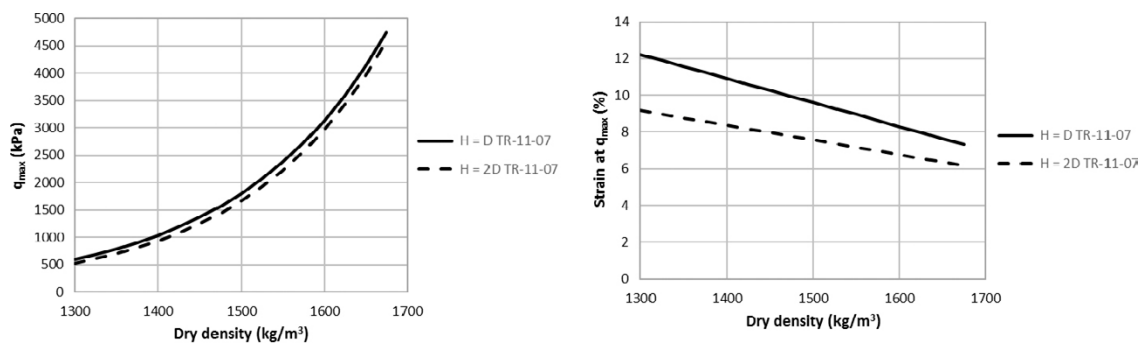


Figure A1-2. Maximum deviator stress as a function of dry density from small ($H = D$) and tall specimens ($H = 2D$), based on results from Dueck et al. (2011a).

Table A1-4. Test series of unconfined compression tests.

Study	Test series	Material	Preparation of specimens						
			Method of ion- exchange or ref material ¹	Excess salt added	Special stress paths	Exposure to heat, T_{max}	Fluid used ³	Stresses measured during prep	Number of specimens
TMS1	UCA	Calcigel	ref				DI-water		6
	UCA10	Calcigel	ref				DI-water		10
	UCB	Dep Ca-N	ref				DI-water		6
	UCBI	Dep Ca-N	ie B				DI-water	Yes ²	6
	UCC	FEBEX	ref				DI-water		6
	UCCI	FEBEX	ie B				DI-water	Yes ²	6
	UCD	GMZ	ref				DI-water		6
	UCDI	GMZ	ie B				DI-water	Yes ²	6
	UCD10	GMZ	ref				DI-water		10
TMS2	PUC1	Asha, Ikosorb, Kunigel	ref				DI-water	Yes	3
	PUC2	Asha, Ikosorb, Kunigel	ref				DI-water	Yes	3
	PUC3	Asha, Ikosorb, Kunigel	ref				DI-water	Yes	3
	UC1	Asha, Ikosorb, Kunigel	ref and ie C				DI-water/1M CaCl ₂		6
	UC2	Asha, Ikosorb, Kunigel	ie C				1M CaCl ₂		10
	UC3	Asha, Ikosorb, Kunigel	ref				DI-water		3
	UC4	Asha, Ikosorb, Kunigel	ref and ie C				DI-water/1M CaCl ₂		6
TMS3	PUC1	MX-80, Ikosorb, GMZ	ie D				DI-water	Yes	3
	PUC2	MX-80, Ikosorb, GMZ	ie D				DI-water	Yes	3
	UC1	MX-80, Ikosorb, GMZ	ie A and ie B				1M CaCl ₂ /DI-water		6
	UC2	MX-80, Ikosorb, GMZ	ie B				DI-water		6
	UC3	MX-80, Ikosorb, GMZ	ie A				1M CaCl ₂		6
	UC4	MX-80, Ikosorb, GMZ	ie C				1M CaCl ₂		10
	UC5	MX-80, Ikosorb, GMZ	ie D				DI-water		10
	UC6	MX-80, Ikosorb, GMZ	ref				DI-water		10
UC7	MX-80, Ikosorb, GMZ	ie D				DI-water		10	

Study	Test series	Material	Preparation of specimens						
			Method of ion- exchange or ref material ¹	Excess salt added	Special stress paths	Exposure to heat, T_{max}	Fluid used ³	Stresses measured during prep	Number of specimens
SC-OE	OEUC_1	MX-80	ref		Constant axial stress		DI-water	Yes	2
	OEUC_2	MX-80	ref		Constant axial stress		DI-water	Yes	2
	OEUC_3	MX-80	ref		Constant axial stress		DI-water	Yes	2
	PUC1	MX-80	ref		No volume change		DI-water		2
	UC1	MX-80	ref		Large swelling		DI-water		6
	UC2	MX-80	ref		Large swelling		DI-water		10
	UC3	MX-80	ref		Water pressure		DI-water		6
	UC4	MX-80	ref		Comp. to saturation		DI-water		10
DS1	PUC1	MX-80	ie C, ie A			90 °C	1M CaCl ₂	Yes	3
	PUC2	MX-80	ie C, ie A			90 °C	1M CaCl ₂	Yes	3
	UC1	MX-80	ie C			90 °C	1M CaCl ₂ or 1M NaCl		6
	UC2	MX-80	ie A	CaCl ₂		90 °C	1M CaCl ₂		10
	UC4	MX-80	ie A	CaCl ₂		90 °C	1M CaCl ₂		10
	UC3	MX-80		CaO or Ca(OH) ₂			DI water		10
	UC5	MX-80		CaO			DI water		10
DS2	PUCA	MX-80	ie D				DI water	Yes	3
	PUCB	MX-80	ie B				DI water	Yes	3
	UCA	MX-80					75 % or 85 % ⁴		16
	UCB	MX-80		CaCl ₂			75 % or 85 % ⁴		20
	UCC	MX-80	ie B	CaCl ₂			DI water		6
	UCD	MX-80	ref				DI water		10
UCT	UCT1	MX-80				240 °C	DI water		2
	UCT2	Asha505				240 °C	DI water		2
	UCT3	Calcigel				240 °C	DI water		2
	UCT4 ⁵	MX-80, Asha505, Calcigel				240 °C/20 °C	DI water		10

¹ The different methods of ion-exchange ie A to ie D which were made according to Table 3-1. Reference, ref, material was also used for some tests.

² These additional specimens were used for measurements of swelling pressure only.

³ The final fluid before dismantling.

⁴ For unsaturated specimens the relative humidity RH is given.

⁵ The specimens heated were unsaturated at the exposure and then subsequently saturated.

Detailed results from TMS1

The preparation of specimens in series TMS1 was described in Section 3.6.2 and the results are presented in Section 4.2. In TMS1 the test series were made according to Table A2-1. Tabulated results are shown in Tables A2-2 and A2-3 and diagrams with results from the unconfined compression tests are shown in Figures A2-1 to A2-5.

Table A2-1. General information about the study TMS1.

Material	Reference specimens	Type of ion-exchange	Ps measured on specimens	Specimens with both Ps and UC
Calcigel	yes	no		
Dep-CaN	yes	i.e. B	i.e. B	no
Febex	yes	i.e. B	i.e. B	no
GMZ	yes	i.e. B	i.e. B	no

Table A2-2. Results from unconfined compression tests. The dry density and water content determined after the test and the maximum deviator stress q_{max} and corresponding strain ϵ are shown for each specimen. In the column with materials the ion-exchanged materials, ion-exchanged to be Ca-dominated, are marked with ie after the material denomination.

Test ID	Material	Final values			At failure	
		Dry density kg/m ³	Water content %	Deg. of saturation %	q_{max} kPa	ϵ %
TMS UC A1	Calcigel	1630	25.4	106	4650	4.1
TMS UC A2	Calcigel	1630	25.5	105	2030	1.8
TMS UC A3	Calcigel	1610	26.5	106	3150	3.2
TMS UC A4	Calcigel	1560	28.6	107	3450	6.8
TMS UC A5	Calcigel	1620	26.3	106	4230	4.4
TMS UC A6	Calcigel	1640	25.3	105	4370	3.3
TMS UC A10-1	Calcigel	1620	25.1	102	5050	5.5
TMS UC A10-2	Calcigel	1610	25.5	103	4640	7.7
TMS UC A10-3	Calcigel	1620	25.6	104	4450	7.3
TMS UC A10-4	Calcigel	1620	25.4	103	4210	7.2
TMS UC A10-5	Calcigel	1580	26.9	102	3430	5.8
TMS UC A10-6	Calcigel	1590	26.6	103	3640	6
TMS UC A10-7	Calcigel	1580	27.1	103	3590	7.2
TMS UC A10-8	Calcigel	1670	23.4	103	5130	5.7
TMS UC A10-9	Calcigel	1660	23.3	101	5140	5.1
TMS UC A10-10	Calcigel	1690	23	104	5700	5
TMS UC B1	Dep Ca-N	1670	23.3	98	5620	7
TMS UC B2	Dep Ca-N	1660	23.9	101	5710	9.1 ¹
TMS UC B3	Dep Ca-N	1650	24	99	5100	6.9
TMS UC B4	Dep Ca-N	1700	22.5	100	5710	4.5
TMS UC B5	Dep Ca-N	1650	24.2	100	5230	6.2
TMS UC B6	Dep Ca-N	1590	26.4	100	3790	9.6
TMS UC BI1	Dep Ca-N ie B	1640	24.5	100	4780	8.2
TMS UC BI2	Dep Ca-N ie B	1640	24.3	99	4620	8.6
TMS UC BI3	Dep Ca-N ie B	1620	25.1	99	4020	9.2
TMS UC BI4	Dep Ca-N ie B	1570	27.5	100	2990	8.6
TMS UC BI5	Dep Ca-N ie B	1630	24.6	98	4430	8.2
TMS UC BI6	Dep Ca-N ie B	1640	24.3	99	4670	8

Test ID	Material	Final values			At failure	
		Dry density kg/m ³	Water content %	Deg. of saturation %	q _{max} kPa	ε %
TMS UC C1	FEBEX	1590	26.6	101	4470	8.9
TMS UC C2	FEBEX	1590	26.9	102	4290	8.3
TMS UC C3	FEBEX	1580	26.8	100	4160	9.2
TMS UC C4	FEBEX	1530	29.1	101	3060	8.5
TMS UC C5	FEBEX	1570	27.4	101	3930	8.5
TMS UC C6	FEBEX	1600	26	100	4920	8.1
TMS UC CI1	FEBEX ie B	1610	25.3	99	6860	4
TMS UC CI2	FEBEX ie B	1610	25.4	99	6680	4.5
TMS UC CI3	FEBEX ie B	1590	26	98	6730	6
TMS UC CI4	FEBEX ie B	1560	27.2	98	4940	5
TMS UC CI5	FEBEX ie B	1590	25.6	97	6130	5.7
TMS UC CI6	FEBEX ie B	1630	24.2	98	6920	5
TMS UC D1	GMZ	1690	22.3	100	3990	6.6
TMS UC D2	GMZ	1690	22.4	101	4030	7.9
TMS UC D3	GMZ	1670	23	100	3460	8.9
TMS UC D4	GMZ	1630	24.7	101	2700	9.9
TMS UC D5	GMZ	1680	23	102	3750	6.6
TMS UC D6	GMZ	1700	22	101	4090	6.3
TMS UC DI1	GMZ ie B	1630	23.8	97	3760	2.8
TMS UC DI2	GMZ ie B	1610	24.3	96	3960	4.8
TMS UC DI3	GMZ ie B	1580	25.4	96	4810	3.9
TMS UC DI4	GMZ ie B	1540	27.3	98	3160	4.3
TMS UC DI5	GMZ ie B	1580	25.4	96	3450	4.6
TMS UC DI6	GMZ ie B	1610	25.4	101	4010	4.3
TMS UC D10-1	GMZ	1640	24.6	101	2840	9.5
TMS UC D10-2	GMZ	1630	24.7	101	2740	9.1
TMS UC D10-3	GMZ	1630	24.7	101	2780	9.6
TMS UC D10-4	GMZ	1640	24.2	101	2930	7.5
TMS UC D10-5	GMZ	1590	26.5	102	2230	9.2
TMS UC D10-6	GMZ	1590	26.6	101	2180	9.5
TMS UC D10-7	GMZ	1600	26.2	102	2320	10.1
TMS UC D10-8	GMZ	1690	22.4	100	3650	5.6
TMS UC D10-9	GMZ	1690	22.4	100	3840	6.7
TMS UC D10-10	GMZ	1690	22.3	100	3550	5.9

¹ Somewhat low specimen at shearing.

Table A2-3. Results from swelling pressure tests. The dry density and water content determined after the test are given with the evaluated swelling pressure. The letters ie included in the denomination of the material indicate the ion-exchange of the material.

Test ID	Material	Final values			Swelling pressure
		Dry density kg/m ³	Water content %	Deg. of saturation %	kPa
TMS P BI1	Dep Ca-N ie B	1490	31.2	102	6880
TMS P BI2	Dep Ca-N ie B	1560	28.6	102	11610
TMS P BI3	Dep Ca-N ie B	1600	26.9	102	14810
TMS P CI1	FEBEX ie B	1540	28.6	101	11110
TMS P CI2	FEBEX ie B	1610	26.1	101	21040
TMS P CI3	FEBEX ie B	1610	26.1	102	17560
TMS P DI1	GMZ ie B	1500	29.8	101	3950
TMS P DI2	GMZ ie B	1540	27.6	99	6260
TMS P DI3	GMZ ie B	1570	25.9	96	6510

A2.1 Unconfined compression tests- deviator stress as a function of strain

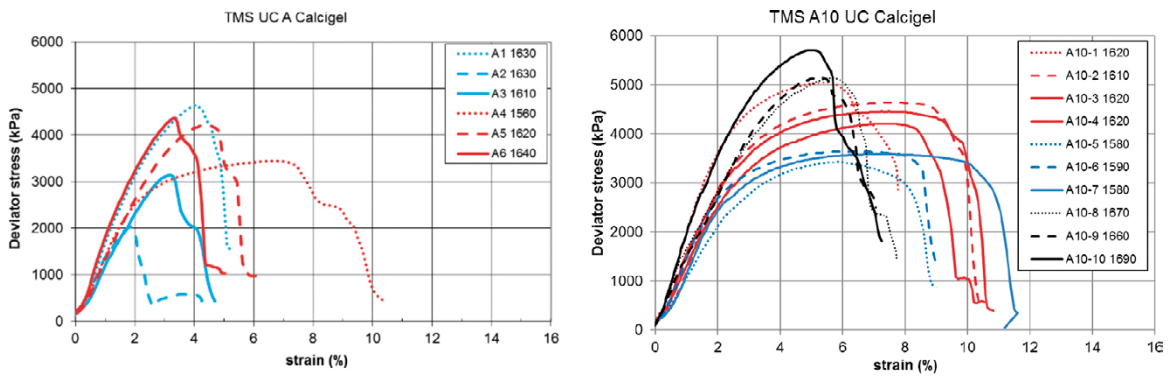


Figure A2-1. Results from unconfined compression tests on Calcigel.

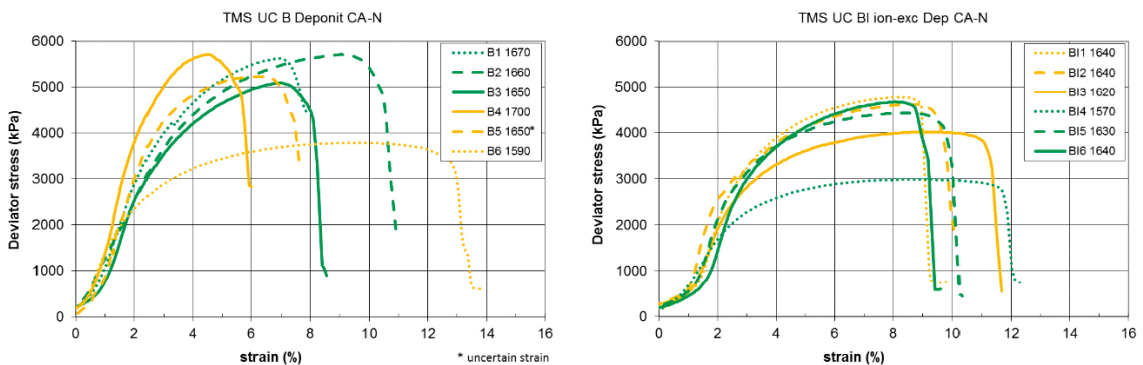


Figure A2-2. Results from unconfined compression tests on Deponit Ca-N (left) and ion-exchanged Ca-dominated Deponit Ca-N ie B(right).

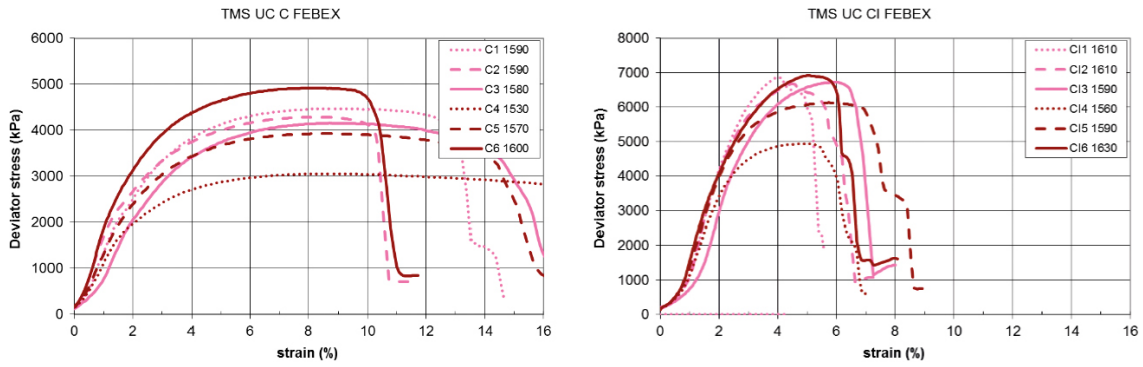


Figure A2-3. Results from unconfined compression tests on Febex (left) ion-exchanged Ca-dominated Febex ie B(right).

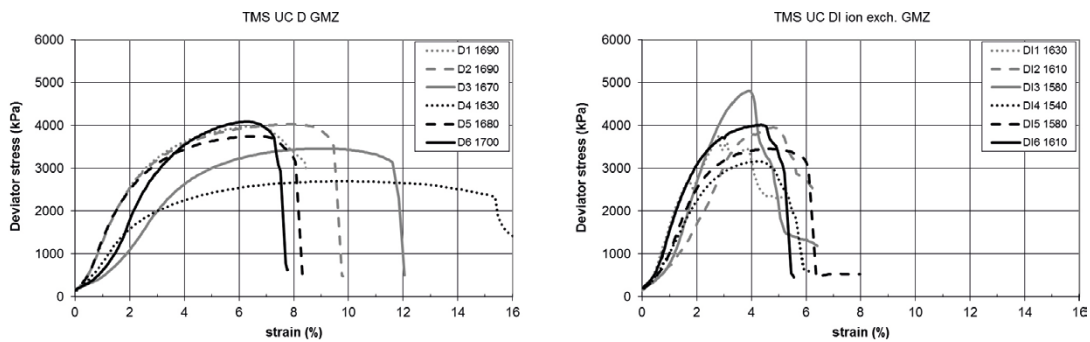


Figure A2-4. Results from unconfined compression tests on GMZ (left) and ion-exchanged Ca-dominated GMZ ie B (right).

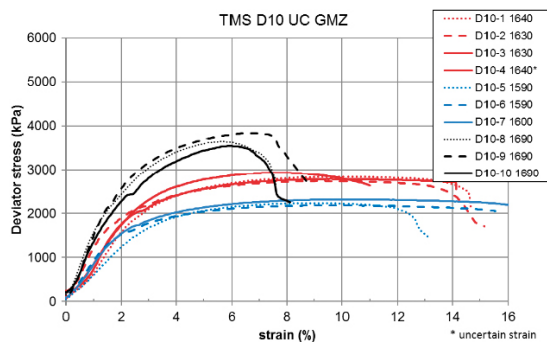


Figure A2-5. Results from unconfined compression tests on GMZ.

Detailed results from TMS2

The preparation of specimens in series TMS2 was described in Section 3.6.2 and the results are presented in Section 4.3. In TMS2 the test series were made according to Table A3-1. Tabulated results are shown in Tables A3-2 and diagrams with results from the unconfined compression tests are shown in Figures A3-1 to A3-4.

Table A3-1. General information about the study TMS2.

Material	Reference specimens	Type of ion-exchange	Ps measured on specimens	Spec. with both Ps and UC
Asha 505	yes	i.e. C	ref	yes
Ikosorb	yes	i.e. C	ref	yes
Kunigel	yes	i.e. C	ref	yes

Table A3-2. Results from unconfined compression tests. The dry density and water content determined after the test and the maximum deviator stress q_{max} and corresponding strain ϵ are shown for each specimen. The swelling pressure is given where this was measured before the unconfined compression test. In the column 'material' gr indicates grained material and ie indicates ion-exchanged materials.

Sample ID	Material	Dry density kg/m ³	Water content %	Degree of saturation %	Swelling pressure kPa	At failure	
						q _{max} kPa	ϵ at q _{max} %
TMS2 PUC1A	Asha505 gr	1654	25.3	99	14810	5160	5.1
TMS2 PUC1I	Ikosorb gr	1627	24.3	97	14160	3870	8.9
TMS2 PUC1K	Kunigel	1911	15.0	100	29250	8260	5.8
TMS2 PUC2A	Asha505 gr	1570	29.1	101	6890	3100	5.3
TMS2 PUC2I	Ikosorb gr	1605	25.5	99	10200	3320	8.0
TMS2 PUC2K	Kunigel	1816	17.7	100	15420	4610	6.3
TMS2 PUC3	Asha505 gr	1633	26.1	99	10150	4410	4.5
TMS2 PUC3I	Ikosorb gr	1561	27.0	98	7210	2530	9.2
TMS2 PUC3K	Kunigel	1774	19.5	102	10680	3440	8.2
TMS2 UC1 1A	Asha505 gr	1657	25.7	101		5270	6.2
TMS2 UC12I	Ikosorb gr	1629	24.5	98		3930	8.6
TMS2 UC13K	Kunigel	1907	15.3	101		7940	5.9
TMS2 UC1 4A	Asha505 gr ie C	1676 ¹	24.5	99		4990	6.0
TMS2 UC1 5I	Ikosorb gr ie C	1639 ¹	23.7	97		3330	9.1
TMS2 UC1 6K	Kunigel ie C	1905 ¹	14.9	98		5870	5.5
TMS2 UC2 1A	Asha505 gr ie C	1630 ¹	26.1	98		3470	5.4
TMS2 UC2 2A	Asha505 gr ie C	1641 ¹	25.5	98		3770	6.4
TMS2 UC2 3A	Asha505 gr ie C	1555 ¹	28.8	98		1840	5.2
TMS2 UC2 4I	Ikosorb gr ie C	1606 ¹	25.1	97		2450	9.2
TMS2 UC2 5I	Ikosorb gr ie C	1638 ¹	23.8	97		3350	9.2
TMS2 UC2 6I	Ikosorb gr ie C	1604 ¹	25.2	97		2440	9.3
TMS2 UC2 7K	Kunigel ie C	1900 ¹	15.1	98		5740	6.9
TMS2 UC2 8K	Kunigel ie C	1914 ¹	14.8	99		6750	7.0
TMS2 UC2 9K	Kunigel ie C	1864 ¹	15.9	97		4420	9.3
TMS2 UC2 10K	Kunigel ie C	1832 ¹	16.9	98		3360	9.8
TMS2 UC3 1A	Asha505 gr	1577	28.9	101		3260	6.1
TMS2 UC3 2I	Ikosorb gr	1617	24.8	98		3510	8.8
TMS2 UC3 3K	Kunigel	1838	17.4	102		4810	6.3
TMS2 UC4 1A	Asha505 gr ie C	1674 ¹	25.1	101		5040	4.4
TMS2 UC4 2I	Ikosorb gr ie C	1608 ¹	25.1	98		2500	7.2
TMS2 UC4 3K	Kunigel ie C	1794 ¹	18.3	99		2860	7.7
TMS2 UC4 4K	Kunigel	1765	19.7	102		3060	8.4
TMS2 UC4 5I	Ikosorb gr ²	1561	26.8	97		2520	9.6
TMS2 UC4 6K	Kunigel	1724	21.1	102		2230	10.7

¹ Original determined dry density without correction of excess salt.

² Corrected material.

A3.1 Unconfined compression tests – deviator stress as a function of strain

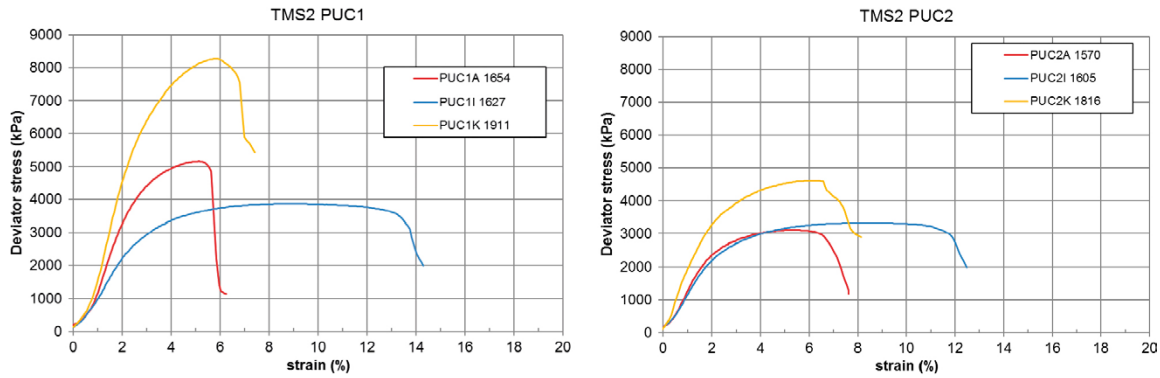


Figure A3-1. Test results from unconfined compression tests in the series PUC1 and PUC2. The legends contain the specimen ID and the dry density of the specimens, not corrected for any excess salt. The colours red, yellow and blue are used for the materials Asha505, Ikosorb and Kunigel, respectively.

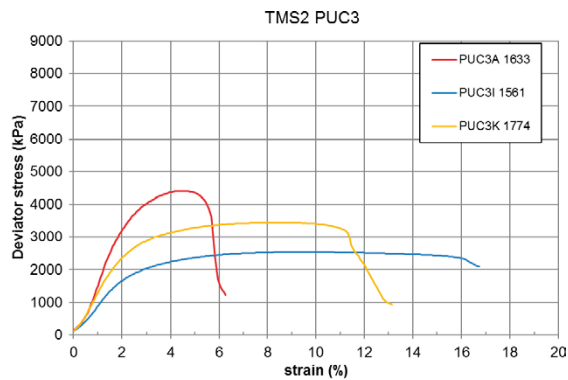


Figure A3-2. Test results from unconfined compression tests in the series PUC3. For the denominations given in the legend the colours used see Figure A3-1.

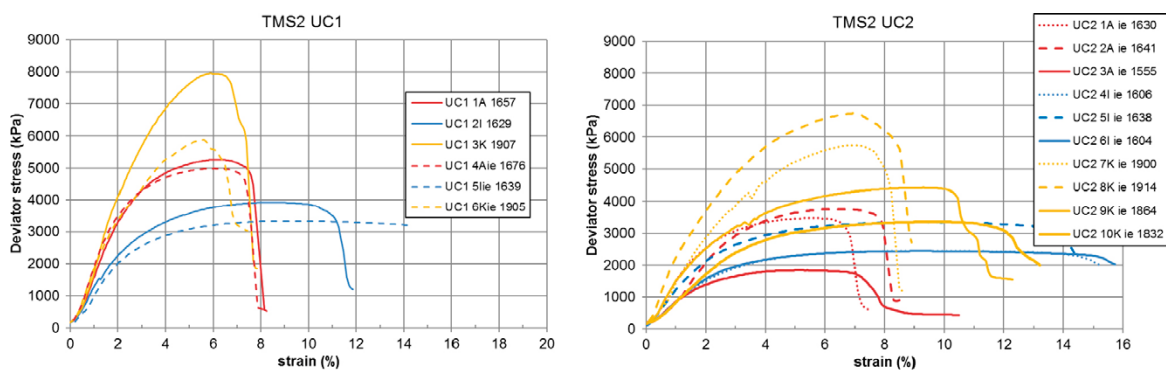


Figure A3-3. Test results from unconfined compression tests in the series UC1 and UC2. For the denominations given in the legend the colours used see Figure A3-1.

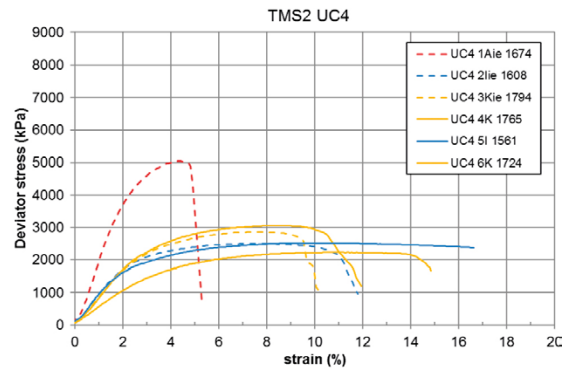
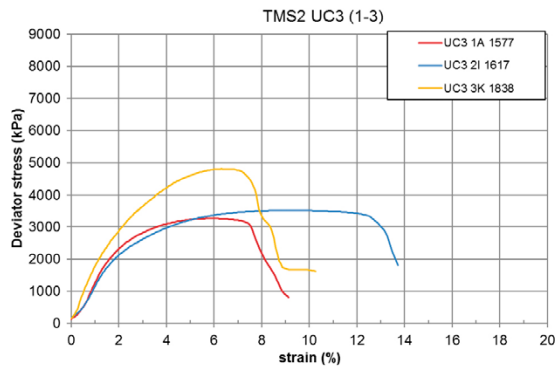


Figure A3-4. Test results from unconfined compression tests in the series UC3 and UC4. For the denominations given in the legend the colours used see Figure A3-1.

Detailed results from TMS3

The preparation of specimens in series TMS3 was described in Section 3.6.2 and the results are presented in Section 4.4. In TMS3 the test series were made according to Table A4-1. Tabulated results are shown in Tables A4-2 and diagrams with results from the unconfined compression tests are shown in Figures A4-1 to A4-5 and the time evolution of the swelling pressure in Figure A4-6.

Table A4-1. General information about the study TMS3.

Material	Reference specimens	Type of ion-exchange	Ps measured on specimens	Spec. with both Ps and UC
MX-80	yes	i.e. A,B,C,D	i.e. D (ref, ie C)	yes
Ikosorb	yes	i.e. A,B,C,D	i.e. D (ref, ie C)	yes
GMZ	yes	i.e. A,B,C,D	i.e. D (ref, ie C)	yes

Table A4-2. Resulting unconfined compressive strength q_{max} and corresponding strain ϵ together with final water content w , bulk density ρ and dry density ρ_d determined after dismantling. The type of ion-exchange (ie) refers to the four methodologies A–D, see Table 3-1, and reference specimens with no ion-exchange are denoted ref.

	Specimen ID	Material	Type of ion-exchange	w %	Density kg/m ³	Dry density kg/m ³	Degree of saturation %	At failure	
								q_{max} kPa	ϵ at q_{max} %
PUC1	PUC1M	MX-80	ie D ²	23.5	2060	1668	98	4216	5.5
	PUC1I	Ikosorb	ie D ²	22.9	2034	1655	96	4325	7.3
	PUC1G	GMZ	ie D ²	21.8	2079	1707	100	4048	4.1
PUC2	PUC2M	MX-80	ie D ²	27.4	2000	1570	99	2459	8.1
	PUC2I	Ikosorb	ie D ²	27.2	1973	1552	97	2241	9.1
	PUC2G	GMZ	ie D ²	26.0	2006	1592	100	2269	8.9
UC1	UC1 1	MX-80	ie A	26.2	2018	1600 ¹	99	1758	10.0
	UC1 2	Ikosorb	ie A	23.8	2045	1652 ¹	99	3034	6.7
	UC1 3	GMZ	ie A	22.4	2053	1678 ¹	98	2246	6.3
	UC1 4	MX-80	ie B	25.6	2035	1620	99	3313	6.8
	UC1 5	Ikosorb	ie B	25.8	2005	1594	98	2813	6.2
	UC1 6	GMZ	ie B	25.2	2023	1616	101	2709	6.4
UC2	UC2 1	MX-80	ie B	28.9	1986	1541	100	2045	7.6
	UC2 2	MX-80	ie B	23.7	2060	1665	99	4155	5.0
	UC2 3	Ikosorb	ie B	29.7	1936	1493	97	1555	7.2
	UC2 4	Ikosorb	ie B	24.2	2014	1622	96	3290	6.5
	UC2 5	GMZ	ie B	28.4	1954	1522	98	1511	5.5
	UC2 6	GMZ	ie B	23.9	2030	1638	99	2841	5.3
UC3	UC3 1	MX-80	ie A	32.2	1914	1448 ¹	97	551	14.3 ³
	UC3 2	MX-80	ie A	28.4	1975	1538 ¹	98	942	12.2
	UC3 3	Ikosorb	ie A	32.9	1881	1415 ¹	96	491	9.0 ³
	UC3 4	Ikosorb	ie A	29.8	1958	1509 ¹	100	895	10.0
	UC3 5	GMZ	ie A	31.6	1899	1442 ¹	97	431	9.5 ³
	UC3 6	GMZ	ie A	28.6	1958	1522 ¹	99	672	10.2
UC4	UC4 1	MX-80	ie C	27.0	1987	1565 ¹	97	1628	9.5
	UC4 2	MX-80	ie C	25.0	2029	1624 ¹	97	2234	6.9
	UC4 3	MX-80	ie C	23.4	2060	1669 ¹	98	3010	6.7
	UC4 4	MX-80	ie C	24.7	2037	1634 ¹	98	2369	6.2
	UC4 5	Ikosorb	ie C	26.1	1982	1571 ¹	96	1831	7.0
	UC4 6	Ikosorb	ie C	24.2	2013	1621 ¹	96	2635	6.9

	Specimen ID	Material	Type of ion-exchange	w %	Density kg/m ³	Dry density kg/m ³	Degree of saturation %	At failure	
								q _{max} kPa	ε at q _{max} %
	UC4 7	Ikosorb	ie C	22.9	2044	1664 ¹	97	3313	6.7
	UC4 8	GMZ	ie C	25.5	2019	1609 ¹	101	1481	6.3
	UC4 9	GMZ	ie C	24.1	2045	1648 ¹	101	1975	5.5
	UC4 10	GMZ	ie C	21.9	2073	1700 ¹	100	2730	6.6
UC5	UC5 1	MX-80	ie D	27.0	1993	1569	97	2218	9.6
	UC5 2	MX-80	ie D	25.8	2021	1607	98	2648	9.4
	UC5 3	MX-80	ie D	24.1	2044	1647	97	3289	7.0
	UC5 4	MX-80	ie D	25.8	2020	1605	98	2689	7.4
	UC5 5	Ikosorb	ie D	27.1	1965	1546	96	1987	9.5
	UC5 6	Ikosorb	ie D	24.8	1995	1599	95	2595	8.4
	UC5 7	Ikosorb	ie D	23.2	2022	1641	95	3384	8.1
	UC5 8	GMZ	ie D	26.1	1992	1579	99	1826	9.5
	UC5 9	GMZ	ie D	24.2	2027	1631	99	2521	9.3
	UC5 10	GMZ	ie D	22.2	2060	1686	99	3381	7.6
UC6	UC6 1	MX-80	ref	30.3	1973	1514	101	1938	8.4
	UC6 2	MX-80	ref	27.1	2020	1589	101	2585	8.4
	UC6 3	MX-80	ref	25.8	2047	1627	101	3159	6.7
	UC6 4	MX-80	ref	26.7	2018	1592	100	2710	6.8
	UC6 5	Ikosorb	ref	28.7	1945	1511	97	1666	11.9
	UC6 6	Ikosorb	ref	25.7	1993	1586	97	2711	8.9
	UC6 7	Ikosorb	ref	25.0	2016	1612	98	3402	8.3
	UC6 8	GMZ	ref	28.7	1981	1540	102	1629	7.6
	UC6 9	GMZ	ref	25.6	2025	1613	102	2400	7.7
	UC6 10	GMZ	ref	22.8	2066	1683	101	3738	6.7
UC7	UC7 1	MX-80	ie D	30.1	1958	1504	99	1772	8.7
	UC7 2	MX-80	ie D	26.6	2008	1585	98	2524	7.6
	UC7 3	MX-80	ie D	24.9	2043	1636	99	3243	6.7
	UC7 4	MX-80	ie D	26.6	2011	1589	99	2621	7.4
	UC7 5	Ikosorb	ie D	29.0	1942	1506	97	1578	9.4
	UC7 6	Ikosorb	ie D	25.4	1987	1585	95	2720	9.3
	UC7 7	Ikosorb	ie D	24.1	2019	1627	97	3345	8.1
	UC7 8	GMZ	ie D	28.2	1971	1537	100	1530	9.5
	UC7 9	GMZ	ie D	25.5	2014	1605	100	2310	9.7
	UC7 10	GMZ	ie D	22.9	2066	1681	101	3547	8.3

¹ Original determined dry density without correction of excess salt.

² Including swelling pressure measurement during saturation.

³ Special evaluation of ε due to relatively low stress, uncertain value.

A4.1 Unconfined compression tests – deviator stress as a function of strain

In the diagrams below the results from all unconfined compression tests are shown. The colours (blue, red, grey) indicate the materials (MX-80, Ikosorb, GMZ). The legends contain information about the sample ID, letters indicating the material and type of preparation and the dry density determined after dismantling (e.g. PUC2 1 MD 1570). The letters (M, I, G) indicate the materials (MX-80, Ikosorb, GMZ) and the letters (A, B, C, D) indicate the methodology used for the ion-exchange to Ca²⁺ dominated material, see sections 4.4.2.

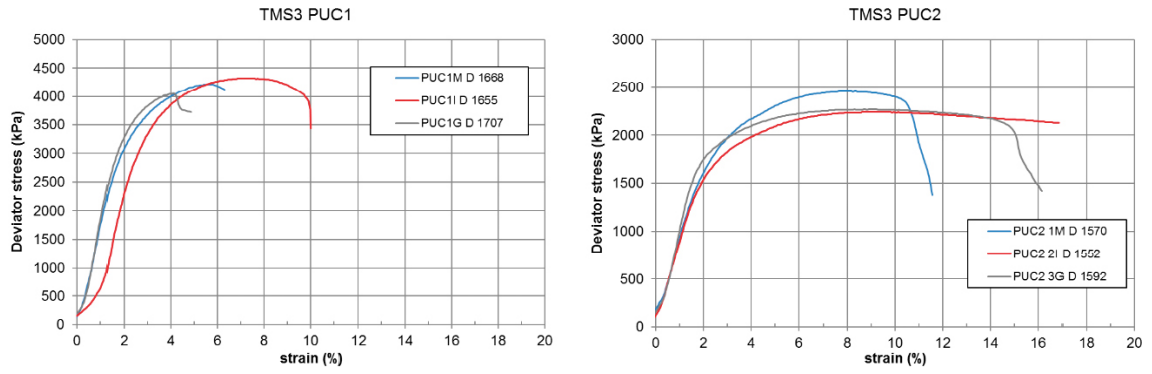


Figure A4-1. Unconfined compression tests on MX-80, Ikosorb and GMZ from the series PUC1 and PUC2 where swelling pressure was measured during preparation, see below.

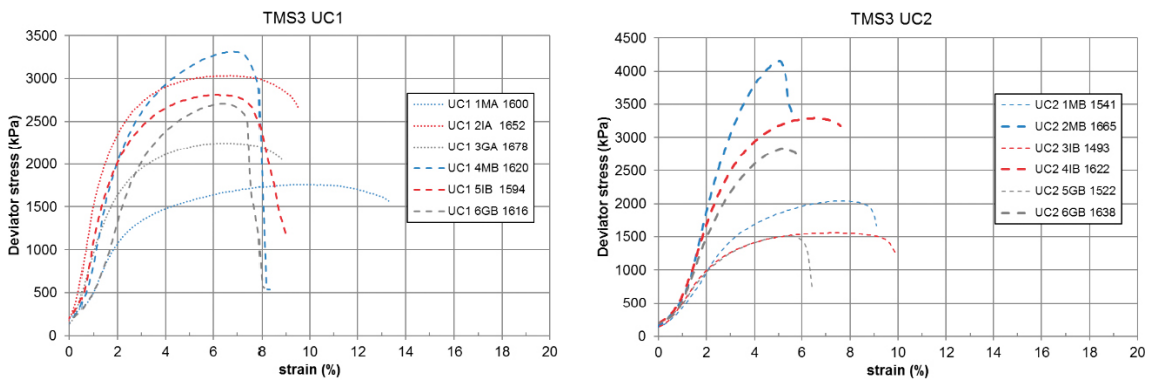


Figure A4-2. Unconfined compression tests on MX-80, Ikosorb and GMZ from the series UC1 and UC2.

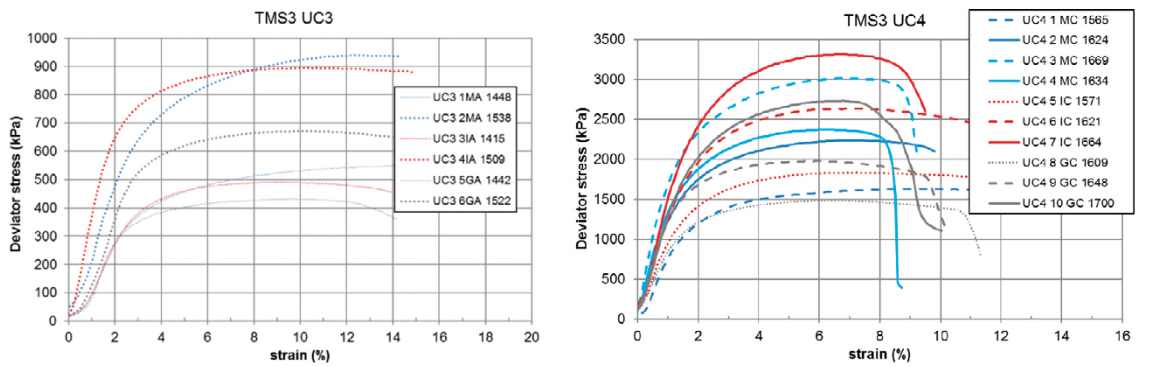


Figure A4-3. Unconfined compression tests on MX-80, Ikosorb and GMZ from the series UC3 and UC4.

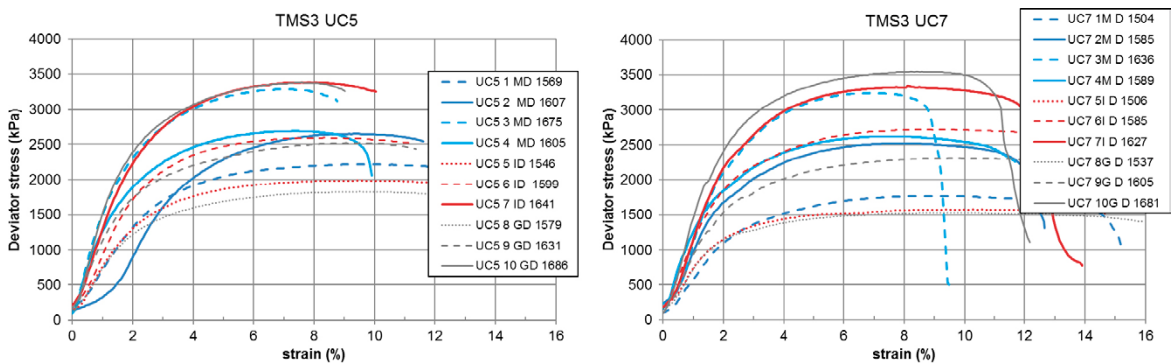


Figure A4-4. Unconfined compression tests on MX-80, Ikosorb and GMZ from the series UC5 and UC7.

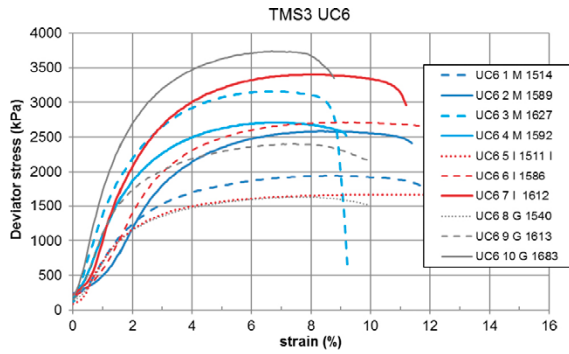


Figure A4-5. Unconfined compression tests on reference specimens of MX-80, Ikosorb and GMZ from the series UC6.

A4.2 Swelling pressure measurements – time evolution

In two series (PUC1 and PUC2) the swelling pressure was determined during the saturation with DI-water, ion-exchange with 1M CaCl₂ and during the final equilibrium with DI-water. The legend contains information about the sample ID and the material (MX-80, Ikosorb, GMZ) and in the diagrams the colours (blue, red, grey) indicate the materials, respectively. See also Section 4.4.3.

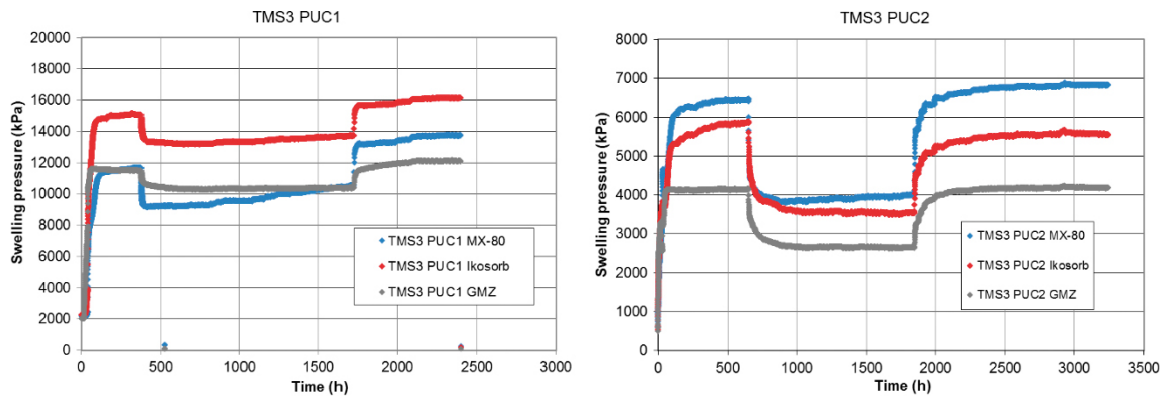


Figure A4-6. Swelling pressure measurement during preparation of specimens in the series PUC1 and PUC2. The marked change in swelling pressure at 400–600 h and 1700–1800 h occurred when the fluid was exchanged from the initial DI-water to 1M CaCl₂ and then back to DI-water. After dismantling the specimens were used for unconfined compression tests and the results are shown in Figure A4-1.

Detailed results from SC-OE

The preparation of specimens in the series SC-OE was described in Section 3.6.3 and the results are presented in Section 4.5. The results from the preparation with constant axial stress and no radial deformation during saturation (SCOE) are tabulated in Table A5-1 and the results from the unconfined compression tests on these specimens are shown in Table A5-2, cf. Section 4.5.2. The results from the series prepared at constant or almost constant volume during saturation (SCP) are given in Table A5-3 and Table A5-4, cf. Section 4.5.3. The amount of swelling given in Table A5-1 and Table A5-2 were calculated from the initial and final densities where the initial density was calculated from the density at compaction recalculated with the final diameter of the device and the final density was measured after dismantling.

Table A5-1. Results from the preparation of the specimen with constant axial stress. Water content, dry density and degree of saturation for the initial and final states are given together with the measured axial and radial stresses, the volume change and the time used for the preparation.

Sample ID	Initial state			Final state			Axial stress kPa	Radial stress kPa	Avr. stress kPa	Swell ² $\rho_{dif}/\rho_{dif}-1$ %	Time days
	Water content %	Dry density ¹ kg/m ³	degree of saturation %	Water content %	Dry density kg/m ³	Degree of saturation %					
SCOE_A_1c	40.2	1254	92	40.2	1327	102	1713	1295	1434	-5	55
SCOE_A_1s	21.8	1692	94	34.1	1425	100	1736	2280	2099	19	56
SCOE_A_2c	41.5	1251	94	36.7	1388	102	3499	2270	2679	-10	72
SCOE_B_2s	22.0	1675	93	30.5	1516	102	3707	4562	4277	10	72
SCOE_B_3c	40.4	1262	93	31.0	1484	99	7073	4397	5289	-15	56
SCOE_B_3s	20.4	1679	86	26.3	1625	103	7356	7001	7120	3	55

¹ Dry density with no gaps.

² Swell – positive values, consolidation – negative values.

Table A5-2. Results from unconfined compression tests on specimens in Table A5-1. The water content, dry density and degree of saturation after the tests and the maximum deviator stress q_{max} and corresponding strain ϵ are shown for each specimen.

Test ID	Final values			At failure	
	Water content %	Dry density kg/m ³	Degree of saturation %	q_{max} kPa	ϵ %
SCOEUC_1c	39.6	1336	102	576	10.8
SCOEUC_1s	33.5	1432	99	893	13.6
SCOEUC_2c	35.9	1406	102	1001	7.9
SCOEUC_2s	29.7	1533	101	1712	11.2
SCOEUC_3c	30.4	1500	99	1601	8.2
SCOEUC_3s	25.3	1632	100	2832	10.1

Table A5-3. Results from the preparation of specimens in the test series aiming at constant volume conditions. Water content, dry density and degree of saturation for the initial and final states are given together with the measured axial and radial stresses, the volume change and the time used for the preparation.

Test ID	Initial state			Final state			Axial stress kPa	Radial stress kPa	Avr. stress kPa	Swell ² $\rho_{dif}/\rho_{dif}-1$ %	Time days
	Water content %	Dry density ¹ kg/m ³	Degree of saturation %	Water content %	Dry density kg/m ³	Degree of saturation %					
SCPUC_A1	35.5	1346	93	37.9	1374	103	1866	1857	1860	-2	27
SCPUC_B1	27.5	1503	90	32.6	1484	104	4067	3022	3370	1	27

¹ Dry density with no gaps.

² Swell – positive values, consolidation – negative values.

Table A5-4. Results from unconfined compression tests on specimens prepared according to Table A5-3. The water content, dry density and degree of saturation after the test and the maximum deviator stress q_{max} and corresponding strain ϵ are shown for each specimen.

Test ID	Final values			At failure	
	Water content %	Dry density kg/m ³	Degree of saturation %	q_{max} kPa	ϵ %
SCPUCA1	35.9	1403	102	703	9.5
SCPUCB1	29.5	1539	102	1809	11.9

The results of the specimens prepared with a controlled final volume without stress measurements are presented in Table A5-5. Three different types of preparation were used; large swelling from high degree of saturation, minimized swelling from a high degree of saturation or applied water pressure during and after saturation, cf. Section 4.5.4.

Table A5-5. Results from unconfined compression tests. The water content, dry density and degree of saturation after the test and the maximum deviator stress q_{max} and corresponding strain ϵ are shown for each specimen.

Test ID	Final values			At failure		Preparation	
	Water content %	Dry density kg/m ³	Degree of saturation %	q_{max} kPa	e %	Type of prep. description ¹	Volume change %
SCUC1 1	31.0	1504	102	1478	15.0	axially	16
SCUC1 2	35.6	1408	102	844	15.0	axially	26
SCUC1 3	42.0	1295	102	423	15.0	axially	36
SCUC1 4	29.8	1527	101	1713	10.2	radially	16
SCUC1 5	36.1	1398	101	860	10.5	radially	27
SCUC1 6	42.1	1276	99	375	8.7	radially	39
SCUC2 1	32.4	1475	102	1303	15.1	axially	16
SCUC2 2	33.7	1447	102	1176	10.0	radially	18
SCUC2 3	32.2	1469	100	1272	15.0	axially	16
SCUC2 4	33.8	1450	102	1184	9.6	radially	18
SCUC2 5	32.3	1477	102	1241	15.0	axially	23
SCUC2 6	32.5	1486	104	1461	9.5	radially	19
SCUC2 7	32.6	1468	101	1284	14.9	axially	28
SCUC2 8	33.4	1443	100	1189	9.7	radially	30
SCUC2 9	32.3	1470	101	1338	14.4	axially	27
SCUC2 10	34.5	1422	101	1032	8.2	radially	31
SCUC3 1	46.2	1215	100	345	12.1	$P_w > 1\text{MPa}$	8
SCUC3 2	37.0	1365	99	751	13.0	$P_w > 1\text{MPa}$	7
SCUC3 3	30.8	1483	98	1498	11.4	$P_w > 1\text{MPa}$	10
SCUC3 4	46.8	1204	99	325	14.1	$P_w > 1\text{MPa}$	10
SCUC3 5	37.9	1342	98	621	14.0	$P_w > 1\text{MPa}$	7
SCUC3 6	31.4	1475	99	1437	10.4	$P_w > 1\text{MPa}$	9
SCUC4 1	48.3	1198	102	233	15.0	$S_{r,ini} = 89$	2
SCUC4 2	47.8	1200	101	229	11.0	$S_{r,ini} = 91$	4
SCUC4 3	32.0	1483	102	1231	12.8	$S_{r,ini} = 98$	5
SCUC4 4	40.1	1321	101	470	10.8	$S_{r,ini} = 94$	3
SCUC4 5	40.6	1321	102	468	13.3	$S_{r,ini} = 95$	3
SCUC4 6	39.9	1326	101	471	10.6	$S_{r,ini} = 95$	3
SCUC4 7	31.4	1492	101	1348	12.3	$S_{r,ini} = 97$	4
SCUC4 8	35.3	1414	102	835	11.1	$S_{r,ini} = 93$	3
SCUC4 9	35.3	1415	102	841	13.5	$S_{r,ini} = 95$	4
SCUC4 10	34.7	1424	101	854	9.6	$S_{r,ini} = 95$	3

¹ The types of preparation are swelling axially or radially (SCUC1 and SCUC2), introduction of water pressure, $P_w > 1$ MPa (SCUC3) or minimized swelling but starting from high degree of saturation $S_{r,ini}$ (SCUC4).

A5.1 Unconfined compression tests

The results from the unconfined compression tests are shown as deviator stress as a function of strain in Figure A5-1 to Figure A5-4.

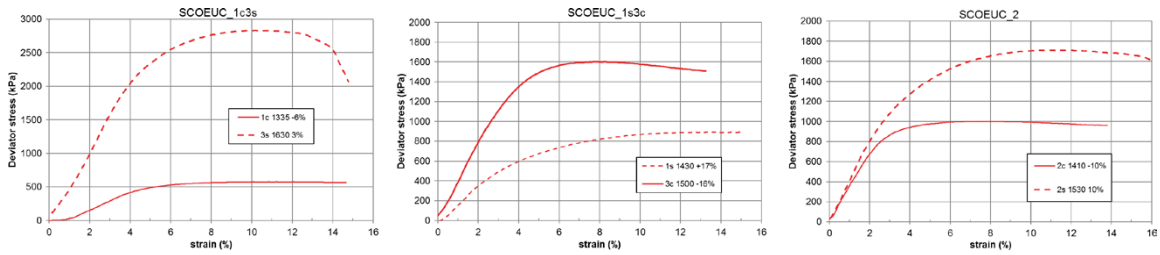


Figure A5-1. Results from unconfined compression tests on specimens in the SCOEUC series.

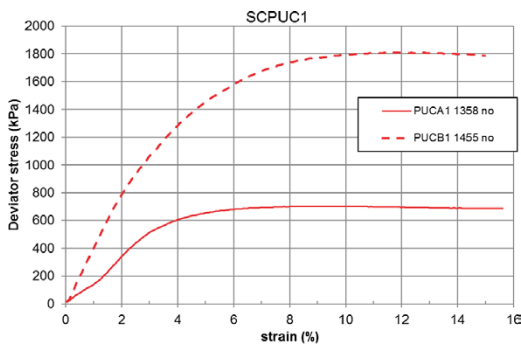


Figure A5-2. Results from unconfined compression tests on specimens in the SCPUC series.

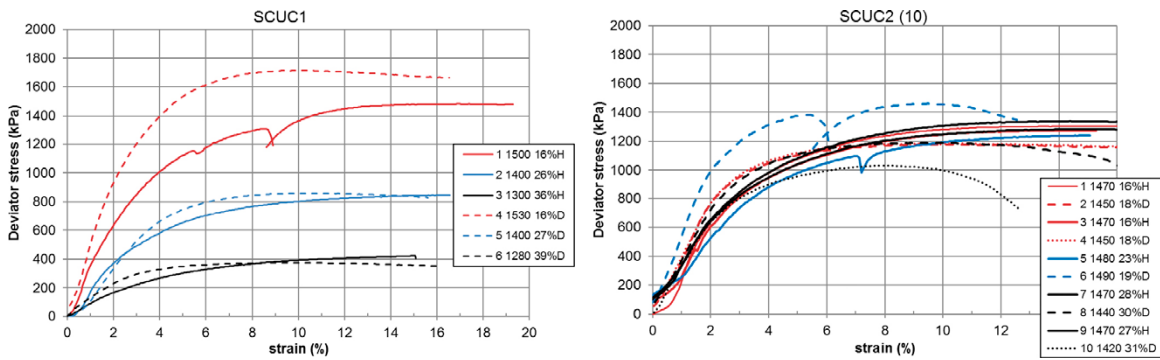


Figure A5-3. Results from unconfined compression tests on specimens in the series SCUC1 and SCUC2.

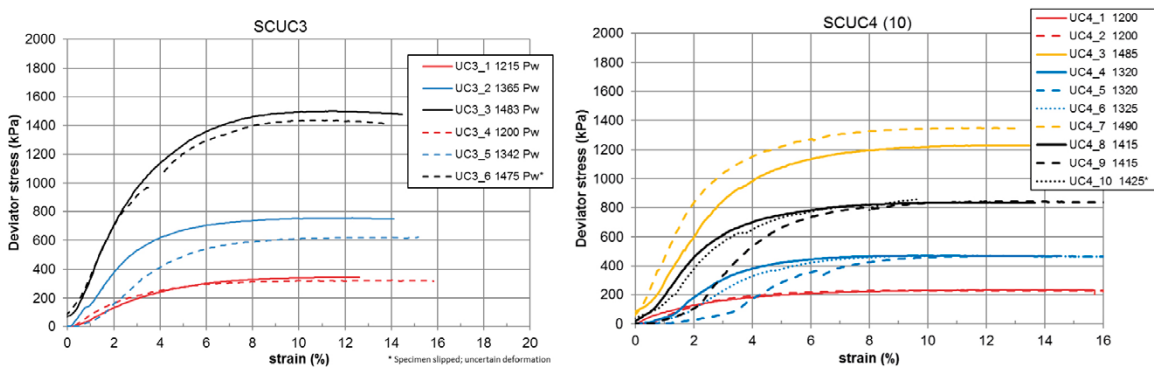


Figure A5-4. Results from unconfined compression tests on specimens in the series SCUC3 and SCUC4 series.

Detailed results from DS1

The preparation of specimens in the series DS1 was described in Section 3.6.4 and the results are presented in Section 4.6. Tabulated test results from the test series on the combined effect of content of chloride salts and drying at 90 °C are shown in Table A6-1 and Table A6-2 and from the test series on the effect of content of calcium oxide in Table A6-3.

Table A6-1. Resulting unconfined compressive strength q_{max} and corresponding strain ϵ together with base variables determined after the tests. Different preparations are mentioned as type of ion-exchange or amount of initially added salt and in addition, the maximum temperature (T_{max}) is given.

Series	Specimen ID	Ion-exchange ¹	Initially added salt ³ % of m_s	T_{max} °C	Water content %	Density kg/m ³	Dry density kg/m ³	Degree of saturation %	At failure	
									q_{max} kPa	ϵ at q_{max} %
PUC1	PUC1-1 ²	ie C		90	24.8	2026	1624	97	1836	5.6
	PUC1-2 ²	ie C		90	21.8	2079	1707	96	3493	5.1
	PUC1-3 ²	ie A		90	37.3	1830	1333	96	131	8.6
PUC2	PUC2-1 ²	ie C		90	23.7	2030	1641	95	2253	5.1
	PUC2-2 ²	ie C		90	21.7	2094	1721	98	3966	4.4
	PUC2-3 ²	ie A		90	28.8	1931	1499	94	373	8.0
UC1	UC1-1	ie C		90	25.4	2004	1599	95	1807	6.0
	UC1-2	ie C		90	22.9	2034	1656	94	2492	5.5
	UC1-3	ie C		90	21.8	2063	1694	94	3217	4.2
	UC1-4	ie C		90	27.3	1981	1556	96	1678	7.0
	UC1-5	ie C		90	25.1	2016	1611	96	2183	4.9
	UC1-6	ie C		90	23.2	2050	1664	96	3080	5.2
UC2	UC2-1			90	25.5	1969	1569	92	917	4.5
	UC2-2			90	24.6	1971	1581	90	1201	5.0
	UC2-3			90	23.0	2004	1630	90	1599	5.0
	UC2-4		17 % CaCl ₂	90	25.7	1934	1539	88	780	6.3
	UC2-5		24 % CaCl ₂	90	26.1	1934	1534	89	753	5.9
	UC2-6		15 % CaCl ₂	90	23.4	2019	1636	93	1544	5.5
	UC2-7		22 % CaCl ₂	90	25.4	1946	1551	89	899	6.3
	UC2-8	ie A		90	40.6	1809	1287	97	103	13.1 ^{4,5}
	UC2-9	ie A		90	40.1	1810	1293	97	98	12.9 ^{4,5}
	UC2-10	ie A		90	33.2	1865	1401	94	319	8.8 ⁴
UC4	UC4-1			90	22.0	1957	1605	83	694	3.3
	UC4-2			90	22.1	1996	1635	88	927	3.9
	UC4-3			90	21.3	2027	1671	89	1126	3.8
	UC4-4		14 % CaCl ₂	90	21.5	1934	1592	80	398	4.0
	UC4-5		20 % CaCl ₂	90	22.1	1927	1577	81	293	4.6
	UC4-6		13 % CaCl ₂	90	21.0	1998	1652	85	1279	4.5
	UC4-7		20 % CaCl ₂	90	22.0	1960	1606	84	896	4.8
	UC4-8	ie A		90	37.3	1785	1300	91	119	15.0 ^{4,5}
	UC4-9	ie A		90	33.6	1814	1358	89	191	10.2 ^{4,5}
	UC4-10	ie A		90	31.1	1857	1417	90	246	12.4 ^{4,5}

¹ Type of ion-exchange.

² Swelling pressure was measured during the preparation.

³ The amount of salt is given as the mass of salt to the dry mass of the specimen.

⁴ Special evaluation of ϵ due to relatively low maximum stress.

⁵ No clear failure was observed.

Table A6-2. Measured swelling pressure P_{s2} presented with water content and dry density measured after dismantling.

Series	Specimen ID	Water content %	Dry density kg/m ³	$P_{s2}(\text{CaCl}_2)$ kPa
PUC1	PUC1-1	24.8	1624	3436
	PUC1-2	21.8	1707	7132
	PUC1-3	37.3	1333	77
PUC2	PUC2-1	23.7	1641	4336
	PUC2-2	21.7	1721	8372
	PUC2-3	28.8	1499	440

Table A6-3. Resulting unconfined compressive strength q_{max} and corresponding strain ϵ together with base variables determined after the tests. The type and amount of added salt is given together with the maximum temperature (T_{max}) used.

Series	Specimen ID	Ion-exchange	Initially added salt ¹ % of m_s	T_{max} °C	Water content %	Density kg/m ³	Dry density kg/m ³	Degree of saturation %	At failure	
									q_{max} kPa	ϵ at q_{max} %
UC3	UC3-1		5 % CaO	20	31.1	1942	1481	99	2226	1.2
	UC3-2		5 % CaO	20	29.7	1937	1494	96	1558	1.6
	UC3-3		5 % CaO	20	28.4	1963	1529	97	1291	4.0 ²
	UC3-4		5 % CaO	20	26.0	2007	1592	97	1366	4.0 ²
	UC3-5		5 % CaO	20	26.5	1999	1580	97	3211	2.2
	UC3-6		5 % Ca(OH) ₂	20	33.0	1870	1405	94	959	3.7
	UC3-7		5 % Ca(OH) ₂	20	29.6	1911	1474	93	1065	2.9
	UC3-8		5 % Ca(OH) ₂	20	29.5	1916	1479	93	1352	2.4
	UC3-9		5 % Ca(OH) ₂	20	27.7	1963	1537	95	1879	3.3 ³
	UC3-10		5 % Ca(OH) ₂	20	27.2	1974	1552	96	1834	3.3
UC5	UC5-1		4 % CaO	20	32.8	1894	1426	96	1881	2.0
	UC5-2		4 % CaO	20	31.7	1902	1443	95	2020	1.7
	UC5-3		4 % CaO	20	25.2	1958	1564	90	3389	2.6
	UC5-4		4 % CaO	20	24.8	2048	1641	99	-	- ²
	UC5-5		4 % CaO	20	24.0	2016	1626	94	4568	3.1
	UC5-6		8 % CaO	20	28.1	1979	1544	98	4428	1.4
	UC5-7		8 % CaO	20	28.6	1995	1551	100	4077	1.9
	UC5-8		8 % CaO	20	24.6	2029	1628	97	6373	1.6
	UC5-9		8 % CaO	20	21.4	2096	1726	98	10363	2.8
	UC5-10		8 % CaO	20	21.5	2088	1719	97	9706	2.5

¹ The amount of salt is given as the mass of salt to the dry mass of the specimen.

² Very brittle specimens and two out of three such specimens were still sheared.

³ Somewhat low specimen at shearing.

A6.1 Results from unconfined compression tests

In the diagrams below, A6-1 to A6-4, the results from all unconfined compression tests are shown. The legends contain information about the specimen ID and the dry density determined after dismantling (e.g. PUC1-1 1624). The preparation of specimens is commented in the captions but are further described in Section 3.6.

A6.2 Results from swelling pressure measurement

In the test series PUC1 and PUC2 the swelling pressure was determined during the saturation with DI-water and the ion-exchange with 1M CaCl₂ (shown to the left of Figures A6-5 and A6-6 below) and during the final equilibrium with 1M CaCl₂ (shown to the right of Figures A6-5 and A6-6). No measurements were made during drying for 48h. Estimated water contents and dry densities after the ion-exchange from the first part of the preparation (shown to the left in the diagrams) are shown in Table A6-4.

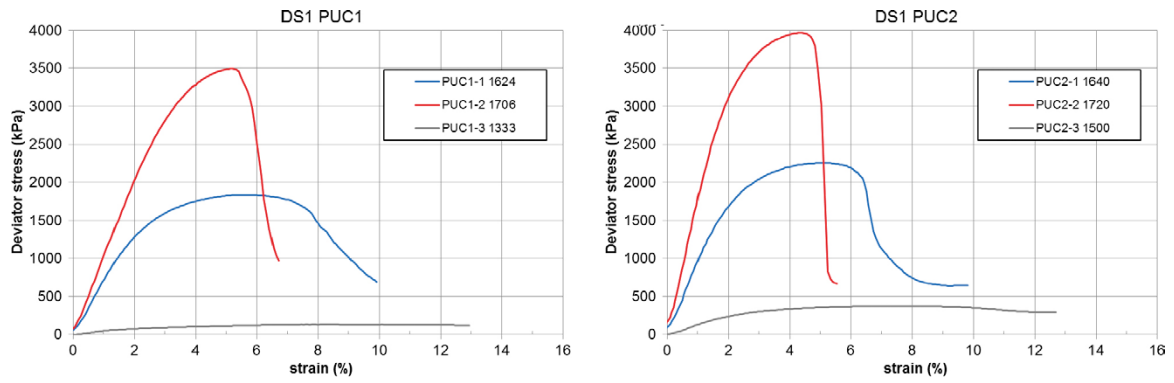


Figure A6-1. Unconfined compression tests on specimens of MX-80 ion-exchanged in-situ (red and blue lines) or ion-exchanged as powder (grey line). After the ion-exchange the dominating ion was Ca^{2+} . The specimens were dried at $90\text{ }^{\circ}\text{C}$ and then saturated with 1M CaCl_2 . Results from series PUC1 and PUC2.

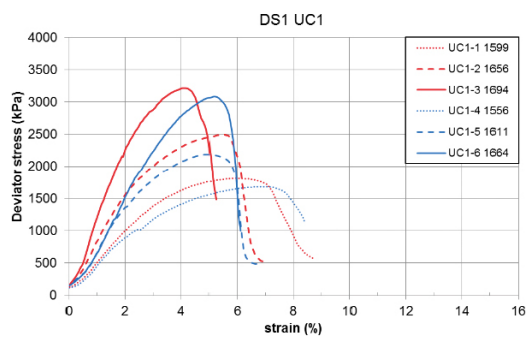


Figure A6-2. Unconfined compression tests on specimens of MX-80 ion-exchanged in-situ. After ion-exchange the dominating ions were Ca^{2+} (red lines) and Na^{+} (blue lines). The specimens were dried at $90\text{ }^{\circ}\text{C}$ and then saturated with 1M CaCl_2 and 1M NaCl , respectively. Results from series UC1.

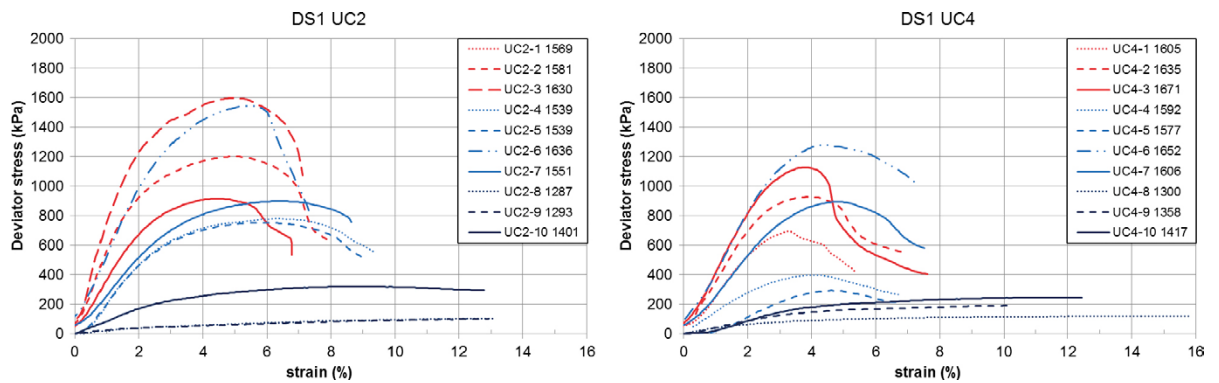


Figure A6-3. Unconfined compression tests on specimens of MX-80. Salt was added initially to some specimens (light blue lines) and some specimens were prepared from ion-exchanged powder (dark blue lines). All specimens were dried at $90\text{ }^{\circ}\text{C}$ and then saturated with 1M CaCl_2 . Results from series UC2 and UC4.

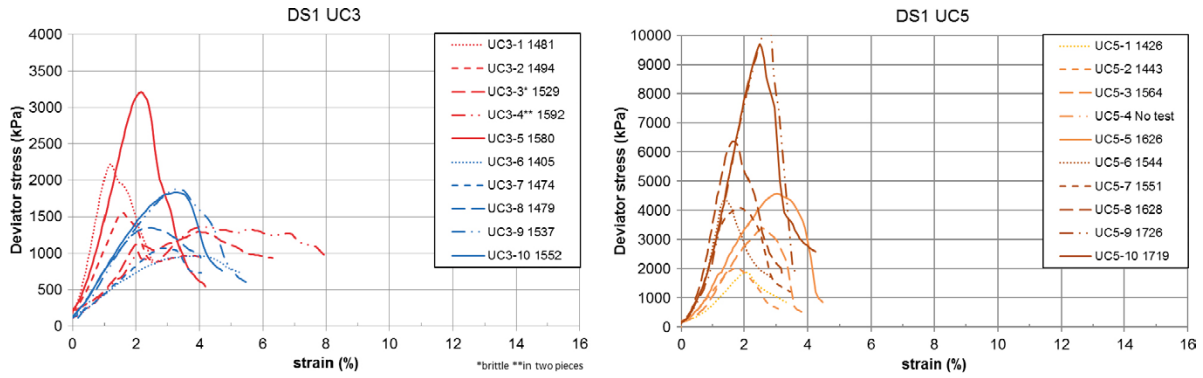


Figure A6-4. Unconfined compression tests on specimens of MX-80 with contents of CaO (red, orange and brown lines) and Ca(OH)₂ (blue lines). The specimens were saturated with de-ionized water. Results from series UC3 and UC5. Observe the high values on the y-axis in the diagram to the right.

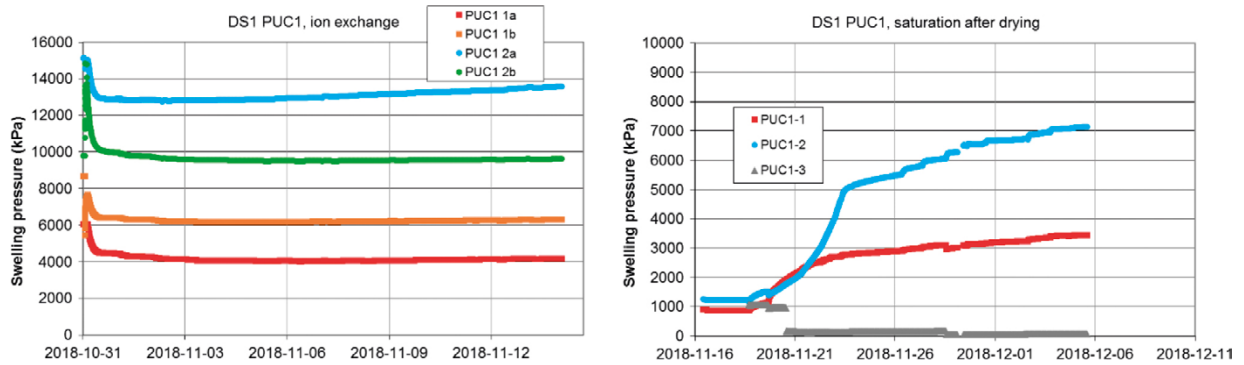


Figure A6-5. Swelling pressure measurement during preparation of specimens in the series PUC1.

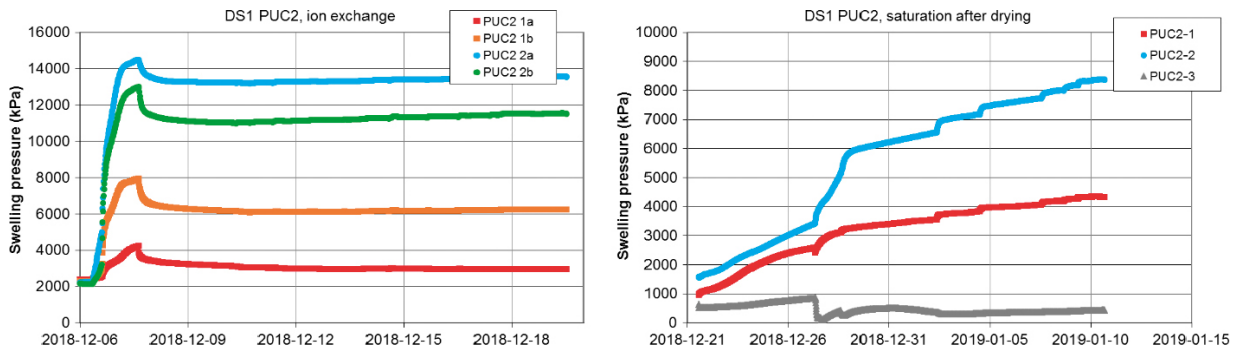


Figure A6-6. Swelling pressure measurement during preparation of specimens in the series PUC2.

Table A6-4. Results from the ion-exchange made on compacted specimens in series PUC1 and PUC2. Measured swelling pressure and estimated water contents and dry densities after the first part of the tests.

Series	Specimen ID	Water content %	Dry density kg/m ³	P_{s0} (H ₂ O) kPa	P_{s1} (CaCl ₂) kPa
PUC1	PUC1-1	27.30	1563	6524	5244
	PUC1-2	22.90	1642	14217	11592
PUC2	PUC2-1	27.8	1529	6073	4598
	PUC2-2	26.8	1578	13729	12558

Detailed results from DS2

The preparation of specimens in the series DS2 was described in Section 3.6.4 and the results are presented in Section 4.7. Tabulated results from the unconfined compression tests on dried and unsaturated specimens are given in Table A7-1, from the test series on complementary saturated specimens in Table A7-2 and from the series with subsequent determinations of characterizing properties in Table A7-3.

Table A7-1. Resulting unconfined compressive strength q_{max} and corresponding strain ϵ together with base variables determined after the tests. Different preparations are mentioned, e.g. type of ion-exchange or amount of initially added salt and the initial water content. The temperature used for the preparation was 25 °C.

Series	Specimen ID	Ion-exchange ¹	Initially added salt ² % of m_s	RH %	Aim initial water content %	Water content %	Density kg/m ³	Dry density kg/m ³	Degree of saturation %	At failure	
										q_{max} kPa	ϵ at q_{max} %
UCA	UCA1-1a			85	18	19.7	2054	1716	88	5224	3.4
	UCA1-2a			85	18	19.5	2046	1712	87	5201	3.4
	UCA1-4a			85	20	20.2	2080	1731	93	6732	3.8
	UCA1-5a			85	20	19.5	1983	1660	80	4101	2.3
	UCA1-6a			85	30	21.5	2080	1713	96	7045	5.0
	UCA1-7a			85	30	21.4	2085	1717	96	7319	5.3
	UCA1-8a			85	35	21.5	2075	1707	95	6747	7
	UCA1-9a			85	35	21.8	2077	1705	96	6898	7
		UCA1-1b			75	18	17.3	2110	1799	88	8706
	UCA1-2b			75	18	17.2	2096	1789	86	8026	6.5
	UCA1-4b			75	20	18.2	2116	1790	91	9723	7.9
	UCA1-5b			75	20	17.4	2015	1716	78	6133	6.1
	UCA1-6b			75	30	19.4	2099	1758	93	9135	10.0
	UCA1-7b			75	30	19.3	2103	1763	93	9795	9.2
	UCA1-8b			75	35	19.4	2098	1757	93	8684	6
	UCA1-9b			75	35	19.4	2111	1768	94	8519	5
	UCA2-1a	ie B		85	30	22.3	2072	1694	97	6386	4.1
	UCA2-2a	ie B		85	30	22.0	2071	1697	96	6573	4.4
	UCA2-1b	ie B		75	30	19.0	2085	1752	90	7428	7.4
	UCA2-2b	ie B		75	30	19.1	2083	1748	90	7453	7.1
UCB	UCB1-1a		5	85	18	30.4	1887	1448	92	304	11 ³
	UCB1-2a		5	85	18	30.0	1890	1454	91	282	10 ³
	UCB1-4a		5	85	20	30.7	1910	1461	95	337	11 ³
	UCB1-5a		5	85	20	30.7	1897	1452	93	356	11 ³
	UCB1-6a		5	85	30	31.3	1912	1456	96	491	15 ³
	UCB1-7a		5	85	30	30.7	1893	1448	93	467	10 ³
	UCB1-8a		5	85	35	30.9	1914	1463	95	575	10 ³
	UCB1-9a		5	85	35	29.9	1885	1451	91	570	10 ³
		UCB1-1b		5	75	18	22.7	1995	1626	89	925
	UCB1-2b		5	75	18	22.8	1980	1613	87	851	8
	UCB1-4b		5	75	20	23.1	2025	1645	93	1126	7
	UCB1-5b		5	75	20	23.0	2014	1637	92	1122	7
	UCB1-6b		5	75	30	24.3	2020	1625	95	1556	9
	UCB1-7b		5	75	30	24.2	1995	1606	92	1414	8
	UCB1-8b		5	75	35	24.3	2004	1613	93	1634	9
	UCB1-9b		5	75	35	24.1	1964	1583	88	1421	8

¹ Type of ion-exchange.

² The amount of salt is given as the mass of salt to the dry mass of the specimen.

³ Special evaluation of ϵ due to relatively low maximum stress.

Table A7-2. Test results from unconfined compression tests from series UCC and UCD.

Series	Specimen ID	Ion-exchange ¹	Initially added salt ² % of m _s	T _{max} °C	Water content %	Density kg/m ³	Dry density kg/m ³	Degree of saturation %	At failure	
									q _{max} kPa	ε at q _{max} %
UCC	UCC-1	ie B		22	27.6	1990	1560	98	2712	8.6
	UCC-2	ie B		22	26.0	2016	1600	98	3327	7.5
	UCC-3	ie B		22	24.2	2037	1640	97	4378	7.0
	UCC-4		20	22	25.7	2022	1609	98	2788	8.7
	UCC-5		14	22	25.8	2019	1606	98	2763	8.7
	UCC-6		20	22	26.2	2015	1597	98	2491	8.5
UCD	UCD-1			22	28.5	1973	1535	98	2144	7.8
	UCD-2			22	28.8	1964	1526	97	2057	8.1
	UCD-3			22	28.6	1970	1531	98	2096	8.0
	UCD-4			22	26.6	2000	1580	97	2547	7.2
	UCD-5			22	26.9	1994	1572	97	2503	7.5
	UCD-6			22	27.1	1997	1571	98	2437	7.9
	UCD-7			22	24.9	2020	1617	96	3194	7.5
	UCD-8			22	25.2	2025	1617	98	3150	7.5
	UCD-9			22	25.3	2026	1617	98	3125	7.0
	UCD-10			22	24.3	2027	1630	96	3409	6.5

¹ Type of ion-exchange.

² The amount of salt is given as the mass of salt to the dry mass of the specimen.

Table A7-3. Results from unconfined compression tests and swelling pressure determination in series PUCA and PUCB.

Series	Specimen ID	Ion-exchange ¹	Initially added salt ² % of m _s	T _{max} °C	Water content %	Density kg/m ³	Dry density kg/m ³	Degree of saturation %	At failure q _{max} kPa	ε at q _{max} %	Swelling pressure kPa
PUCA	PUCA-1	ie D		22	25.7	2013	1601	97	2980	7.2	8848
	PUCA-2	ie D		22	22.4	2045	1671	94	4416	6.0	13594
	PUCA-3	ie D		22	21.7	2061	1694	94	5006	5.3	14890
PUCB	PUCB 1	ie B		22	27.0	1997	1572	98	2427	7.5	6435
	PUCB 2	ie B		22	24.3	2030	1633	96	3338	5.4	12071
	PUCB 3	ie B		22	23.6	2043	1652	96	4123	6.3	15149

¹ Type of ion-exchange.

² The amount of salt is given as the mass of salt to the dry mass of the specimen.

A7.1 Results from the determination of retention curves of the material used for the tests PUCB ieB (labelled MX-80Ca)

Table A7-4. Water retention curve of ion-exchanged MX-80Ca. Resulting water contents after approximately 2000 h from the initial water contents of approximately 3 % and 64 %.

Sample ID	Initial w	mol. Sieve RH=0 %	LiCl RH=11.3 %	MgCl ₂ RH=32.8 %	NaBr RH=57.6 %	NaCl RH=75.3 %	KCl RH=84.4 %	NaCl_2m RH=93.1 %	K ₂ SO ₄ RH=97.3 %
MX-80Ca 3 %	3.5	0.8	7.0	12.6	16.2	18.8	20.6	24.0	29.7
MX-80Ca 64 %	65.2	0.9	8.2	14.6	18.3	20.9	23.0	26.8	33.2

To evaluate whether an equilibrium was reached the parameter Ω was calculated according to Equation 2-5. For all specimens the limit value $\Omega \leq 5 \times 10^{-9}$ 1/s was achieved when using the final parameter value or an average of the last three measured values. The equilibrium or the stability of the final values is further illustrated by the measured values 500 h before the termination, given in Table A7-5. There were some uncertainties in the salt solution of the LiCl and 2 m NaCl and these salts were changed during the last 500 h which gave relatively large changes.

Table A7-5. Differences between maximum and minimum water contents Δw evaluated during the last 500h of each test.

Sample ID	Initial w	mol. Sieve RH=0 %	LiCl RH=11.3 %	MgCl ₂ RH=32.8 %	NaBr RH=57.6 %	NaCl RH=75.3 %	KCl RH=84.4 %	NaCl_2m RH=93.1 %	K ₂ SO ₄ RH=97.3 %
MX-80Ca 3 %	3.5	0.03	0.24	0.03	0.03	0.02	0.03	0.29	0.16
MX-80Ca 64 %	65.2	0.08	0.79	0.00	0.05	0.03	0.03	0.19	0.26

A7.2 Results from preparation of the unsaturated specimens, drying and water uptake

In the preparation of specimens in series UCA and UCB the specimens were exposed to relative humidity of 75 % and 85 %. The resulting water content w , dry density ρ_d and degree of saturation S_r are shown in Table A7-6. Series UCA1 was made on MX-80, UCA2 on ion-exchanged Ca-dominated MX-80 and UCB on MX-80 with added contents of CaCl₂.

The resulting water contents and dry density after the preparation in the climate chambers are also shown in Figure A7-1 to Figure A7-3 where the initial values are marked with open circles, the values after the preparation are marked with solid circles and the values determined after the unconfined compression tests are marked with plus signs. The test series A1, A2 and B1 are shown separately.

Table A7-6. Results from preparation of specimens in series UCA and UCB. The specimen ID are shown with the actual RH, the aim of the initial water content and the initial condition of the specimens (w_{ini} , $\rho_{d,ini}$, $S_{r,ini}$) the condition after exposure (w_{prep} , $\rho_{d,prep}$, $S_{r,prep}$) and the condition determined after the unconfined compression test (w_f , $\rho_{d,f}$, $S_{r,f}$). The base variables have not been corrected in series UCB where excess salt was used.

Series	Specimen ID	RH %	w_{aim} %	w_{ini} %	$\rho_{d,ini}$ kg/m ³	$S_{r,ini}$ %	w_{prep} %	$\rho_{d,prep}$ kg/m ³	$S_{r,prep}$ %	w_f %	$\rho_{d,f}$ kg/m ³	$S_{r,f}$ %
UCA	A1-1a	85	17.5	18.0	1816	92	20.2	1688	87	19.7	1716	88
	A1-2a	85	17.5	18.0	1797	89	20.3	1678	86	19.5	1712	87
	A1-4a	85	20	20.1	1751	95	21.2	1711	94	20.2	1731	93
	A1-5a	85	20	20.1	1661	82	20.8	1635	83	19.5	1660	80
	A1-6a	85	30	30.8	1498	97	21.9	1701	96	21.5	1713	96
	A1-7a	85	30	30.8	1485	96	22.3	1694	97	21.4	1717	96
	A1-8a	85	35	35.0	1389	97	23.0	1659	94	21.5	1707	95
	A1-9a	85	35	35.0	1388	97	23.4	1648	95	21.8	1705	96
	A1-1b	75	17.5	18.0	1800	89	18.0	1769	88	17.3	1799	88
	A1-2b	75	17.5	18.0	1780	87	17.9	1761	86	17.2	1789	86
	A1-4b	75	20	20.1	1747	94	19.4	1763	93	18.2	1790	91
	A1-5b	75	20	20.1	1658	82	19.0	1670	80	17.4	1716	78
	A1-6b	75	30	30.8	1500	98	20.2	1739	94	19.4	1758	93
	A1-7b	75	30	30.8	1502	98	19.9	1731	91	19.3	1763	93
	A1-8b	75	35	35.0	1385	97	21.2	1683	90	19.4	1757	93
	A1-9b	75	35	35.0	1396	98	20.9	1686	90	19.4	1768	94
	A2-1a	85	30	31.6	1468	93	21.4	1699	94	22.3	1694	97
	A2-2a	85	30	31.6	1461	92	21.5	1690	93	22.0	1697	96
	A2-1b	75	30	31.6	1488	96	19.6	1714	88	19.0	1752	90
	A2-2b	75	30	31.6	1477	95	19.6	1694	85	19.1	1748	90

Series	Specimen ID	RH %	W _{aim} %	W _{ini} %	ρ _{d,ini} kg/m ³	S _{r,ini} %	W _{prep} %	ρ _{d,prep} kg/m ³	S _{r,prep} %	W _f %	ρ _{d,f} kg/m ³	S _{r,f} %
UCB	B1-1a	85	17.5	16.6	1822	92	33.3	1369	90	30.4	1448	92
	B1-2a	85	17.5	16.6	1794	88	32.9	1357	87	30.0	1454	91
	B1-4a	85	20	21.1	1715	89	31.7			30.7	1461	95
	B1-5a	85	20	21.1	1714	89	31.9			30.7	1452	93
	B1-6a	85	30	31.1	1486	96	33.5			31.3	1456	96
	B1-7a	85	30	31.1	1460	92	33.2			30.7	1448	93
	B1-8a	85	35	35.0	1384	97	34.3			30.9	1463	95
	B1-9a	85	35	35.0	1353	92	34.6			29.9	1451	91
	B1-1b	75	17.5	17.0	1792	88	24.4	1565	87	22.7	1626	89
	B1-2b	75	17.5	17.0	1764	84	24.4	1553	86	22.8	1613	87
	B1-4b	75	20	20.2	1731	92	24.6	1604	93	23.1	1645	93
	B1-5b	75	20	20.2	1700	87	24.6	1593	92	23.0	1637	92
	B1-6b	75	30	30.7	1489	96	26.5	1564	95	24.3	1625	95
	B1-7b	75	30	30.7	1471	94	26.4	1541	91	24.2	1606	92
	B1-8b	75	35	34.8	1395	98	27.4	1535	94	24.3	1613	93
	B1-9b	75	35	34.8	1364	94	27.6	1506	91	24.1	1583	88

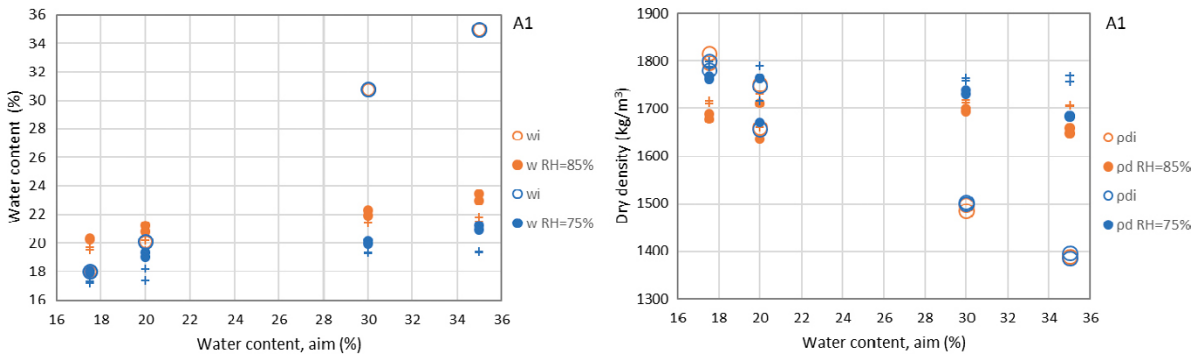


Figure A7-1. Results from the preparation of specimens used in the test series UCA1 on MX-80. Water content and dry density at start (unfilled circles) and after conditioning in a climate chamber with a controlled relative humidity of 75 % or 85 % and a temperature of 25 °C (filled circles). The variables were also determined after the unconfined compression tests (plus signs).

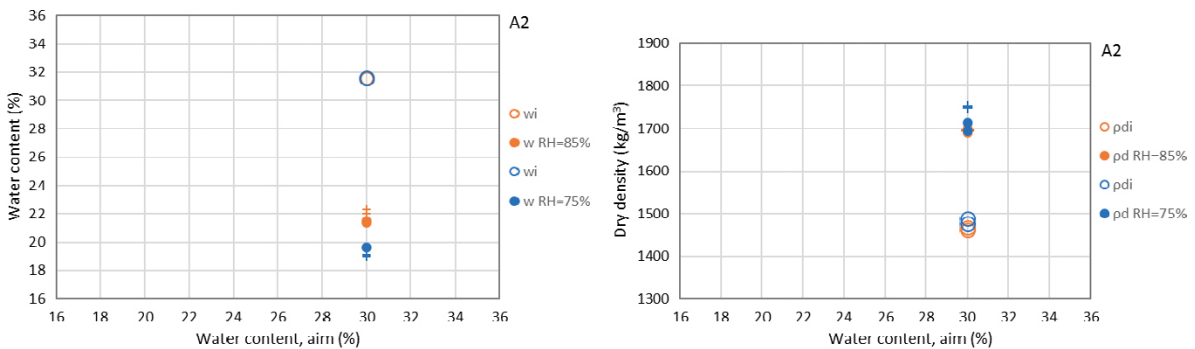


Figure A7-2. Results from the preparation of specimens used in the test series UCA2 on ion-exchanged Ca-dominated MX-80. Water content and dry density at start (unfilled circles) and after conditioning in a climate chamber with a controlled relative humidity of 75 % or 85 % and a temperature of 25 °C (filled circles). The variables were also determined after the unconfined compression tests (plus signs).

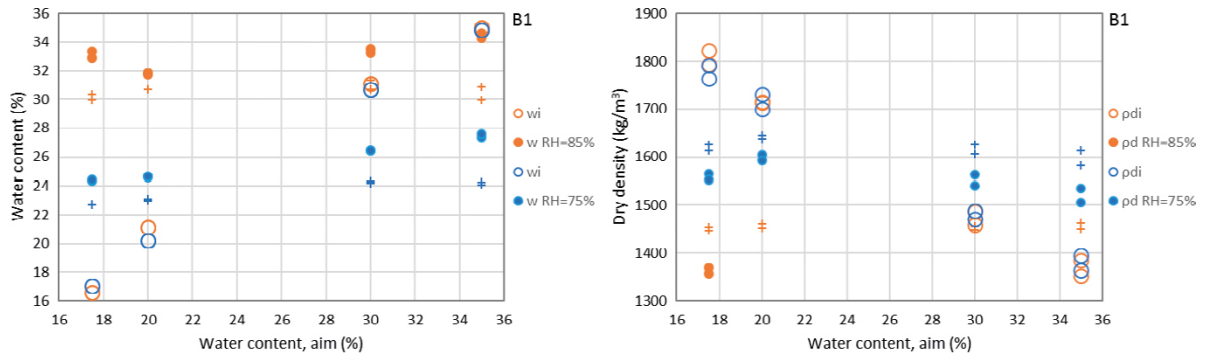


Figure A7-3. Results from the preparation of specimens used in the test series UCB1 on MX-80 with added contents of CaCl_2 . Water content and dry density at start (unfilled circles) and after conditioning in a climate chamber with a controlled relative humidity of 75 % or 85 % and a temperature of 25 °C (filled circles). The variables were also determined after the unconfined compression tests (plus signs).

A7.3 Results from unconfined compression tests

In the diagrams below the results from all unconfined compression tests are shown. The legends contain information about the specimen ID and the dry density in kg/m^3 determined after dismantling (e.g. UCD-1 1540). In the unsaturated test series UCA and UCB the legends also contain information about the aim initial water content in %. Where the material was not MX-80 this is indicated in the final part of the legends either with the ion-exchanged method used (ieB or ieD) or with the word *salt* indicating that an amount of excess salt (CaCl_2) was added at preparation.

Series with saturated specimens are shown in Figure A7-4 and Figure A7-5 while the series with unsaturated specimens are shown in Figure A7-6 to A7-8.

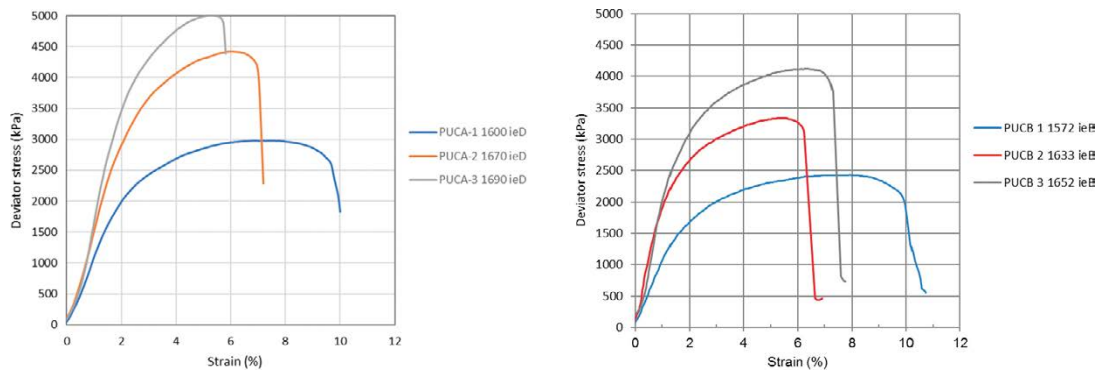


Figure A7-4. Deviator stress as a function of strain from unconfined compression tests on saturated specimens of ion-exchanged Ca-dominated MX-80 from tests series PUCA and PUCB where the dry density in kg/m^3 is given in the labels together with the method used for the ion-exchange (ieB or ieD).

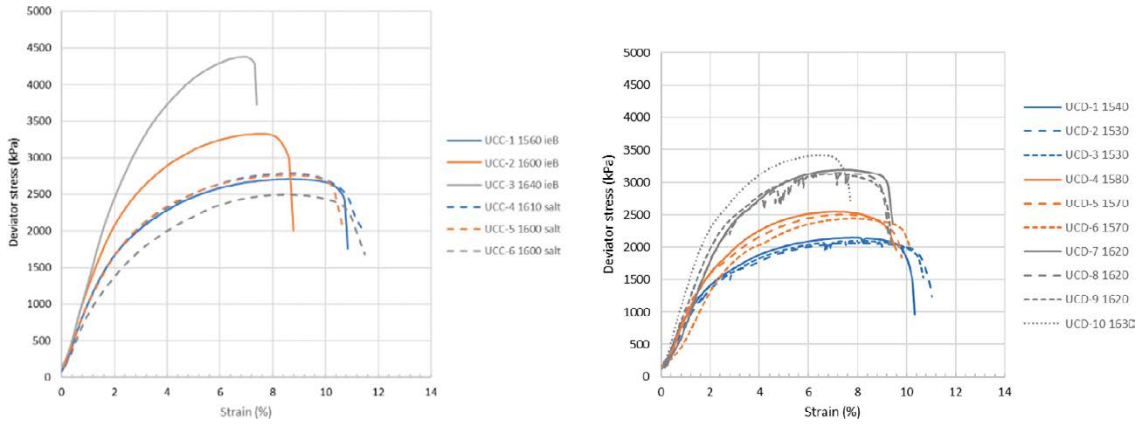


Figure A7-5. Deviator stress as a function of strain from unconfined compression tests on saturated specimens from test series UCC and UCD where the dry density in kg/m^3 is given in the labels. The material in UCC was based on MX-80 and was either ion-exchanged Ca-dominated material (ieB) or included amounts of CaCl_2 which are indicated with the word salt in the labels. The material in series UCD was MX-80.

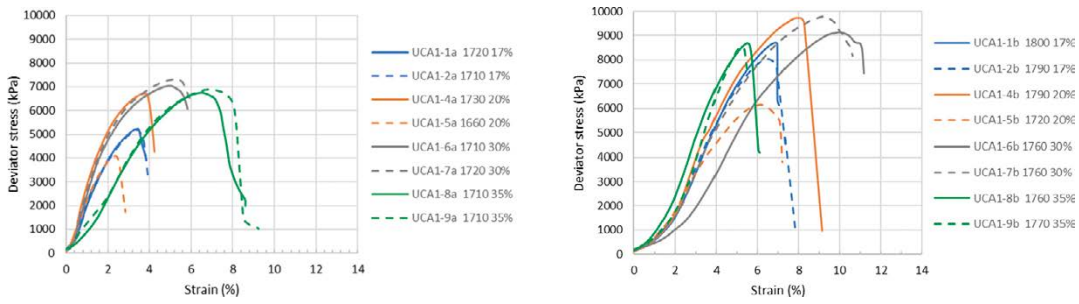


Figure A7-6. Deviator stress as a function of strain from unconfined compression tests on unsaturated specimens of MX-80 from tests series UCA1 where the labels contain information about the sample ID, dry density in kg/m^3 and the aim initial water content in %.

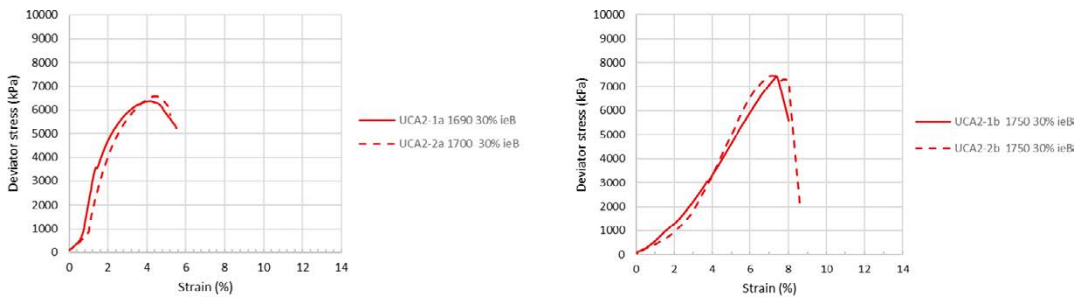


Figure A7-7. Deviator stress as a function of strain from unconfined compression tests on unsaturated specimens of ion-exchanged Ca-dominated MX-80 from tests series UCA2 where the labels contain information about the sample ID, dry density in kg/m^3 , the aim initial water content in % and the method used for the ion-exchange (ieB).

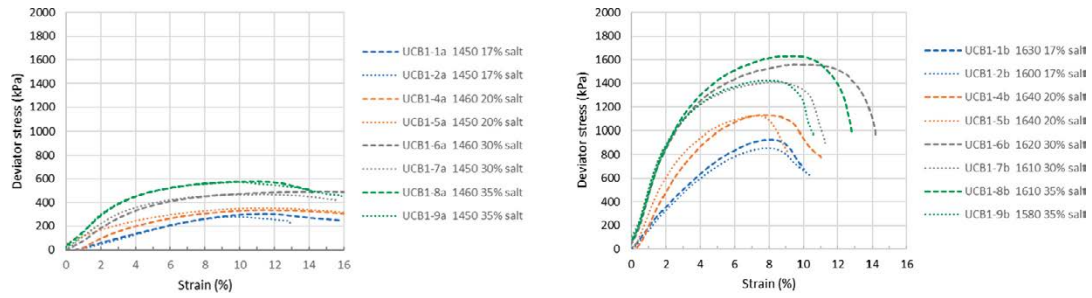


Figure A7-8. Deviator stress as a function of strain from unconfined compression tests on unsaturated specimens of MX-80 with added amounts of CaCl_2 from tests series UCB1 where the labels contain information about the sample ID, dry density in kg/m^3 , the aim initial water content in % and the word salt indicate added amounts of CaCl_2 .

A7.4 Results from swelling pressure measurements

In the test series PUCA and PUCB the swelling pressure was determined during the saturation with DI-water, the ion-exchange with 1M CaCl_2 and during the final equilibrium with DI-water. The swelling pressure during the preparation are shown in Figure A7-9, Figure A7-10 and Table A7-7.

Table A7-7. Results from specimens, ion-exchange in-situ (ieD) in series PUCA and ion-exchange on powder (ieB) in series PUCB. Measured swelling pressure and estimated water contents and dry densities after the first part of the tests.

Series	Specimen ID	Type of ion-exchange	Water content %	Dry density kg/m^3	Degree of saturation %	P_{s0} (H_2O) kPa	P_{s1} (CaCl_2) kPa	P_{s3} (H_2O) kPa
PUCA	PUCA 1	ie D	25.7	1601	97.1	7686	5784	8848
	PUCA 2	ie D	22.4	1671	93.7	11284	9739	13594
	PUCA 3	ie D	21.7	1694	94.0	12125	10876	14890
PUCB	PUCB 1	ie B	27.0	1572	98			6435
	PUCB 2	ie B	24.3	1633	96			12071
	PUCB 3	ie B	23.6	1652	96			15149

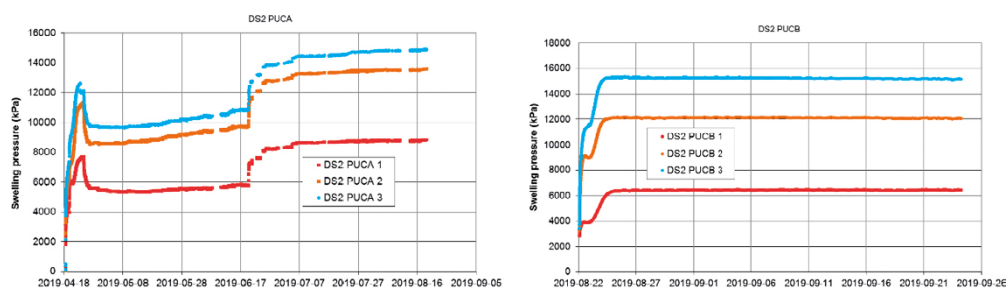


Figure A7-9. Swelling pressure measurement during preparation of specimens in the series PUCA and PUCB.

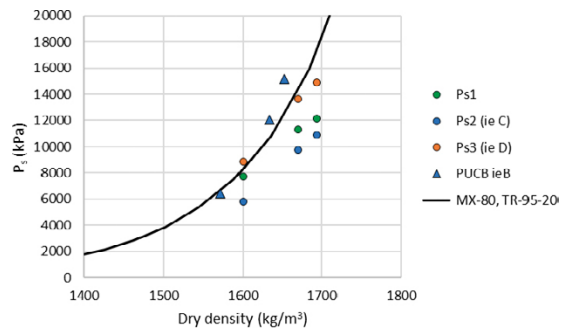


Figure A7-10. Swelling pressure measurement at saturation, ion-exchange and washing of PUCA and at saturation of PUCB.

Detailed results from UCT

The preparation of specimens in the test series were described in Section 3.6.5 and the results were presented in Section 4.8. Details of the procedure of heating at saturated conditions are shown in Figure A8-1 where the protocol of water pressure and temperature are shown as a function of time.

Below the tabulated test results are shown in Table A8-1. In Figure A8-2 to Figure A8-5 the deviator stress as function of strain from all test series, UCT1–UCT4, are shown separately. In series UCT1–UCT3 all specimens were heated at saturated and confined conditions. In series UCT4 specimens 1 to 6 were heated at unsaturated and drying conditions and specimen 7–10 were reference specimens. Photos of all specimens in series UCT1–4 are given in Figure A8-6 to Figure A8-9.

Table A8-1. Resulting unconfined compressive strength q_{max} and corresponding strain ϵ together with base variables determined after the tests from the series UCT. Maximum temperature and the condition at heating are also shown. All specimens were saturated before the unconfined compression test and de-ionized water was used for the saturation.

Test ID	Material	T_{max} °C	Condition at heating	Dry density kg/m ³	Water content %	Degree of saturation %	At failure	
							q_{max} kPa	Strain at q_{max} %
UCT1-1	MX-80	240	saturated	1606	25.9	99	3513	3.0
UCT1-2	MX-80	240	saturated	1681	23.2	99	5735	1.8
UCT2-1	Asha505	240	saturated	1543	30.0	100	4090	2.3
UCT2-2	Asha505	240	saturated	1614	27.2	100	6557	2.1
UCT3-1	Calcigel	240	saturated	1555	27.5	101	2942	2.0
UCT3-2	Calcigel	240	saturated	1632	24.1	100	2516	3.2 ¹
UCT4-1	MX-80	240	unsaturated	1552	28.1	99	2254	7.2
UCT4-2	MX-80	240	unsaturated	1623	25.2	98	3151	6.5
UCT4-3	Asha505	240	unsaturated	1527	30.6	100	2624	6.1
UCT4-4	Asha505	240	unsaturated	1618	27.0	100	4349	5.9
UCT4-5	Calcigel	240	unsaturated	1512	28.7	99	2057	3.7
UCT4-6	Calcigel	240	unsaturated	1593	25.2	98	2978	3.3
UCT4-7	MX-80	20		1549	27.7	97	2337	7.5
UCT4-8	Asha505	20		1543	29.9	100	3085	6.4
UCT4-9	Calcigel	20		1538	28.2	101	2676	4.0
UCT4-10	MX-80	20		1636	24.3	96	3528	6.2

¹ Somewhat uncertain result, specimen stuck to the filter at dismantling from the saturation device, low height at shearing.

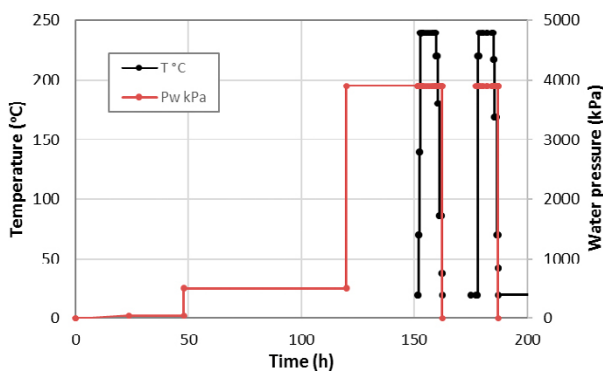


Figure A8-1. Water pressure (red line) and temperature (black line) as a function of time from test series UCT1–3.

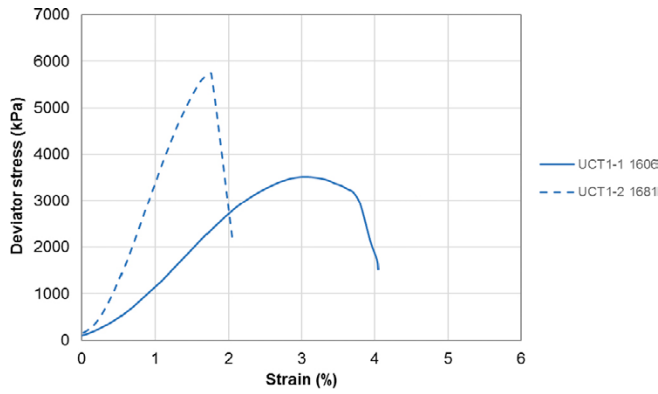


Figure A8-2. Deviator stress as a function of strain from unconfined compression tests on MX-80 (UCT1). The labels contain the Test ID and the dry density (kg/m^3).

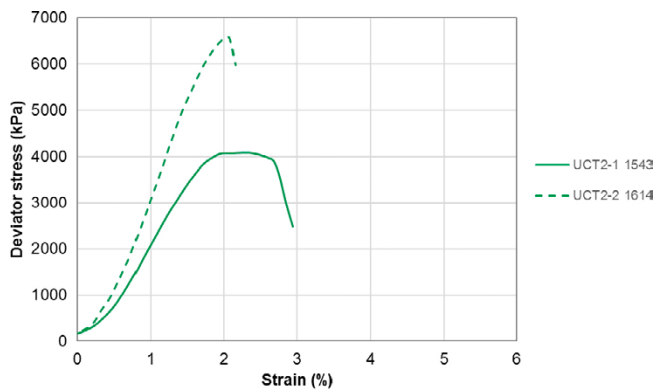


Figure A8-3. Deviator stress as a function of strain from unconfined compression tests on Asha505 (UCT2). The labels contain the Test ID and the dry density (kg/m^3).

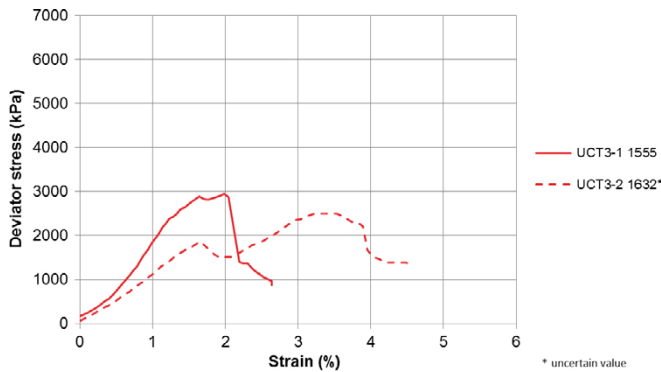


Figure A8-4. Deviator stress as a function of strain from unconfined compression tests on Calcigel (UCT3). The labels contain the Test ID and the dry density (kg/m^3).

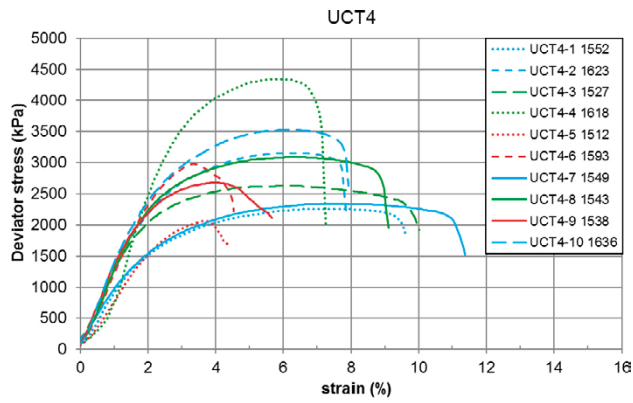


Figure A8-5. Deviator stress as a function of strain from unconfined compression tests on MX-80 (blue lines), Asha505 (green lines) and Calcigel (red lines) in series UCT4. The labels contain the Test ID and the dry density (kg/m^3).

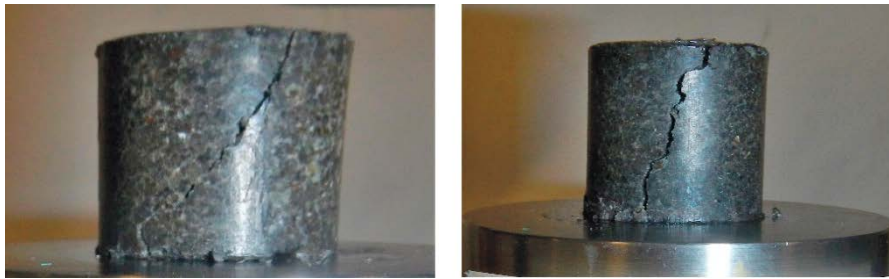


Figure A8-6. Photos of specimens of MX-80 heated at saturated conditions, test series UCT1.

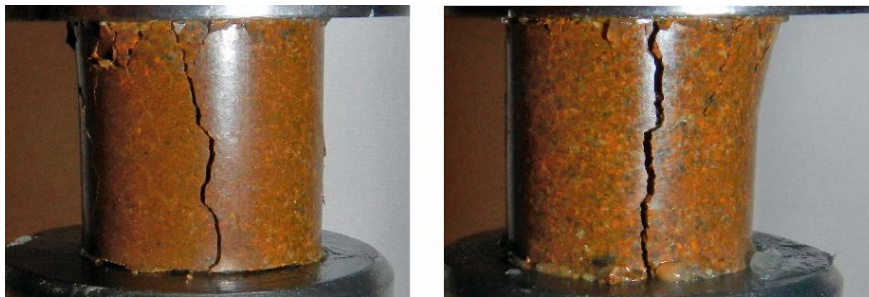


Figure A8-7. Photos of specimens of Asha 505 heated at saturated conditions, test series UCT2.



Figure A8-8. Photos of specimens of Calcigel heated at saturated conditions, test series UCT3.



Figure A8-9a. Photos of specimens of MX-80 heated at unsaturated conditions. Test series UCT4.



Figure A8-9b. Photos of specimens of Asha505 heated at unsaturated conditions. Test series UCT4.



Figure A8-9c. Photos of specimens of Calcigel heated at unsaturated conditions. Test series UCT4.



Figure A8-9d. Photos of reference specimens of MX-80. Test series UCT4.



Figure A8-9e. Photos of reference specimens of Asha505 (left) and Calcigel (right). Test series UCT4.

Expected accuracy in unconfined compression tests

When analysing deviating results from unconfined compression tests, as in Chapter 5, the accuracy in the results should be known. The accuracy was evaluated by determination of a best fit line and then subtracting values according to the adopted line from the original data and analysing the residuals. The analysis was done by calculation of the average and standard deviation. Similar evaluation of accuracy has been reported by e.g. Dueck (2014) and Svensson et al. (2019).

In this study the accuracy was evaluated from three series where each of the series contained more than ten tests on specimens of the same material and treated in the same way but at different densities. The test series were run on Calcigel and GMZ (series TMS1, Section 4.2.5) and on MX-80 (series DS2 UCD, Section 4.7.3). The results are tabulated in Table A9-1 and Table A9-2 and illustrated in Figure A9-1 to A9-4.

In Table A9-1 the average and standard deviation for the residual deviator stress at failure are evaluated for the three test series. The best fit lines were evaluated as exponential relationships between the maximum deviator stress at failure and the dry density. A fourth evaluation was done where the residual between the original MX-80 data and the reference line TR-11-07 (Dueck et al. 2011a) was calculated, i.e. the results from this study is compared to results from another batch of the material. This evaluation was done since the specific reference line has been frequently used in the report. The illustrations in Figure A9-1 to Figure A9-4 show the original data with the best fit line or reference line (to the left) and the residual stress (to the right).

In Table A9-2 the average and standard deviation for the residual strain at q_{max} are evaluated. The best fit lines were evaluated as linear relationships between the corresponding strain and the dry density.

Table A9-1. Mean and standard deviation for residual deviator stress at failure.

Material, Reference	Number of tests	Average kPa	Standard deviation kPa	See Figure below
MX-80, DS2 UCD	10	-1	48	Figure A9-1
Calcigel, TMS1	15	12	347	Figure A9-2
GMZ, TMS1	16	3	104	Figure A9-3
MX-80, TR-11-07 ¹	10	-197	225	Figure A9-4

¹ The residuals have been calculated from a reference referred to by Dueck et al. (2011a).

Table A9-2. Mean and standard deviation in percentage points for residual strain at q_{max} .

Material, Reference	Number of tests	Average %	Standard deviation %
MX-80, DS2 UCD	10	0.0003	0.26
Calcigel, TMS1	15	0.226	1.32
GMZ, TMS1	16	0.001	0.85
MX-80, TR-11-07 ¹	10	-1.069	1.11

¹ The residuals have been calculated from a reference referred to by Dueck et al. (2011a).

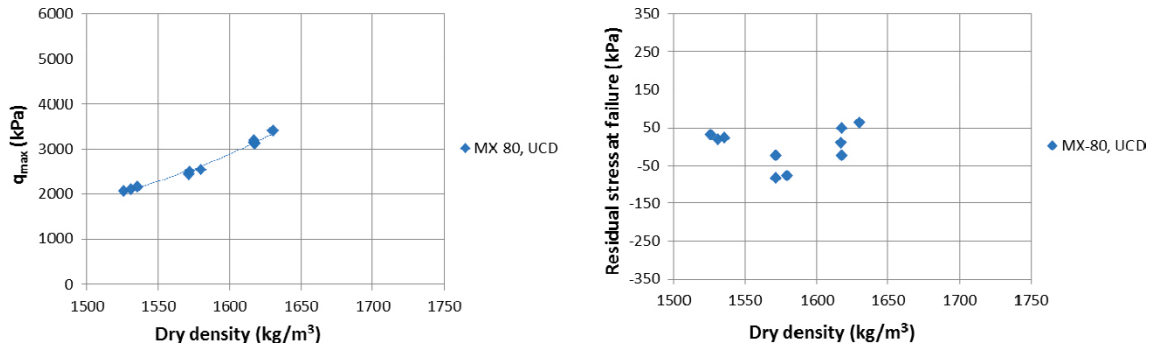


Figure A9-1. Maximum deviator stress from test series DS2 UCD on MX-80 (cf. Figure 4-45) with an exponential best fit line (left) and the residual stress (right) plotted as a function of dry density.

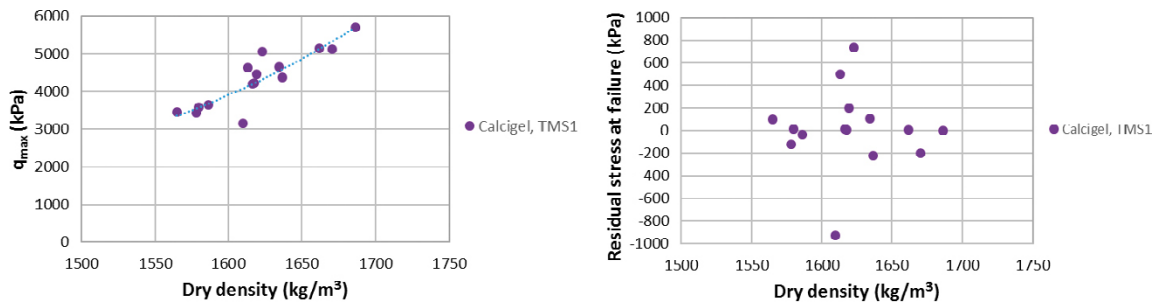


Figure A9-2. Maximum deviator stress from test series TMS1 on Calcigel (cf. Figure 4-1) with an exponential best fit line (left) and the residual stress (right) plotted as a function of dry density.

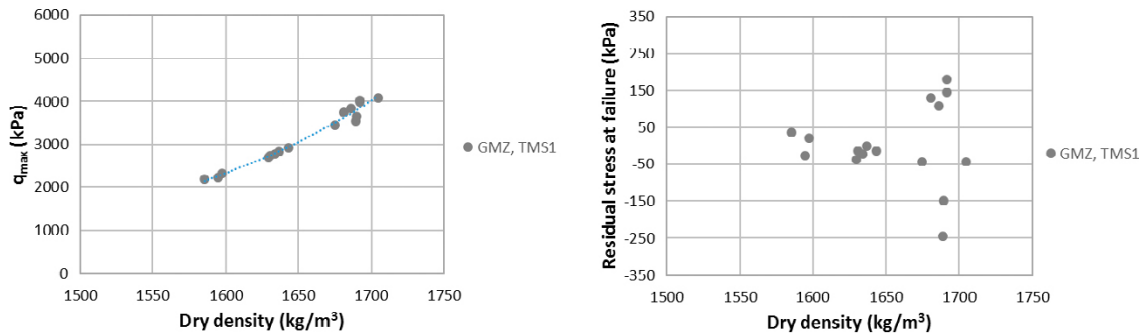


Figure 91-3. Maximum deviator stress from test series TMS1 on GMZ (cf. Figure 4-4) with an exponential best fit line (left) and the residual stress (right) plotted as a function of dry density.

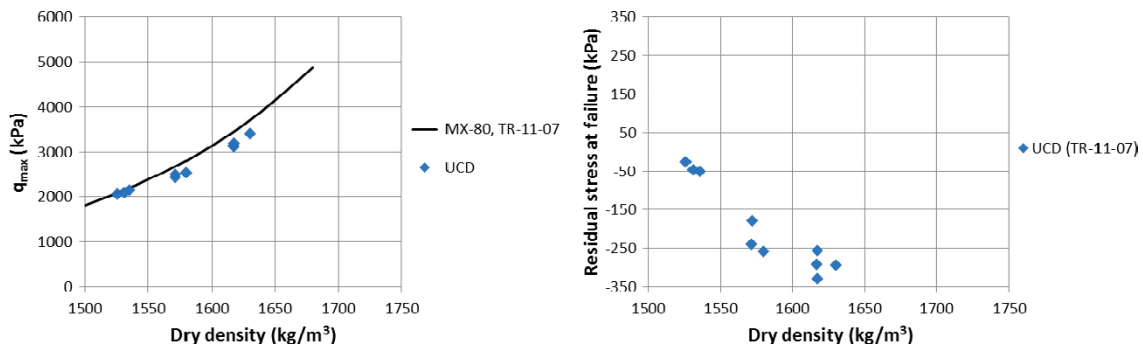


Figure A9-4. Maximum deviator stress from test series DS2 UCD (cf. Figure 4-45) with an exponential best fit line from TR-11-07 (Dueck et al. 2011a) (left) and the residual stress (right) plotted as a function of dry density.

